Unravelling the biology of the Southern African Sauropodomorph dinosaurs, *Plateosauravus* and the 'Maphutseng dinosaur'.

Emil Darius Krupandan

Thesis presented for the degree of Doctor of Philosophy

In the Department of Biological Sciences

University of Cape Town

February, 2019

Declaration of Free Licence

I hereby grant the University free license to reproduce the above thesis in whole or in part, for the purpose of research.
I declare that the above thesis is my own unaided work, both in conception and execution, and that apart from the normal guidance of my supervisors, I have received no assistance apart from that stated below.

Except as stated below, neither the substance or any part of the thesis has been submitted in the past, or is being, or is to be submitted for a degree at this University or any other University.

I am now presenting the thesis for examination for the Degree of PhD.

Signed by candidate

––––––––––––––––

Emil Darius Krupandan

11th day of February 2019 at the University of Cape Town

I confirm that I have been granted permission by the University of Cape Town's Doctoral Degrees Board to include the following publication(s) in my PhD thesis, and where co-authorships are involved, my co-authors have agreed that I may include the publication(s):

1. Krupandan, E., Chinsamy-Turan, A. & Pol, D. 2018. The long bone histology of the sauropodomorph, Antetonitrus ingenipes. *The Anatomical Record.* 301(9):1506-1518.

SIGNATURE: Signed by candidate DATE: 03/07/2019

STUDENT NAME: Emil Darius Krupandan

STUDENT NUMBER: KRPEMI001

Abstract

The *nomen dubium* "*Euskelosaurus*" has functioned as a waste-basket taxon for decades, with large bodied sauropodomorph material from South Africa assigned to it without proper analysis. Following the collapse of *Euskelosaurus*, material previously assigned to it was summarily referred to *Plateosauravus cullingworthi*. Based on this, material referred to *Euskelosaurus* from Maphutseng, Lesotho (NMQR 1705) would technically also be referrable to *Plateosauravus*. In light of the tenuous nature of the taxonomic affinity of these materials, a thorough analysis of material associated with both taxa follows. The validity of *Plateosauravus* was evaluated and the taxonomic affinity of material previously reffered to *Euskelosaurus* (NMQR 1705) tested.

The *Plateosauravus cullingworthi* hypodigm was subject to a rigorous anatomical and phylogenetic analyses in order to test its taxonomic validity. Undescribed material from Maphutseng, Lesotho (NMQR 1705) was also analysed. It was hypothesised that *Plateosauravus* was a valid non-Massopodan dinosaur and that NMQR 1705 represented a basal sauropod, with concomitant growth dynamics.

Skeletal elements from *Plateosauravus* and NMQR 1705 were anatomically described and taxonomically identified based on comparisons with other sauropodomorph taxa. Anatomical data was scored in a character matrix and subject to phylogenetic analyses. The growth dynamics of NQMR 1705 was investigated through histological analysis of thin sections of long bones.

The material referred to *Plateosauravus* shows that some of the material belongs to a non-Massopodan basal sauropodomorph that, but there also exists material that should

be excluded from this taxon based on doubtful provenance and association.

The Maphutseng material (NMQR 1705) can be referred to *Antetonitrus ingenipes*. New elements described, including a complete sacrum, reveal additional adaptations highlighting *Antetonitrus*' position as a transitional basal sauropod, exhibiting a mosaic of basal sauropomorph and derived sauropod characterisitcs. The phylogenetic analysis corroborates the position of *Antetonitrus* as the sister taxon of *Lessemsaurus sauropoides* (Bonaparte, 1999), but the new information from the pes indicates that both taxa are more derived than *Blikanasaurus cromptoni* (Galton & Van Heerden, 1998).

Growth patterns in the youngest individuals of NMQR 1705 exhibit uninterrupted fibrolamellar bone without any growth marks. Sub-adult individuals, also exhibit highly vascularised fibrolamellar bone throughout the cortex, as in more derived sauropods and the basal sauropodiforme *Mussaurus patagonicus*, but growth lines occur intermittently throughout the cortex as in *Lessemsaurus*. *Antetonitrus* (NMQR 1705) does not exhibit the growth dynamics previously considered characteristic of Sauropoda.

Growth marks are decoupled from bone size, indicating a level of developmental plasticity in this taxon. Modulations in the pattern of vascular canal arrangements throughout the fibrolamellar bone in the cortex may be related to resource availability. Localised bands of radial fibrolamellar bone, followed by resumption of normal growth in two samples indicate disease infliction, and subsequent recovery.

“If it looks like a duck, and quacks like a duck, we have at least to consider the possibility that we have a small aquatic bird of the family anatidae on our hands.”

-Douglas Adams

Acknowledgements

Firstly, I'd like to express my thanks to my two supervisors, A. Chinsamy-Turan and D. Pol, without whom this work would not have been possible. Both of them have provided me with countless opportunities and funding to learn new techniques, visit collections across South Africa and Argentina and generally become a fully-fledged palaeontologist.

I am grateful to J. Botha-Brink and E. Butler (National Museum, Bloemfontein, South Africa) for allowing for the histological analysis of NMQR 1705; as well as to B. Rubidge and B. Zipfel (Evolutionary Studies Institute, Johannesburg, South Africa) for access to the holotype of *Antetonitrus ingenipes* and other comparative material on countless occasions.

I'd also like to extend thanks to S. Kaal, Z Skosana and R. Smith at Iziko Natural History Museum for access to the collections throughout my work. Further acknowledgments go to C. Apaldetti and A. Otero for advice, discussion and assistance in South Africa and Argentina throughout my studies.

Lastly, I'd like to thank my family and friends for supporting me throughout this endeavour.

This research was supported by a South African National Research Foundation (NRF) Scarce Skills Bursary and Palaeontological and Scientific Trust (PAST) grant to E. Krupandan.

TABLE OF CONTENTS

LIST OF TABLES

LIST OF FIGURES

Page

Chapter 2:

Chapter 3:

Chapter 4:

Chapter 1

Introduction

1.1 Outline of Thesis Structure

This chapter provides a general introduction to the area of study and the rationale for doing so. In addition, the aims and objectives of this work are outlined here as well. Following the first chapter, three research aspects of the study (Chapters 2-4) are presented to address specific research questions listed in Chapter 1

Each research chapter is a self-contained study, that looks at particular aspects of the study material assigned to and historically associated with the now recognised *nomen dubium* - *Euskelosaurus browni*.

Chapter 5 is the concluding chapter, which provides a summary and synthesis of the key findings of chapters 2 - 4, and provides suggestions as to how future work in addressing the phylogeny and biology of South African Sauropodomorph taxa should proceed.

1.2 General Introduction

Late Triassic- Early Jurassic dinosaur assemblages from southern Gondwana (viz. South Africa, Lesotho, Argentina and Brazil) present a host of sauropodomorph dinosaurs, spanning the spectrum from basal sauropodomorphs (or ‘prosauropods’), members of the obligatory quadrupedal clade (*Melanosaurus* + Sauropoda [see Yates et al.,2010]) and their immediate out-group comprising *Aardonyx celestae*, *Mussaurus patagonicus* and *Leonerasaurus taquetrensis* (Yates et al., 2010; Pol et

al.,2011 and Otero & Pol, 2013). The latter two groups comprise the clade Sauropodiformes (Sereno, 2007; Otero & Pol, 2013), early members of which show a mosaic of both basal sauropodomorph and sauropod characteristics (refer to Table 1. for definition of clades used throughout study).

Focusing on Southern Africa (South Africa and Lesotho specifically) the Elliot Formation (EF) serves as an exemplar of Late Triassic–Early Jurassic sauropodomorphs. Within the Elliot, we find the basal sauropodomorphs *Massospondylus carinatus*, *Plateosauravus cullingworthi*, *Eucnemesaurus fortis, Arcusaurus pereirabdalorum*; the basal sauropodiformes *Aardonyx celestae*, *Sefapanosaurus zastronesis*, *Meroktenos thabanensis*; the facultative and obligatory quadrupeds (*Melanorosaurus* + Sauropoda) *Melanorosaurus readi, Antetonitrus ingenipes* , *Blikanasaurus cromptoni*, *Pulanesaura eocollum*, *Ledhumahadi mafube* and the now discredited nomen dubium – *Euskelosaurus browni* (Yates & Kitching, 2003; Yates et al., 2010; Yates et al., 2011; Galton & Van Heerden, 1998; Galton & Upchurch, 2004; Otero et al., 2015; Peyre de Fabregues & Allain, 2016; McPhee et al. 2015,2018).

This range of taxa has been significant in that they span the transition from smaller bipedal basal sauropodomorphs to quadrupedal sauropods (*sensu* Yates, 2007a), providing an opportunity to understand how more basal sauropodomorphs changed in terms of their morphology and growth as they approached Sauropoda.

However, in the course of research over the past century some of these taxa still suffer from poor descriptions and issues surrounding their taxonomic validity. For example, *Melanorosaurus*, *Plateosauravus* and *Euskelosaurus* are currently considered taxonomically problematic genera.

In order to provide a better assessment of sauropodomorph evolution in southern Africa it is essential that the confusion around these poorly/undescribed fossils is cleared up, since they could potentially shed even more light on what was occurring in the sauropodomorph hyperspace during the Mesozoic in southern African. As work is currently underway by other researchers on re-evaluating the *Melanorosaurus* hypodigm (see Nair & Yates, 2014; McPhee et al., 2017), this work will focus on material ascribed to *Plateosauravus* and *Euskelosaurus* exclusively.

Table 1. Phylogenetic nomenclature for clades mentioned throughout the text

Clade	**Definition**	**Source**
Sauropodomorpha	The most inclusive clade containing *Saltasaurus* but not *Passer* and *Triceratops*	Sereno, 2007
Unaysaurids	The most inclusive clade containing *Unaysaurus* but not *Plateosaurus engelhardti* and *Saltasaurus*	Müller et al., 2018
Massopoda	The most inclusive clade that contains *Saltasaurus* but not *Plateosaurus*	Yates, 2007a, b
Massospondylidae	All taxa more closely related to *Massospondylus carinatus* than to *Platoesaurus engelhardti* and *Saltasaurus loricatus*	Sereno, 1998
Anchisauria	*Anchisaurus* and *Melanorosaurus,* their common ancestor, and all its descendants.	Galton & Upchurch, 2004
Sauropodiformes	The least inclusive clade containing *Mussaurus* and *Saltasaurus.*	Sereno,2007
Sauropoda	The most inclusive clade that contains *Saltasaurus loricatus* but not *Melanorosaurus readi*	Yates, 2007a, b

Lessemsaurids	*Lessemsaurus* and *Antetonitrus*, their common ancestor, and all its descendants.	Apaldetti et al., 2018
Vulcanodontidae	All sauropods closer to *Vulcanodon* than to eusauropods (i.e. *Vulcanodon* and *Tazoudausaurus*).	Allain *et al*., 2004
Eusauropoda	The least inclusive clade containing *Shunosaurus* and *Saltasaurus*	Upchurch *et al*., 2004

1.3 Rationale for this research

Although much work has already been done on the Southern African sauropodomorphs, it is evident that uncertainties still remain around the taxonomy and phylogeny of *Plateosauravus* and the '*Euskelosaurus* problem'.

In an attempt to better understand sauropodomorph biology (including anatomy, taxonomy, phylogeny and growth dynamics) during the South African Mesozoic, this study will focus on a portion of the material previously referred to the genus "*Euskelosaurus*". Material assigned to this taxon is present in abundance in collections in South Africa, however this taxon is now considered a *nomen dubium* as its diagnosis is not based on any autapomorphies or unique combination of characters present in the holotype - BMNH R 1625 (Yates,2003; Yates & Kitching, 2003; Yates, 2007b; Galton et al, 2005). Van Heerden (1979) subjectively assigned material previously belonging to *Plateosauravus*, *Melanosaurus* and *Eucnemesaurus* to *Euskelosaurus*, thereby collapsing those taxa. Following this Kitching & Raath (1984) assigned most large bodied Lower Elliot Formation (LEF) sauropodomorph material to *Euskelosaurus*. Effectively *Euskelosaurus* became a 'waste-basket' taxon. Following the recent recognition that

Melanorosaurus, *Plateosauravus* and *Eucnemesaurus* were distinct taxa, material previously assigned to them was re-assigned as such (Galton & Van Heerden, 1998; Yates, 2003a; Yates, 2007b and Galton & Upchurch, 2004). However, in addition to the holotype and referred specimens, a host of material of undetermined taxonomic identity still assigned to *Euskelosaurus* remains in the collections at Iziko South African Museum (SAM), Evolutionary Studies Institute (ESI) and National Musuem Bloemfontein (NMB).

According to Yates (2003a) the material assigned to *Euskelosaurus* should be referred to *Plateosauravus cullingworthi* (Yates & Kitching, 2003; Yates, 2007b and Galton et al, 2005). Although Yates (2003) has suggested that *Plateosauravus* can be diagnosed by an “unusual combination of characters”, this diagnosis has not been formalised. Following Yate’s (2003a) assignation of *Plateosauravus* as the next available valid taxon for material assigned to *Euskelosaurus*, the problem remains that *Plateosauravus* suffers from the same ill-definition that has plagued *Euskelosaurus* - there are still issues surrounding the taxonomic identity and monospecificity of material assigned to *Plateosauravus* in the SAM and BPI collections. So, while it may be possible that some material identified as “*Euskelosaurus*” may belong to the same taxon as that represented by the material currently identified as *Plateosauravus* - it is first necessary to evaluate whether *Plateosauravus* is actually a valid taxon and whether all the material referred to it is monospecific. McPhee et al (2017), have suggested that *Plateosauravus* may be a chimera. The research here will seek to clarify the issue about the validity of *Plateosauravus*.

In order to start making sense of the confusion created around the wholesale “lumping” of material into “*Euskelosaurus*”(e.g. Van Heerden, 1979; Gauffre, 1993; Yates, 2003a), the analysis of the validity of the designated next available taxon (*Plateosauravus*) will provide much needed clarity on what this taxon is and isn’t – and will go a long way towards separating out material that has been conflated with both taxa for over 100 years.
A second major component of this study will examine the taxonomic identity of a significant amount of skeletal remains that were recovered from Maphutseng in Lesotho (NMQR 1705) and which was referred to as “*Euskelosaurus*” (Gauffre, 1993).

The so-called “Maphutseng material” comprises a monospecific, assemblage of sauropodomorph material of indeterminate taxonomic identity excavated from the “Red Beds” (i.e. corresponding to the Lower Elliot Formation) near Maphutseng, Mohale’s Hook District, in Lesotho, which ended up being split between the Museum National d’Histoire Naturelle, Paris (MNHN) and the National Museum, Bloemfontein (NMB) (Ellenberger & Ellenberger, 1956; Ellenberger, 1970; Charig et al., 1965; Gauffre, 1993). We will be focusing on the South African (NMB) portion of the material. Peyre de Fabregas et al. (2015) have used some of the MNHN material for comparison with *Meroktenos*, but a comprehensive analysis still awaits that portion of the material.

Without any evidence or detailed taxonomic assessment, Ellenberger & Ellenberger (1956) stated that the material (NMQR 1705) was probably either a large plateosaurid or melanorosaurid. Apart from this, Gauffre (1993) provided a brief description that was not formally published and referred the MNHN material to *Euskelosaurus* based on subjective, non-diagnostic characteristics. Until now no detailed taxonomic or

phylogenetic analysis has been undertaken on the Maphutseng dinosaur material. Therefore, this study will for the first time assess whether the Maphutseng fossils have any affinity with the material referred to *Plateosauravus* over the years or if they represent a different taxon.

In addition to the taxonomic assessment, the third major component of this research is an osteohistological analysis of the Maphutseng material to obtain information about its growth patterns. By comparing the results obtained for the Maphutseng dinosaur with other published data on basal sauropodomorphs and early sauropods valuable information will be obtained to assess the changes that occurred in the growth dynamics *en route* to Sauropoda. In conjunction with anatomical data this study will provide much greater clarity on how Sauropodomorpha changed as they approached Sauropoda.

The multiple approaches utilised in this PhD research will increase our understanding of the phylogenetic relationships amongst Gondwanan Sauropodomorpha, and the order and degree of acquisition of eventual sauropod synapomorphies (e.g. the trajectory of characteristics associated with the acquisition of quadrupedality as we approach Sauropoda, such as the increase in forelimb length relative to hindlimb length, rapid bone growth). Together, these approaches will be able to tell us more about the diversification of the southern Africa Sauropodmorpha at about the time of the initial radiation of sauropods. Thus, this study will increase our understanding of Gondwanan sauropodomorph diversity and inter-relationships during the Late Triassic- Early Jurassic.

1.4 Aims and Objectives of Study

Aims

The aim of this thesis is to examine the taxonomic identity, morphology and phylogenetic position of undescribed material that was assigned to the 'waste-basket" taxon *Euskelosaurus*, as well as *Plateosauravus*, which Yates (2003) identified as the next available taxon following the collapse of *Euskelosaurus*. This will provide a better understanding of taxonomic diversity and morphology, *en route* to Sauropoda, in southern Africa during the Late Triassic – Early Jurassic.
A comprehensive review of material assigned to *Plateosauravus* is undertaken in order to determine the taxonomic identity and phylogenetic placement of this material.

Following this, a thorough investigation into the taxonomic identity and phylogenetic position of the Maphutseng material will be conducted. Furthermore, osteohistological studies will be undertaken to assess the ontogenetic age and growth dynamics of the taxa represented by this material - in order to ascertain changes in the growth patterns and probably physiological adaptations that eventually permitted the attainment of the large body sizes seen in eusauropods.

Research Objectives

1. Provide a formal diagnosis of *Plateosauravus*, followed by anatomical description, revision of the taxonomic identity and phylogenetic analysis of material currently ascribed to *Plateosauravus* from SAM.

Hypothesis 1 – *Plateosauravus* is a distinct/valid taxon.

Hypothesis 2 – *Plateosauravus* is a non-Massopodan taxon that lies outside Sauropodiformes.

2. Provide an anatomical description, taxonomic assessment and phylogenetic analysis of the Maphutseng assemblage including material from NMQR.

Hypothesis 3 - The Maphutseng material is monospecific and represents a basal sauropod dinosaur.
Hypothesis 4 – Part of the current material assigned to *Euskelosaurus* corresponds to *Antetonitrus* and/or *Plateosauravus.*

3. a) Analyse the bone histology of the long bones and ribs of the Maphutseng dinosaur in order to determine the ontogenetic stage and histological variation in the skeleton.

b) Compare the growth dynamics of the Maphutseng dinosaur and the published results of other Sauropodiformes in order to determine if the histology of taxa show increasing approximation of the sauropod condition concomitant with phylogenetic closeness to Sauropoda.

Hypothesis 5 – As seen in Sauropod dinosaurs, the bone histology of the Maphutseng material will exhibit highly vascularised fibrolammelar bone (FLB), with lines of arrested growth (LAGs) only occurring late in ontogeny (in keeping with the general trend seen in sauropods). Therefore, early bone histology as determined from smaller femora and tibia will show the same azonal bone growth pattern seen in larger specimens with the

exception of LAGs occurring in the outer circumferential layer (OCL) of the latter.

Hypothesis 6 – Similar to the condition found in basal sauropodmorphs such as *Massospondylus* and *Plateosauravus*, we expect a high degree of developmental plasticity in the Maphutseng sample. Due to this, we do not expct a correlation between age and body size in this sample.

Hypothesis 7 - As continuous growth is a feature of taxa more closely related to Sauropoda than Massopoda, we expect NMQR 1705 to share this feature based on its phylogenetic proximity to Sauropoda.

Chapter 2

Assessment of the taxonomic validity of *Plateosauravus cullingworthi* (Haughton, 1924)

2.1 Introduction

Amongst the host of Sauropodomorpha found in southern Africa, *Plateosauravus* is currently considered a taxonomically problematic genus. Since it was assigned to *Euskelosaurus browni*, which about two decades ago was conclusively shown to be a *nomen dubium* (Yates & Kitching, 2003; Yates, 2003a; Yates, 2004), it is essential to evaluate both the type and referred material of *Plateosauravus* to assess whether or not it is a valid taxon and to aid in our identification of the mass of material still labelled *Euskelosaurus spp*. Therefore, the current research focuses on the taxonomic validity of the currently accepted and utilised *Plateosauravus* hypodigm (see Yates, 2003a, b).

In addition, this study investigates the issues surrounding the referral of former *Euskelosaurus africanus* (Haughton, 1924; Van Heerden, 1979; Yates, 2003a) material to *Plateosauravus,* and the implications this has for uncovering the taxonomic identity of material previously assigned to and still accessioned as *Euskelosaurus* sp. in South African museum collections.

2.2 Historical Context

Plateosauravus cullingworthi was originally erected by Haughton (1924) based on material collected from Kromme Spruit, near Herschel in the Eastern Cape as *Plateosaurus cullingworthi*. Von Huene (1932) identified it as being distinct

from *Plateosaurus* and renamed it *Plateosauravus*. The initial (syn)type material was composed of elements from multiple individuals found in situ at the top of the koppie ,referred to in this study as Kromme Spruit B, (SAM PK 3345 – 3356) *and* ex-situ on the side of the same koppie (SAM PK 3602-3603), refered to as Kromme Spruit A. Haughton (1924) also referred material found 30km away from Lady Grey (SAM PK 2780) to *Plateosauravus*, however only a fragmented ilium was described.

Huxley (1886) initially erected *Euskelosaurus browni* (BMNH R1625) based on the proximal portion of a right femur and fragmented postcranial remains; including - part of an astragalus and the incomplete proximal ends of a fibula and tibia (Haughton and Brink, 1954; Van Heerden, 1979), fragmentary vertebrae and part of a pubis (Haughton and Brink, 1954). Haughton (1924) also erected *Euskelosaurus africanus* based on the additional Kromme Spruit material (excluding SAM PK 3602-3) found exposed on the side of the koppie, two sacral vertebrae and a conjoined ischium forming the holotype (SAM PK 3608).

Van Heerden (1979) synonymised material previously belonging to *Plateosauravus* with *E. browni*. Following this Raath & Kitching (1984) assigned most large bodied Lower Elliot Formation (LEF) sauropodomorph material to *Euskelosaurus* sp. Thus, effectively the genus *Euskelosaurus* became a ‘waste-basket’ taxon for any robust sauropodomorph material from the LEF.

The consequences of Van Heerden's (1979) synonymisation of discrete taxa as *Euskelosaurus spp*.

All the above material (SAM PK 2780,3341-3356,3602-3603,3607-3609), were re-designated as paratypes of *E. browni* by Van Heerden (1979). However, Van Heerden (1979) did not describe SAM PK 2780 – and no description exists in the literature apart from a figure and description of a right ilium in Haughton (1924, p 412).

E. browni served as the type species for *Euskelosaurus* (Haughton, 1924; Van Heerden, 1979). After the recognition of *E. browni* as a *nomen dubium* (Yates, 2003a;2004), the next available type species for *Euskelosaurus* would have been *Euskelosaurus capensis*, followed by *E. africanus*, however neither of these taxa are viable alternatives as they are also of dubious taxonomic validity due to paucity of material (i.e. *E. capensis* is based on an undiagnostic fragment of a tibia) and the lack of diagnostic features to further differentiate them from Sauropodomorpha in general (*E.africanus* does not appear to have any diagnostic features).

According to Yates (2003a; 2004; 2006) at least some of the material assigned to "*Euskelosaurus*" by Van Heerden (1979) - SAM PK 3341-3356,3602-3,3607-3609- should be referred to *P. cullingworthi* as "the next available valid" taxon after the collapse of the "*Euskelosaurus*" hypodigm (Yates & Kitching, 2003; Yates, 2003a; Yates, 2004; Yates, 2007b and Galton et al, 2005). It appears that Yates (2003a) also added the holotype and referred material for *E. africanus* (SAM PK 3607-3609) to that of the syntype series material for *Plateosauravus* during the deconstruction of *Euskelosaurus* and reconstitution of *P. cullingworthi*.

Since the resurrection of *Plateosauravus* (Yates, 2003a), it is generally accepted as a valid taxon and has been uncritically included in phylogenetic analyses since Yates (2003b) onwards. Yet, *Plateosauravus* lacks specified autapomorphies, it is not formally diagnosed, the monospecificity of its syntype material is not established and a comprehensive assessment of all the material collected at Kromme Spruit and Lady Grey associated with this taxon has not yet been done (Yates, 2003a ; McPhee et al., 2014).

It is imperative that these questions surrounding the taxonomic validity and phylogeny of *Plateosauravus* be addressed before undiagnosed material assigned to *Euskelosaurus* be definitively assigned to it. It is possible that some of this material informally referred to *Euskelosaurus* over the years may be referable to *Antetonitrus* (as in the case of BPI/1/4952a & NMQR 1705), another EF sauropodomorph or could even be representative of new as yet undescribed taxa.

This study seeks to provide the first step in clarifying the conundrum around material assigned to *Euskelosaurus* sp. by providing an accurate anatomical description and formal diagnosis for *Plateosauravus*. The aim of this investigation is to determine whether there are any autapomorphies or unique combination of characters in the type material of *Plateosauravus* that justifies the validity of this taxon.

The invalidity of *Euskelosaurus browni* (Huxley, 1866)

Both Van Heerden (1979) and Yates (2003a) indicated that the proximal femur is the only element complete enough to be informative and that the other fragmentary remains provide no data. This proximal femur differed from that of the *Melanorosaurus readi* in having a sinuous femoral shaft, lesser

trochanter positioned away from the lateral margin of the femur (in anterior view) and a proximally placed fourth trochanter (Galton, 1985; Yates, 2003a). However, these features are plesiomorphic for Sauropodomorpha and also present among other taxa in the materials upon which two basal sauropodomorph genera from the LEF were erected *Plateosauravus* and *Eucnemesaurus* spp. (Yates, 2003a; McPhee et al., 2015; 2017). The lack of any autapomorphies or unique combination of characters in this material make diagnosis of *Euskelosaurus* impossible, rendering *E. browni* a *nomen dubium* and invalidating the type species for *Euskelosaurus* as a valid genus (Yates,2003a; Yates, 2004; Yates & Kitching, 2003; Yates, 2007b; Galton et al, 2005).

Following the re-recognition that *Plateosauravus* was a distinct taxon, material previously comprising the syntpe series was re-assigned to it by Yates (2003a), in addition to the original syntpe series (SAM PK 3345-3356, 3602-3603), Yates (2003a) also referred SAM PK 3607-9 to it. This latter material was found with and included the type specimen (SAM PK 3608) for *E. africanus.*

In addition to the holotypes/syntypes and referred specimens pertaining to *Plateosauravus*, a host of material of undetermined taxonomic identity still accessioned as "*Euskelosaurus*" remains in the collections at SAM, ESI and NMQR (pers. obs.). In order to understand what material can be referred to *Plateosauravus* we must carefully analyse its type material.

Materials & Methods

The current *Plateosauravus* syntypes (SAM PK 3341–3356, 3602–3603) and previously referred material (SAM PK 3607–

3609, 2780) are housed at Iziko South African Museum (SAM), Cape Town.

The taxonomic identity of the *Plateosauravus* syntypes and referred specimens attributed to it will be examined by comparing them to the other EF sauropodomorphs in order to gauge if there are any autapomorphic or unique combinations of characters present.

Anatomical terminology employed herein makes use of traditional or "Romerian" directional terms over veterinarian alternatives (e.g. anterior and posterior rather than cranial and caudal). Phylogenetic nomenclature for the clades mentioned in this chapter can be found in Table 1. The anatomical descriptions are based on first-hand observation of SAM 3341–3356, 3602–3603, 3607–3609 and SAM PK 2780. Comparisons made with other members of Sauropodomorpha are based both on first-hand observation of certain taxa and the published literature (see Table.2).

Nomenclatural Acts: This study follows nomenclatural terminology and definitions regarding types as set out in the Fourth Edition of the International Code of Zoological Nomenclature (ICZN).

Table 2. Sources of comparative taxa

Taxon	**Source**
Anchisaurus polyzelus	Galton & Upchurch, 2004
Antetonitrus ingenipes	BPI/1/4952a, 4952b, 4952c; BPI/1/5901; NMQR 1545
Apatosaurus louisae	Gilmore, 1936; Wilhite, 2003
Blikanasaurus cromptoni	SAM-PK K403
Chinshakianosaurus chunghoensis	Upchurch et al., 2007
Chromogisaurus novasi	Ezcurra, 2010

Coloradisaurus brevis	PVL 5904
Glacialasaurus hammeri	Smith & Pol, 2007
Guibasaurus candelariensis	Bonaparte et al, 1999; Bonaparte et al, 2007
Ingentia prima	Apaldetti et al, 2018
Jaklapallisaurus asymmetrica	Novas et al, 2011a
Kotasaurus yamanpalliensis	Yadagiri, 2001
Ledumahadi mafube	McPhee et al, 2018
Leonerasaurus taquetrensis	MPEF-PV 1663
Lessemsaurus sauropoides	PVL 4822
Lufengosaurus hueni	Young, 1941
Macrocollum itaquii	Müller et al, 2018
Massospondylus carinatus	Cooper, 1981
Melanorosaurus readi	SAM 3449, 3450; NMQR 1551; NMQR 3314
Mussaurus patagonicus	MLP 61-III-20-22, 61-III-20-23, 68-II-27-1
Nambalia roychowdhurri	Novas et al, 2011b
Pantydraco caducus	Galton & Kermack, 2010
Plateosaurus engelhaardti	Von Huene, 1936; Malleson, 2010a, 2010b
Plateosaurus longiceps	Galton & Upchurch, 2004
Pulanesaura eocollum	McPhee et al, 2015
Riojasaurus incertus	PVL 3526, 3663, 3808
Ruehleia bedheimensis	Galton, 2001
Saturnalia tupiniqum	Langer, 2003; Langer et al, 2007
Unaysaurus tolentinoi	McPhee et al, 2019
Vulcanodon karibaensis	Cooper, 1984

BMNH, British Museum of Natural History; **ESI,** Evolutionary Studies Institute (formerly Bernard Price Institute), Johannesburg, South Africa; **NMQR**, National Museum Bloemfontein, South Africa; **PVL**, Instituto Miguel Lillo, Tucumán; **MLP**, Museo de La Plata, La Plata, Argentina; **MPEF**, Museo Palaeontológico Egidio Feruglio, Trelew, Argentina; **SAM**, Iziko South African Museum, Cape Town, South Africa.

Cladistic Analysis

Plateosauravus was re-scored, incorporating solely data from the lectotype, in a modified version of the Müller (2018) data

matrix, which is a modified version of the data set originally published by Yates (2007). It includes additional characters (244, 277 and 402) and a taxon (*Ledumahadi*) drawn from McPhee et al (2018) that are not present in the Müller (2018) matrix. Forty-four characters were treated as ordered following Müller (2018). The dataset includes some sauropodomorph outgroups, reaching a total of 76 taxa and 402 characters (see Appendices 1-3 for character list, character-taxon matrix and for details of phylogenetic analysis). The data matrix was created using Mesquite 3.51 (Maddison & Maddison, 2018) and analysed using TNT Version 1.1 (Goloboff et al., 2008).

Systematic Palaeontology

Saurischia Seeley 1888

Sauropodomorpha Von Huene 1932

Massopoda Yates 2007

Genus *Plateosauravus* Von Huene 1932

Type species. *P. cullingworthi* (Haughton, 1924)

Diagnosis. As for the lectotype and only known species.

Lectotype. SAM PK 3341-3344,3346-3349,3356 This material was originally described and figured by Haughton (1924) as being from two individuals found in situ as the name-bearing type, forming part of the syntype series of *P. cullingworthi*. SAM PK 3602-3 have been removed from the syntype series as there is no evidence that these femora are associated with the former material. A complete and two similar partial right ulnae (SAM PK 3345, 3350 & 3351) are of dubious association with the lectotype material. As noted by McPhee et al (2014) the complete ulna (SAM PK 3351) bears a striking resemblance to BPI/1/4952a. It also possesses the standard anterior process common to Saurischia, as well as a lateral process which

delimits a radial fossa of similar depth to *Antetonitrus*, rendering the ulna triradiate in proximal view. This is striking, as this is considered a derived sauropod trait. In proximal outline, it looks similar to *Antetonitrus*. Based on this we remove these ulnae from the lectotypic material, as we cannot be certain that fits in with the rest of the material.

Referred material. A duplicate left humerus (SAM PK 3350) of similar size and morphology found associated with the lectotype material.

Locality and horizon

SAM PK 3341-3344,3346-3350,3356 were found in an in-situ deposit of two individuals at the top of a hill formed from the base of the “Red Beds” near Kromme Spruit (30°33’4.25” S; 27°25’50.55” E), ~ 6km ESE of Sterkspruit, Eastern Cape, South Africa (Haughton, 1924; McPhee et al., 2017). This site and the material from it have been identified as falling within the bounds of the Upper Triassic (Norian – Rhaetian), Lower Elliot Formation, however exactly where within the member it fits is unknown (McPhee et al 2017).

Comments on the association of specimens

At the top of the hill (this site will be referred to as Kromme Spruit B) Haughton (1924) described a “pocket” of in situ bones belonging to a smaller and larger individual. This material formed the syntype series (Haughton, 1924; Haughton & Brink, 1954) and the bulk of Haughton’s (1924) description of *P. cullingworthi* (SAM PK 3341-3356), as mentioned above Haughton (1924) assumed that two femora (SAM PK 3602 and 3603), reconstructed from fragments found weathered out of the slope along with SAM PK 3607-3609, also pertained to these two individuals and incorporated them into the syntype -

despite the lack of evidence to suggest association or monospecificity. SAM PK 3602–3603 and 3607–3609 were found ex-situ, weathered out of the slopes of this steep hill.

Later, Van Heerden (1979) stated that all the Kromme Spruit A (material from the side of the same hill) & B material belonged to one larger and one smaller individual. This is unconvincing based on Haughton's (1924) initial description of the site, the actual material and the fact that two left humeri (SAM PK 3342 & 3350) from Kromme Spruit A form part of the *in situ* material indicating a minimum number (MNI) of at least two individuals for the in situ finds at the top of the hill. In conjunction with Haughton's (1924) description of a more robust morph ("*Euskelosaurus africanus*") apparent amongst material found on the side of the hill, it seems likely that at least three individuals are present in SAM PK 3602-3,3341-3356,3607-3609.

SAM PK 2780 was found ~30km away from the Kromme Spruit site, also from strata within the "Red Beds", in the Kok vicinity, just above the village of Lady Grey (30°42'0"S; 27°13'0"E), Eastern Cape, South Africa (Haughton, 1924; ESI database). This site can also be identified as falling within the Upper Triassic (Norian – Rhaetian), LEF based on Haughton's (1924) description of this material coming from the "Red Beds" of the member, which are well established as conforming to the LEF. This associated material will be described separetly.

Haughton (1924) referred this material to *P. cullingworthi* (SAM PK 3341-3356,3602-3603) based on similarities between a left tibia, right humerus, distal ends of two ischia, distal end of a right femur, proximal end of a left femur, and part of a left scapula. However, most diagnostic features of this material are not preserved, making the referall superficial at best. A right

ilium from SAM PK 2780 was the only element figured and described by Haughton (1924). After 1924, SAM PK 2780 appears to have been neglected in the literature and has not been included in the *Plateosauravus* hypodigm as paratypic material. This material will be described separately from the lectotype and refered material and will not contribute to the character data for *Plateosauravus*.

Revised Diagnosis

Yates (2003a) indicated that while possessing no autapomorphies, *Plateosauravus* was differentiated from other LEF sauropodomorphs by a unique combination of characters. *P. cullingworthi* can now only be identified by the following unique combination of characters: strongly sinuous deltopectoral crest on humerus, anterolateral sulcus on deltopectoral crest (shared with *Antetonitrus*); presence of a bevelled embayment above the descending posterolateral process of the distal tibia.

Description

Comment

SAM PK 3352-55 appear to be missing or misplaced in the collection at SAM. There is no entry for these numbers in the collections catalogue and the bones matching these number could not be located in the collection. Furthermore, this material has never been described or figured in the literature.

Dorsal centrum (SAM PK 3356)

An amphicoelus dorsal centrum is preserved and its sides are constricted with lateral depressions. Evidence of the parapophysis is located in a lateral depression on left side of this element. A ventral keel is present on this centrum.

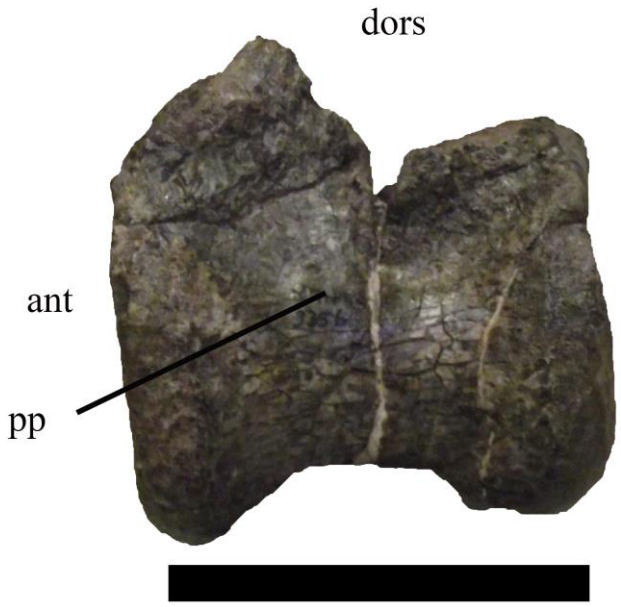

Figure 1. Sam PK 3356, Dorsal centrum in left lateral view. dors, dorsal; ant, anterior; pp, parapophysis. **Scale = 100mm.**

Scapula (SAM PK 3348)

The ventral portion of a left scapula is preserved. The scapula is narrow lateromedially but starts to expand ventrally. The glenoid region is not preserved; however, the acromion process is. It looks very similar to *Mussaurus* and *Macrocollum itaquii* in terms of the angle between it and the long axis of the scapula, but the angle for *Mussaurus* is 75 degrees, while *Macrocullum* in whilst in SAM PK 3348 it is between 45- 60 degrees maximum. As in *Mussauraus* and *Macrocollum*, the lateral surface of the preserved portion of the scapula is convex, whilst the medial surface is flat. The acromiom process is slightly expanded mediolaterally.

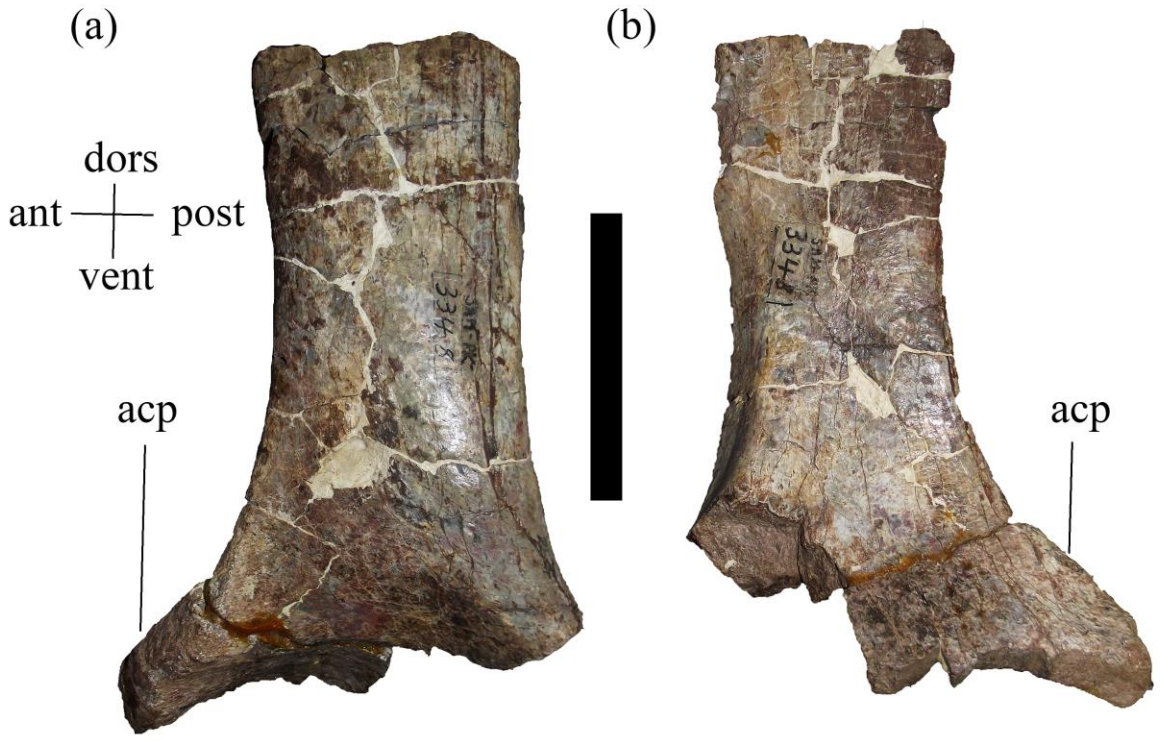

Figure 2. SAM PK 3348, Ventral portion of left scapula. A) lateral view; B) medial view. Scale = 100mm. acp, acromiom process; ant, anterior; dors, dorsal; lat, lateral; vent, ventral.

Humeri (SAM PK 3342, 3350)

Two left humeri are preserved, SAM PK 3342 (450mm in length) and 3350 (405mm). SAM PK 3342 will form the bulk of the description as both humeri are similar in morphology and it appears that humerus SAM PK 3350 has been flattened anteriorly. The humeral heads of both the humeri are both sigmoidal in proximal view, in contrast to the relatively flat condition exhibited by *Macrocollum*.

The deltopectoral crest (DPC) is subrectangular in shape, however the antero-lateral margin is extremely sinuous, deflects medially and lacks rugosity on the lateral margin. A sulcus, as seen in *Antetonitrus*, is also present on the

anterolateral margin of the DPC. The length of the DPC is between 30-50% of the overall length of the bone.

There is a well-defined cuboid fossa on the distal flexor surface of the humerus In SAM PK 3342 this fossa is somewhat more triangular compared to the rounder fossa present in SAM PK 3350. The transverse width of the distal humerus is greater than 33% of the length of the humerus. The distal end is transversely expanded relative the shaft in similar proportion to the humeral head, differing from the moderate transverse expansion seen in *Macrocollum*.

The shape of the entepicondyle differs between SAM PK 3342 and SAM PK 3350, with the former being a flat disto-medially facing surface bounded by a sharp proximal margin and the latter bone having a more rounded shape.

Radius (SAM PK 3347).
A left radius measuring 107mm in length is preserved. The radius is a gracile, rod-like bone, the shaft is subcircular in cross-section. Compared to Unaysaurus the proximal and distal expansions are less pronounced and the shaft is less curved. The proximal end is much more expanded anteroposteriorly than the distal end, but is mediolaterally compressed, rendering an ovoid shape in proximal view. There is a depression on the proximal articular surface that starts on the anterior medial side and extends posterolaterally along the surface terminating midway along the anteroposterior axis of the proximal surface, the posterior half of the articular surface then begins to rise in a proximal direction. On the posterior surface of the proximal part of the radius a ridge begins just

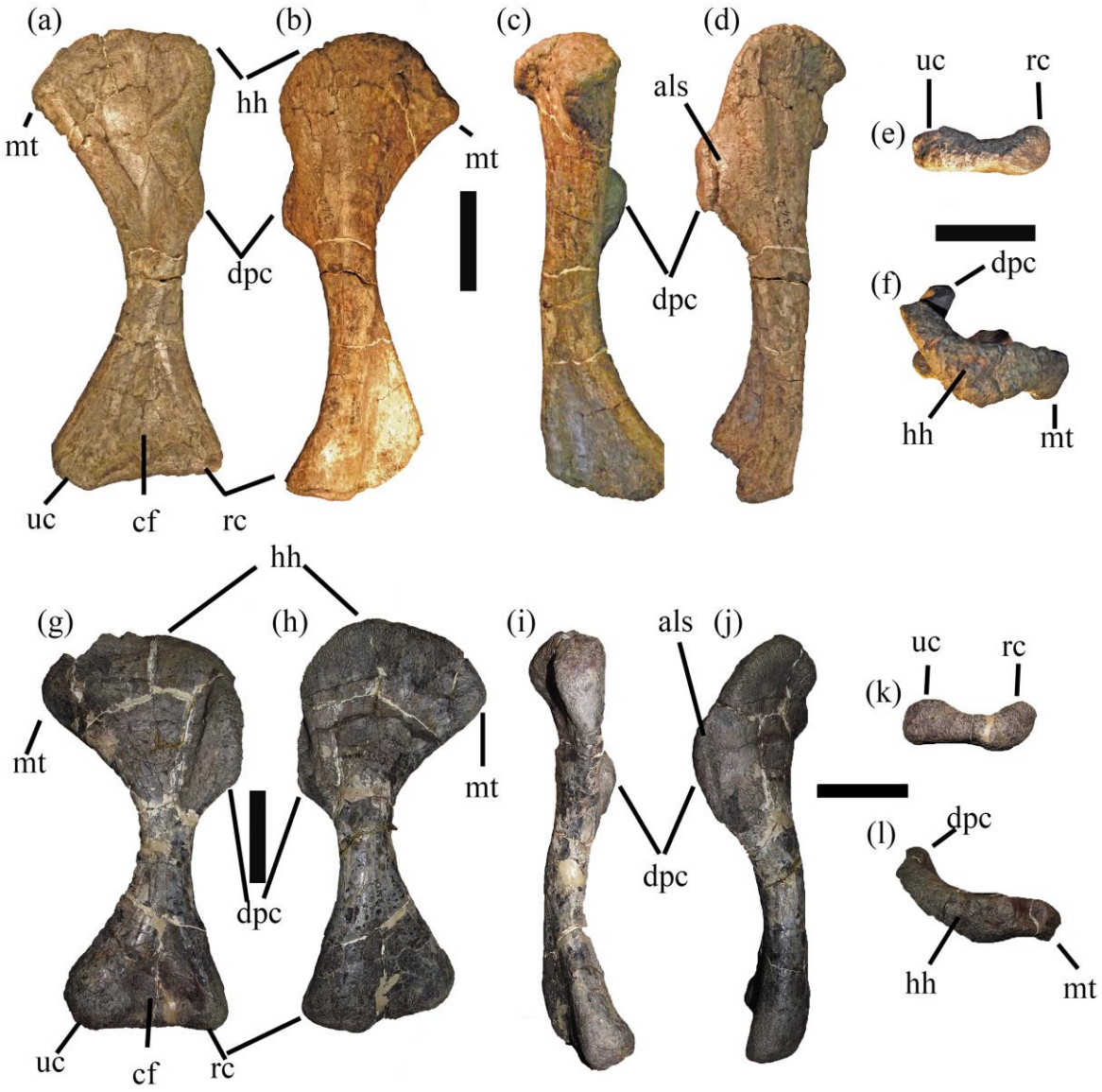

Figure 3. Left humeri. A-F, SAM PK 3342; G-L. SAM PK 3350. A, G) lateral; B, H) medial; C, I) posterior; D, J) anterior; E, K) distal; F, L) Proximal view. als, anterolateral sulcus; cf, cuboid fossa; dpc, deltopectoral crest; hh, humeral head; mt, medial tuberosity; rc, radial condyle; uc, ulnar condyle. **Scale = 100mm.**

distal to the proximal articular surface and extends downwards in a medio-distal direction for 44mm.

On the anterior half of the lateral surface there is a groove distal to the proximal articular surface that runs distally for 57mm. On the medial side, there is a similar groove, but it starts in the middle of the medial surface and extends antero-

distally down the shaft for 104mm. It is not certain whether these are real or artefacts of preservation. There is no evidence of a biceps tubercle/scar.

On the lateral surface of the distal end there is a groove 57mm in length, that terminates just proximal to the distal end. This appears to be a result of damage to the bone as there is evidence of breaks around the region. The medial surface of the distal end is smooth and flat. On the posterior surface, there is a radial ulnar process on the medial half of the posterior surface (46mm), just lateral to it is a faint groove. Lateral to the faint groove is a much more pronounced groove on the posterolateral edge that runs in a distolateral to proximo-medial direction for 50mm. It is unclear if this a result of distortion.

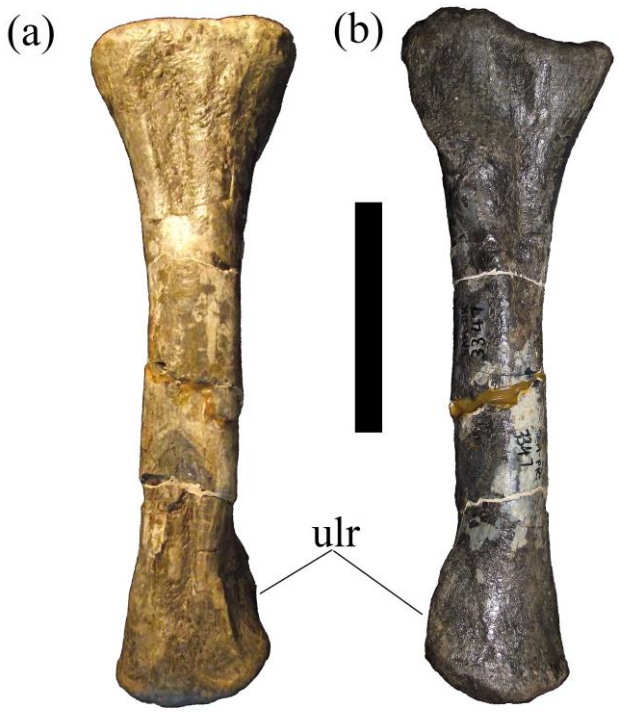

Figure 4. SAM PK 3347 left radius in A) lateral, B) medial view. ulr, ulnar ligament of radius attachment**. Scale = 100mm.**

In distal view, the radius is almost square, the lateral edge is the longest at 60mm and is straight. The medial edge is rounder, but a bit shorter at 48mm. The lateral half of the distal articular surface projects further both anteriorly and posteriorly. The distal articular surface is rounded and slopes from the anterior to posterior ends.

Ischium (SAM PK 3341)

This as yet undescribed material consists of a partial right ischium with only the proximal half preserved, and the ventral portion of obturator plate is absent. The shaft is triangular in cross-section, with the dorsal surface of the shaft beginning to exhibit transverse expansion. A dorsolateral sulcus as present in most sauropodomorphs is visible. The iliac articulatory surface is robust, and lacks the lateral protuberance seen in NMQR1705 on the dorso-lateral corner. The dorsal portion of the obturator region that is preserved is mediolaterally expanded.

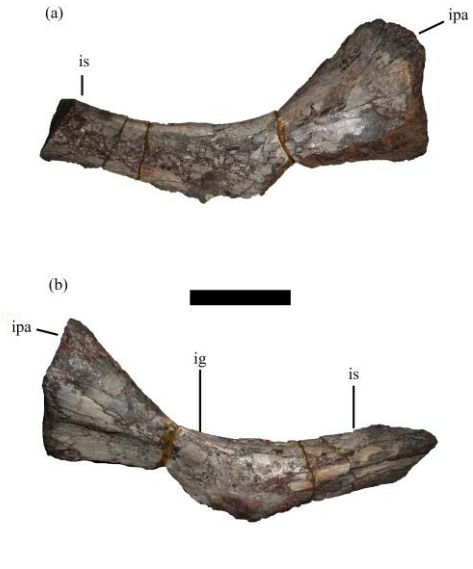

Figure 5. SAM PK 3341. Partial proximal right ischium. A) Medial, B) Lateral view. ig, ischial groove; is, ischial shaft; ipa, ischiadic peduncle articulation area. **Scale = 100mm.**

Tibia (SAM PK 3341)

This specimen is a right complete tibia. A second tibia mentioned by Van Heerden (1979) SAM PK 3349 could not be located in the SAM collection. Proximally below the cnemial crest, the shaft is elliptical in cross-section - with the long axis conforming to that of the proximal surface (i.e. in an anteroposterior direction). However, midway down the shaft the anterior surface begins to expand transversely, resulting in a more triangular cross-section of the shaft with the apex on the posterior side. The angle between the long axis of the distal end (mediolateral) and the proximal end (anteroposterior) is 68 degrees. Overall the tibia is relatively slender compared to that of *Antetonitrus*, but in overall shape it is not too dissimilar.

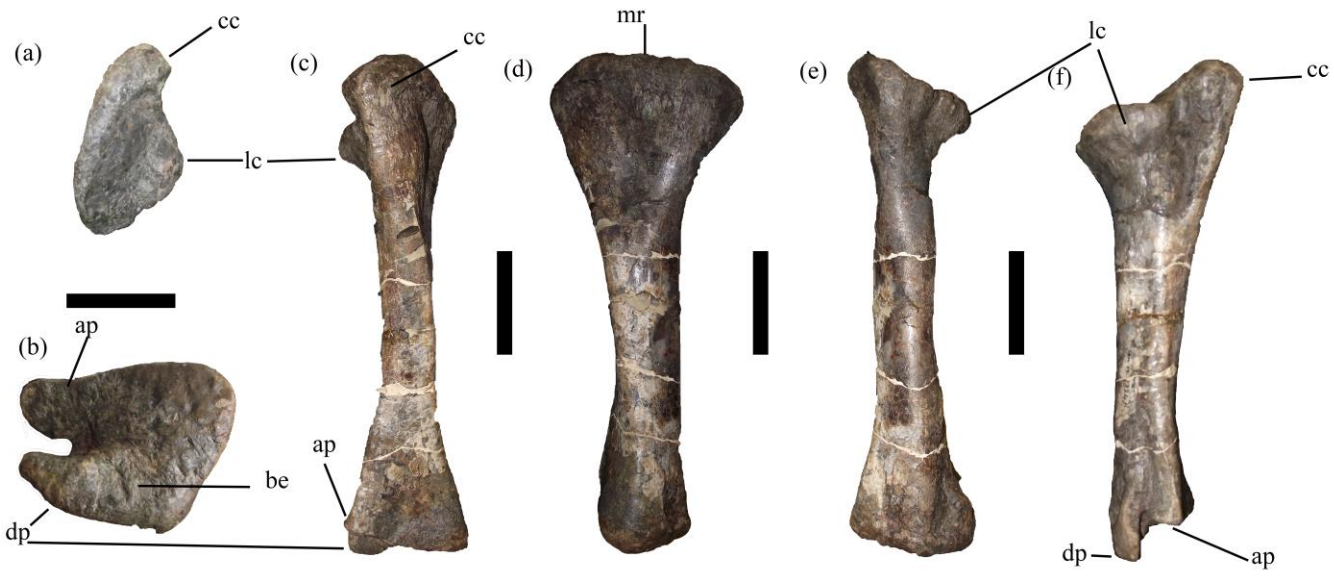

Figure 6. SAM PK 3341. Right tibia A) proximal, B) Distal, C) anterior, D) medial, E) posterior, F) lateral view. ap, ascending process (ascending articular facet); be, bevelled embayment above descending process*; cc, cnemial crest; dp, descending process; lc, lateral condyle; mr, medial ridge. Scale = 100mm.

Second Metatarsal (SAM PK 3343)

In proximal view the articular surface of the second metatarsal is hourglass shaped, with both the dorsal and plantar sides

being straight in proximal view. Both lateral and medial sides are concave, although the medial side is more concave due to the expansion of the ventromedial corner, which McPhee et al. (2014) incorrectly described as a ‘ventrolateral wing’. This expansion of the VMF (ventromedial flange) is seen prominently in *Antetonitrus*. The medial concavity is more pronounced than in *Unaysaurus* and in general more similar to *Antetonitrus* in robusticity and morphology.

The dorsoventral expansion of the proximal surface is larger than the transverse width of the proximal end, more so than in *Antetonitrus*, resulting in a slimmer outline. Despite this, the element is more robust than the elongate, slender condition seen in Unaysaurids and most other non-Massopodan taxa. Furthermore, compared to BPI/1/4952 it is more symmetrical due to almost equal lateral and medial projection of the dorsomedial (plantar-medial) and dorsolateral corners, rendering it more hourglass shaped regardless of the expansion of the ventromedial corner.

The proximal surface is twisted and slopes ventrolaterally with respect to the shaft, resulting in the dorsal surface being more medially located than the plantar surface. On all sides of the proximal end there are concavities distal to the proximal articular surface, the medial surface exhibits the most pronounced one. However, it is also quite marked on the palmar surface where the concavity/groove runs for almost 50% of the length of the element, which results in the medial and lateral edges of the palmar surface forming ridges on either side of this depression with the lateral ridge extending distally for 64mm, whilst the lateral extends to 103mm. On the dorsal surface (plantar surface) there is a raised bump midway down the shaft on the lateral side.

The distal end is slightly turned in medially. The lateral condyle is much more pronounced than the medial condyle transversely and projects slightly more distally than the medial condyle, which would have caused the second digit to be in-turned medially.

The medial condyle is actually dorsoventrally wider due to the palmar projection of the medial condyle. Both condyles exhibit collateral ligament fossae (ligament pits) of similar pronouncement. On the palmar surface of the distal end there is a groove in between the two condyles that continues proximally for 40mm.

Third Metatarsal (SAM PK 3344)
The proximal surface is slightly convex and triangular in outline, with a broad, curved ventrolateral surface similar to *Unaysaurus*. The dorsomedial surface is straight and meets the shorter, straight dorsolateral surface at a right angle and an acute ventromedial apex. This is in contrast to *Unaysaurus* where the ventral-most border is the shortest side and the lateral and medial sides are longer and form an acute apex.

As in *Antetonitrus*, proximally, on the anterolateral surface of the shaft, there is a faintly striated shallow concavity, which potentially represents the insertion area of the M. tibialis anterior (Carrano & Hutchinson, 2002; Smith & Pol, 2007). The shaft is straight and subtriangular in cross-section, tapering gently towards the distal condyles where it becomes elliptical with the long axis running transversely. As in most non-Eusauropodan sauropodomorphs, the distal condyles are deflected slightly medially (e.g. *Massospondylus*; *Aardonyx*; *Lessemsaurus*; *Vulcanodon*). On the distal end of the dorsal surface there is another shallow, striated depression, which is interpreted as the attachment site for the extensor ligament.

The distal condyles are roughly symmetrically developed but the medial condyle is slightly deeper dorsoventrally due to a ventrally projecting “flange” and the lateral condyle is slightly

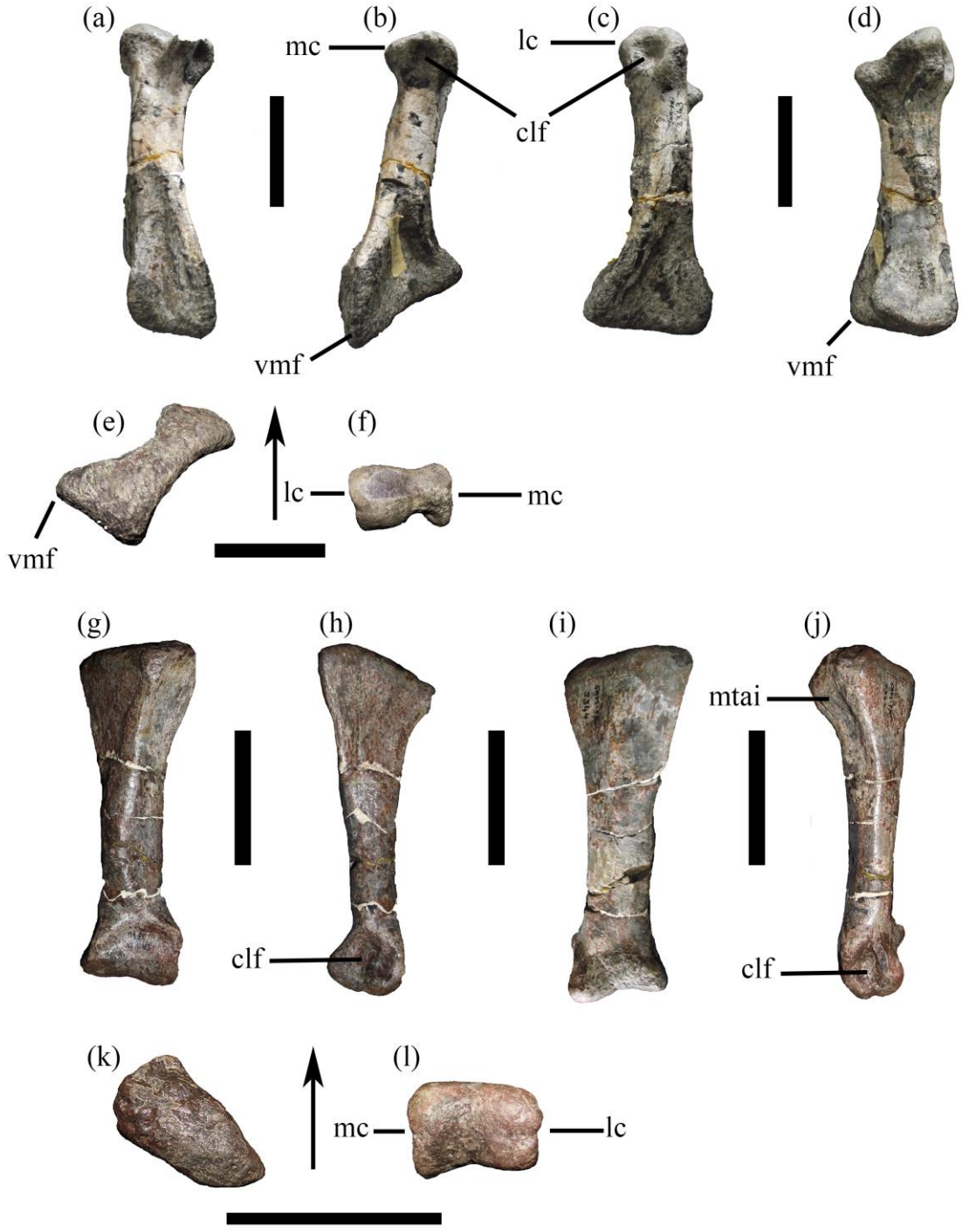

Figure 7. A -F) SAM PK 3343 right MtII; G-L) SAM PK 3344 left MtIII. A, I) ventral (plantar), B, H) medial, C, J) lateral, D, G) dorsal, E, K) proximal, F, L) distal views. Arrow indicates dorsal direction. clf, collateral ligament fossae; lc, lateral condyle; mc, medial condyle; mtai,

insertion area of the M. tibialis anterior; vmf, ventromedial flange. **Scale = 100mm.**

larger than the medial one. Since it projects slightly further distally than the medial condyle it is apparent that the third digit was medially inclined, although not to the same extent as in the second metatarsal. On both the lateral and medial surfaces of the distal condyles obvious collateral ligament fossae can be observed.

The most apparent difference between this taxon and *Antetonitrus* is that the anteromedial surface of the proximal metatarsal three is angled much more laterally, running at about 120 degrees to the transverse axis of the distal end, as opposed to 90 degrees in *Antetonitrus*.

Previously associated material

The following material has historically been associated with the *Plateosauravus* lectotype material. However, there is no evidence of association with the former and thus we treat these two assemblages separately.

Euskelosaurus africanus (Haughton, 1924)

Ilium (SAM PK 3609)
A complete left ilium is preserved.

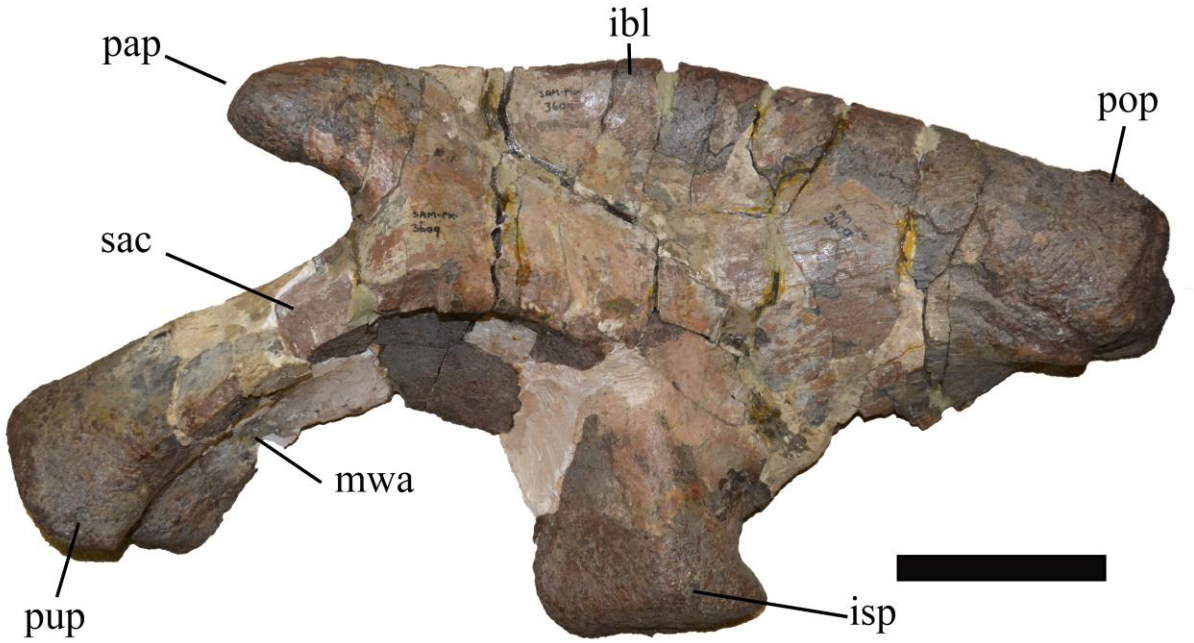

Figure 8. SAM PK 3609. Left ilium in medial view. ibl, iliac blade; isp, ischial peduncle; mwa, medial wall; pap, preacetabular process; pop, postacetabular process; pup, pubic peduncle; sac, supracetabular crest. **Scale = 10mm.**

The general morphology is congruent with that of non-eusauropod sauropodomorphs. The iliac blade is dorsoventrally low above the acetabulum and anteroposteriorly long in relation. The dorsal margin of the ilium in lateral view is slightly convex. In dorsal view it curves slightly laterally anteriorly and posteriorly, thus being weakly convex above the acetabulum region and sub-parallel to the sagittal axis, a similar morphology as in *Lessemsaurus* and NMQR 1705.

The anterior extent of the preacetabular process does not extend further forward than the anterior end of the pubic process, similar to that seen in *Macrocollum*, but contrasting with the anteriorly projected preacetabular process of *Anchisaurus* and *Leonerasaurus*. The preacetabular process is short and triangular with its apex directed anteriorly and dorsoventrally low relative to the iliac blade above the acetabulum as in *Lessemsaurus*, *Leonerasaurus,* and all non-

eusauropod sauropodomorphs (Pol & Powell, 2007). The preacetabular process is not anteriorly expanded as in *Anchisaurus polyzelus*, *Melanorosaurus readi* (NMQR 3314) and eusauropods (Pol et al., 2011). It forms an angle of approximately 70 degrees with the pubic process, similar to that of NMQR 1705. The dorsal margin of the preacetabular process is continuous with the dorsal margin of the iliac blade (Pol & Powell, 2007), like in the left ilium of NMQR 1545 and 1705 it would appear that this taxon did not possess a stepped margin as in some non-eusauropod sauropodomorphs (Pol & Powell, 2007; Galton et al, 2005; McPhee et al., 2014).

The ilium lacks the thick buttress at the base of the preacetabular process which contacts the supraacetabular crest ventrally that is present in basal dinosauriformes and the basal sauropodomorph *Chromogisaurus* (Ezcurra, 2010). The medial wall of the acetabulum circumscribes a fully open acetabulum as in most basal sauropodomorphs more derived than Saturnaliinae, with the medial ventral margin closely approximating the lateral rim of the acetabulum in contrast to the condition seen in *Macrocollum* and *Jaklapallisaurus asymmetrica*, which have a more ventrally invasive expansion of the medial wall.

As in NMQR 1705 and *Melanorosaurus* (NM 1551) the anterior portion of the supracetabular crest is more developed than the posterior portion. The supracetabular crest extends along the entire pubic peduncle as a moderate ridge, resembling the intermediate condition found in *Lessemsaurus* (but slightly more pronounced), between the pronounced crest seen in *Macrocollum*, *Chromogisaurus* and other basal sauropodomorphs and the lack of a large supracetabular crest seen in eusauropods (Ezcurra, 2010; Pol & Powell, 2007).

There is a posteriorly projecting heel at the distal end of the ischial peduncle, the presence of this process is also seen in *Plateosaurus*, *Riojasaurus*, *Lufengosaurus*, *Coloradisaurus*, *Pantydraco*, and *Ruehleia* (pers. obs.). The ischial peduncle is much shorter than the pubic peduncle, resembling the condition seen in NMQR 1705, *Lessemsaurus*, *Leonerasaurus*, *Macrocollum* and *Plateosaurus* (Müller et al, 2018; Pol & Powell, 2007), although not as short as in *Kotasaurus*, *Vulcanodon* and eusauropods (e.g., *Shunosaurus*; Pol & Powell, 2007; Carrano, 2005).

The length of the postacetabular process is 112% of the distance between the pubic and ischial peduncles. Unlike *Lessemsaurus*, where the dorsal margin of the postacetabular process is mildly concave, or NMQR 1705 where it is straight and runs anterodorsally at an angle of approximately 20 degrees to the longitudinal plane - the dorsal margin of SAM PK 3609 is mildly convex.

SAM PK 3609 possesses a brevis fossa and shelf, in contrast to the condition present in the specimen NM 1545 and NMQR 1705 that represents the derived sauropod condition (Upchurch et al, 2004).

The postacetabular process is distinctly square ended. It is similar to the condition seen in both *Melanorosaurus* and *Lessemsaurus*, but differs from that seen in NMQR 1705, *Riojasaurus* and *Macrocollum*, of a pointed ventral corner with a rounded posterodorsal margin.

Ischium (SAM PK 3608)
Two relatively complete conjoined ischia are preserved, although the proximoventral portion of the combined unit has been reconstructed with plaster. The ischium is similar to that

of other basal sauropodomorphs. There is no evidence of a notch separating the posteroventral end of the obturator plate from the shaft (e.g. *Plateosaurus*). An elongate interischial fenestra is absent and conforms to the general sauropodomorph condition. An ischial groove (dorsolateral sulcus) is present along the dorsolateral area of the proximal ischium, this feature is common to Saurischia (except *Herrerasaurus*, Yates 2003; Otero & Pol, 2013). The ischial shaft is long and rod-like, the typical dinosaurian condition. It is sub-triangular in cross section as in most basal sauropodomorphs and is distally dorsoventrally expanded. Thus, in distal view the conjoined ischia are V-shaped as in most basal sauropodomorphs such as *Massospondylus, Plateosaurus, Coloradisaurus*, *and Mussaurus* – but in contrast to the semi-circular outline seen in *Macrocollum.*

The elements show remarkable similarity with that of *Antetonitrus* (NMQR 1705) in terms of dimensions and features, especially the lateral protuberance of the ischiadic peduncle articulation area - but ultimately both taxa exhibit an ischial complex that it indistinguishable from that of basal sauropodomorphs.

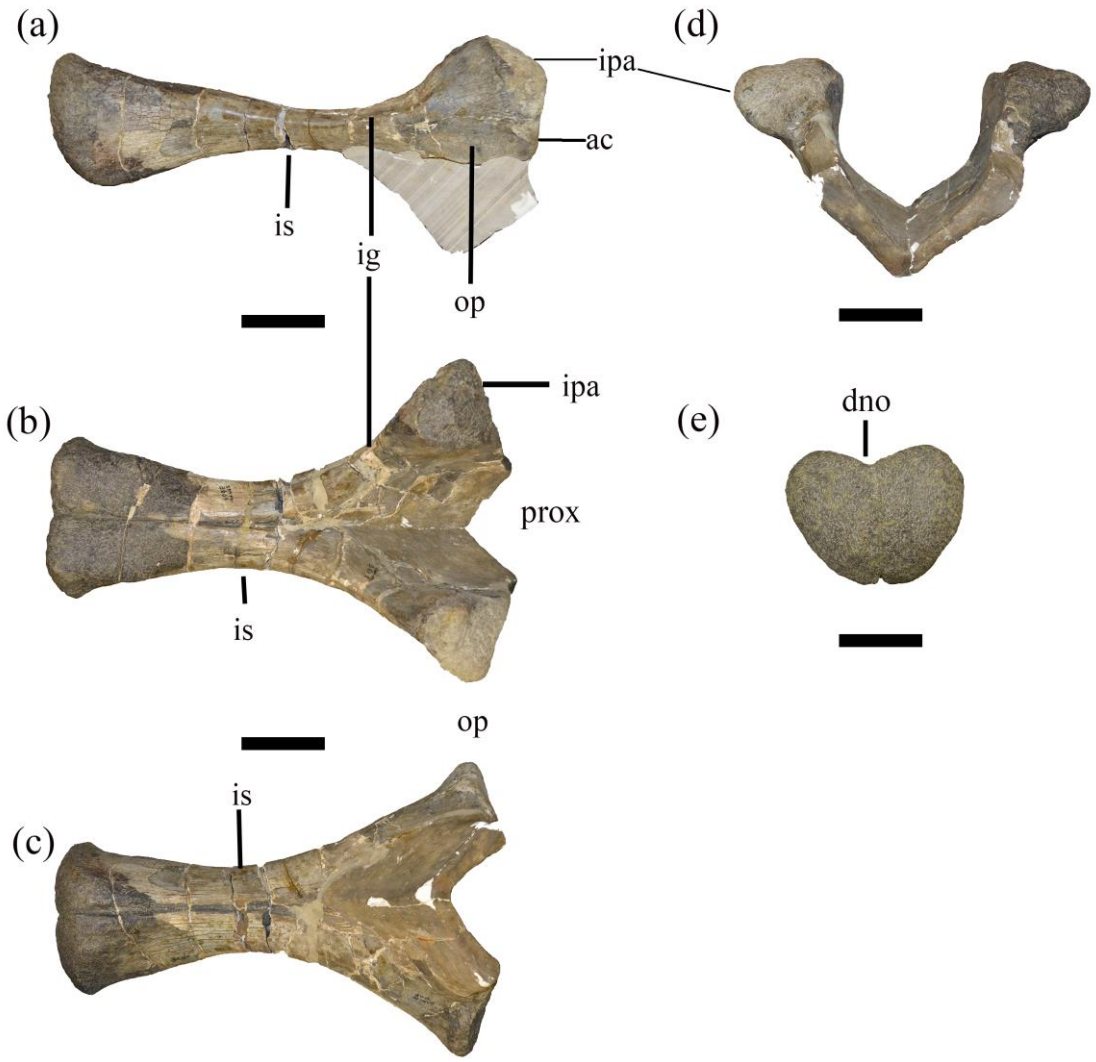

Figure 9. SAM PK 3608. Conjoined ischia. A) Right lateral view, B) Dorsal view, C) Ventral view, D) Proximal view, E) Distal view. op, obturator plate; ig, ischial groove; is, ischial shaft; ipa, ischiadic peduncle articulation area; dno, dorsal notch. **Scale = 10mm.**

Femora (SAM PK 3602-3)

Two right femora are present, one smaller element (SAM PK 3603) at 86% of the length larger one (SAM PK 3602). In anterior, posterior medial and lateral aspects both are sigmoidal in shape, although the smaller one (SAM PK 3603) slightly more so. Both are sub-circular in cross section. The fourth trochanter is located midway between the lateral and medial margins of the posterior surface and in the proximal half of the femur contrary to Van Heerden's (1979) description of it "straddling the midpoint". However, it is more distally placed

than in *Macrocollum*. The distal ends of both femora are expanded mediolaterally and anteroposteriorly. However, the size of the distal condyles relative to each other differ in anteroposterior width, with the medial condyle of SAM PK 3602 being 10mm wider than the fibular and lateral condyle, while the opposite is the case with SAM PK 3603. Despite this, a broad sulcus separates the lateral and medial condyles on both femora, similar to the condition seen in *Macrocollum*. Both SAM PK 3602 and 3603 have a more laterally placed tibiofibular crest (lateral condyle) than *Macrollum*.

Differences between the two femora include: the lack of a distinct medial distal corner on the femoral head of SAM PK 3602 and the presence of this feature in SAM PK 3603; the profile of the fourth trochanter is asymmetrical with a steeper distal slope than the proximal slope and a distinct distal corner in SAM PK 3602 compared to subsymmetrical and lack of a sharp distal corner in SAM PK 3603; the size of the medial condyle of the distal femur is larger than the fibular and lateral condyles in SAM PK 3602 and subequal to them in SAM PK 3603 (although only by 5mm).

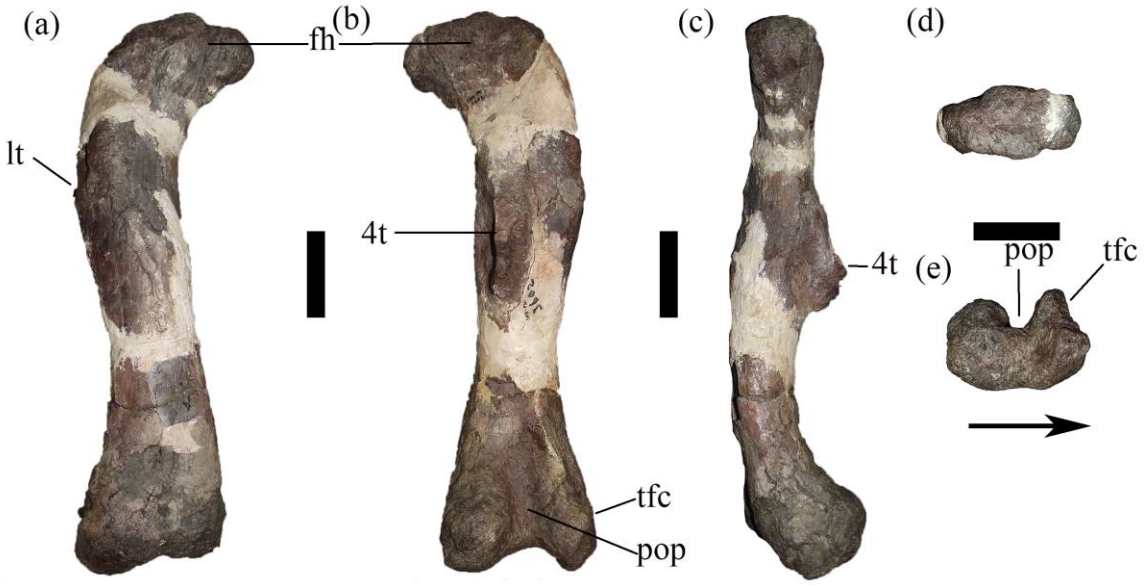

(Above)Figure 10. SAM PK 3602. Right femur. A) Anterior, B) Posterior, C) Medial, D) Proximal, E) Distal. Up is proximal and down is distal. Arrow indicates lateral direction. 4t, fourth trochanter; fh, femoral head; lt, lesser trochanter; pop, popliteal fossa; tfc, tibiofibular crest **Scale = 10mm.**

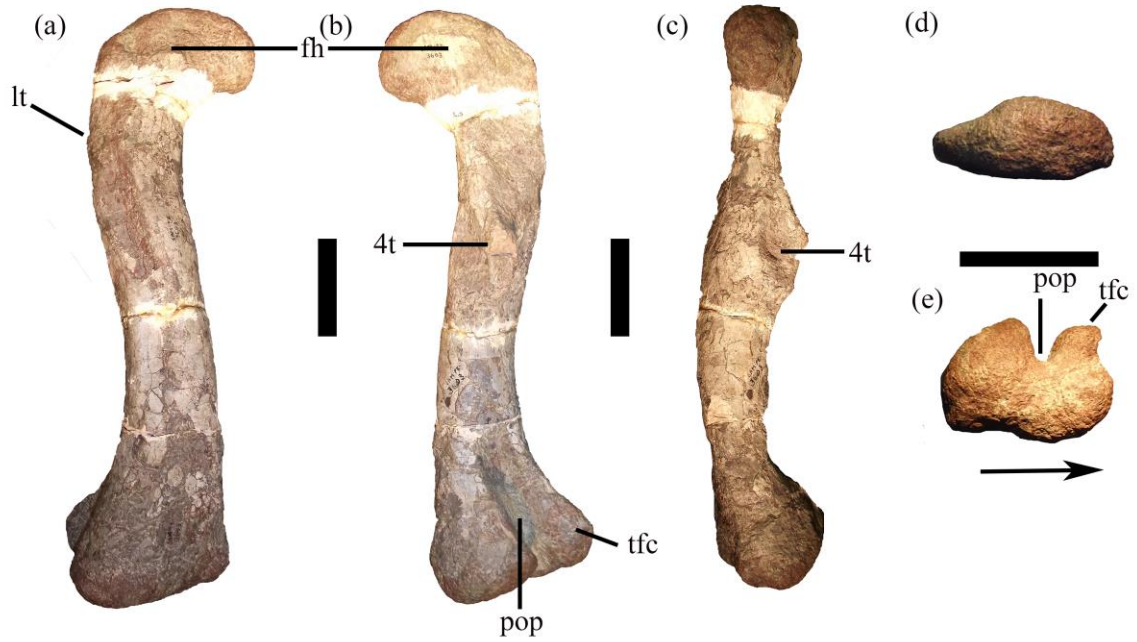

Figure 11. SAM PK 3603. Right femur. A) Anterior, B) Posterior, C) Medial, D) Proximal, E) Distal. Up is proximal and down is distal. Arrow indicates lateral direction. 4t, fourth trochanter; fh, femoral head; lt, lesser trochanter; pop, popliteal fossa; tfc, tibiofibular crest **Scale = 10mm.**

Lady Grey Referred "Plateosauravus" Material SAM PK 2780

Ribs

A proximal fragment of a dorsal rib with a portion of the tuburculum and capitulum preserved. It is of little diagnostic use. Sulci are present on the anterior and posterior surfaces as seen in *Unaysaurus*.

Scapula

A partial ventral portion of the left scapula is preserved; however, it lacks the acromion process, which is where the diagnostic characters are located.

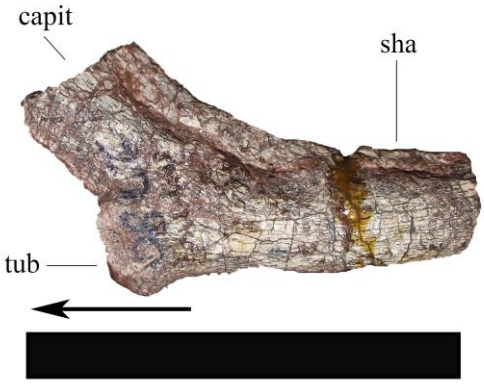

Figure 12. SAM PK 2780. Proximal dorsal rib fragment. Arrow indicates proximal direction. capit, capitulum; tub, tuberculum; sha, shaft. **Scale = 10mm.**

Figure 13. SAM PK 2780. Ventral portion of left scapula in medial view. ant, anterior; dors, dorsal; lat, lateral; vent, ventral. Scale = 10mm.

Humerus

A right humerus missing the anterolateral margin is preserved. It's preserved length (410mm) is similar to that of the smaller humerus, SAM PK 3350 (405mm). It differs from both SAM PK 3342 and 3350 in that the length of the deltopectoral crest (dpc) is less than 30% of the length of the humerus, while the former both exhibit values greater than 30%, but less than 50%. However, this value is most likely due to the incompleteness of the specimen as a value of less than 30% is only seen in non-Dinosaurian archosaurs.

The base of the deltopectoral crest appears straight, however the actual crest is not preserved, rendering us unable to state whether the anterolateral margin of the deltopectoral crest was also straight or sinuous as in SAM PK 3342 and 3350.

A rugose pit as seen in Massospondylids (i.e. *Massospondyolus*, *Lufengosaurus* and *Jingshanosaurus*) is present on the lateral surface of the dpc, this is in contrast to SAM PK 3342 and 3350, which lack this feature. As in SAM PK 3342 and 3350, there is a well-defined fossa on the distal flexor surface of the humerus –a feature that is common to basal sauropodomorphs in general. The transverse width of the distal humerus is greater than 33% of the length of the humerus as in SAM PK 3342 and 3350.

This humerus possesses a rounded entepicondyle as seen in SAM PK 3350, but in contrast to the flatter and sharper shape present in SAM PK 3342. This condition is seen in taxa as phylogenetically disparate as *Cetiosaurus* and *Thecodontosaurus*.

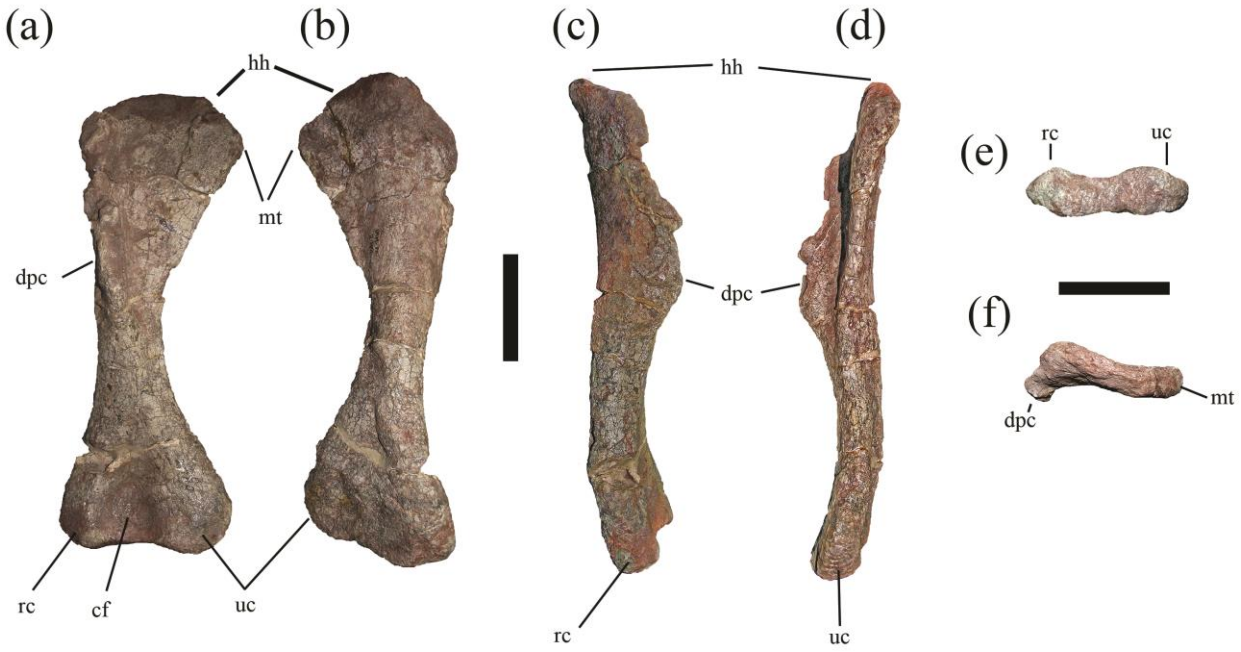

Figure 14. SAM PK 2780. Left humerus. A) lateral; B) medial; C) anteriort; D) posterior; E) distal; F) Proximal view. cf, cuboid fossa; dpc, deltopectoral crest; hh, humeral head; mt, medial tuberosity; rc, radial condyle; uc, ulnar condyle. **Scale = 10mm.**

Ilium

A right ilium was preserved; however, it is missing the dorsal margin and preacetabular process (pap). Unfortunately, we cannot compare its dorsal margin or pap with SAM PK 3609, except in terms of the angle between the pap and the pubic peduncle, which is more obtuse at +- 90 degrees compared to 70 degrees seen in SAM PK 3609.

This ilium also lacks the thick buttress at the base of the preacetabular process which contacts the supraacetabular crest ventrally that is present in basal dinosauriformes and the basal sauropodomorph *Chromogisaurus* (Ezcurra, 2010).

As expected in any sauropodomorph more derived than Saturnaliinae, the medial wall of the acetabulum circumscribes a fully open acetabulum with the medial ventral margin closely approximating the lateral rim of the acetabulum.

As in SAM PK 3609, NMQR 1705 and *Melanorosaurus* (NM 1551) the anterior portion of the supracetabular crest is more developed than the posterior portion. It differs in that the supracetabular crest extends only midway along the pubic peduncle as opposed to the entire length as in SAM PK 3609 (Ezcurra, 2010; Pol & Powell, 2007).

The ischial peduncle is damaged, so we cannot determine if there was a posteriorly projecting heel at the distal end of the ischial. While the ischial peduncle appears much shorter than the pubic peduncle, resembling the condition seen in SAM PK 3609, NMQR 1705, *Lessemsaurus*, *Leonerasaurus*, and *Plateosaurus* (Pol & Powell, 2007), it is not fully preserved and this may be a result of damage.

The length of the postacetabular process is 77% of the distance between the pubic and ischial peduncles, in contrast to 112% in SAM PK 3609. Once again, this could be a preservational artefact.

The area where a brevis fossa and shelf would be, behind the ischial peduncle, is not preserved. However, the postacetabular process is distinctly square ended as in SAM PK 3609 and both *Melanorosaurus* and *Lessemsaurus*. Unfortunately, this element is damaged primarily in regions where diagnostic features are present.

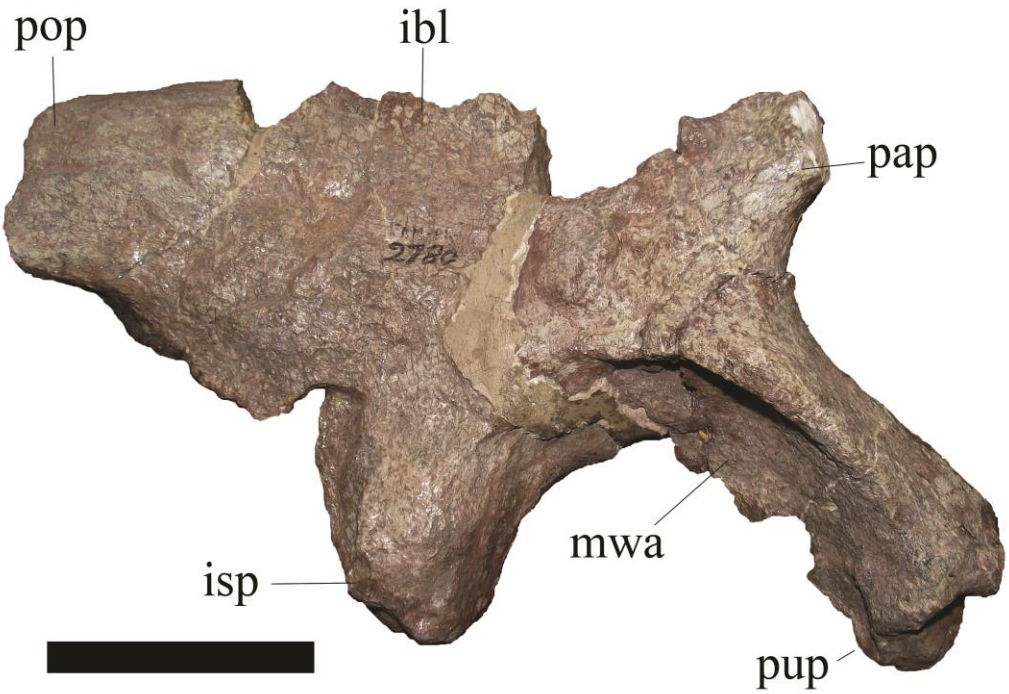

Figure 15. SAM PK 2780. Right ilium in lateral view. ibl, iliac blade; isp, ischial peduncle; mwa, medial wall; pap, preacetabular process; pop, postacetabular process; pup, pubic peduncle; sac, supracetabular crest. **Scale = 100mm.**

Ischia

A partial conjoined proximal ischium is present, the left side preserves more of the proximal portion than the right. The conjoined mediolateral width of shafts is 77mm. Anteroposterior height of right proximal shaft (better preserved) is 38mm, and the singular mediolateral width of same shaft is 40mm.

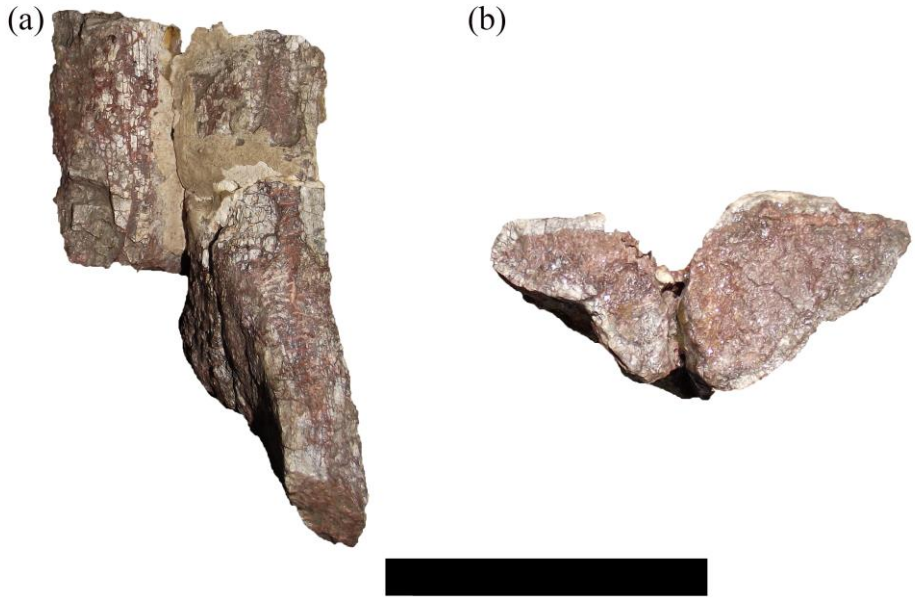

Figure 16. SAM PK 2780. Conjoined proximal ischial fragment. A) dorsal view. B) proximal view. Scale = 10mm.

Pubis

A fragment of the proximal pubis is preserved. It is too fragmented to provide usable data.

Femur

Not much data is discernible from the preserved femoral fragments. A distal end of a right femur and the proximal end of a left femur are present. The proximal portion of the left femur consists of the femoral head, it is roughly hemispherical, with no sharp medial distal corner – a feature common to most basal sauropodomorphs.

The distal right femur preserves a portion of the midshaft and the posterior portion of the bone, the anterior portion of the distal-most end is missing. The cross-section of the midshaft is sub-circular as in most sauropodomorphs. The medial condyle is larger than the fibular and lateral condyles, this is similar to SAM PK 3602 and other basal sauropodomorphs.

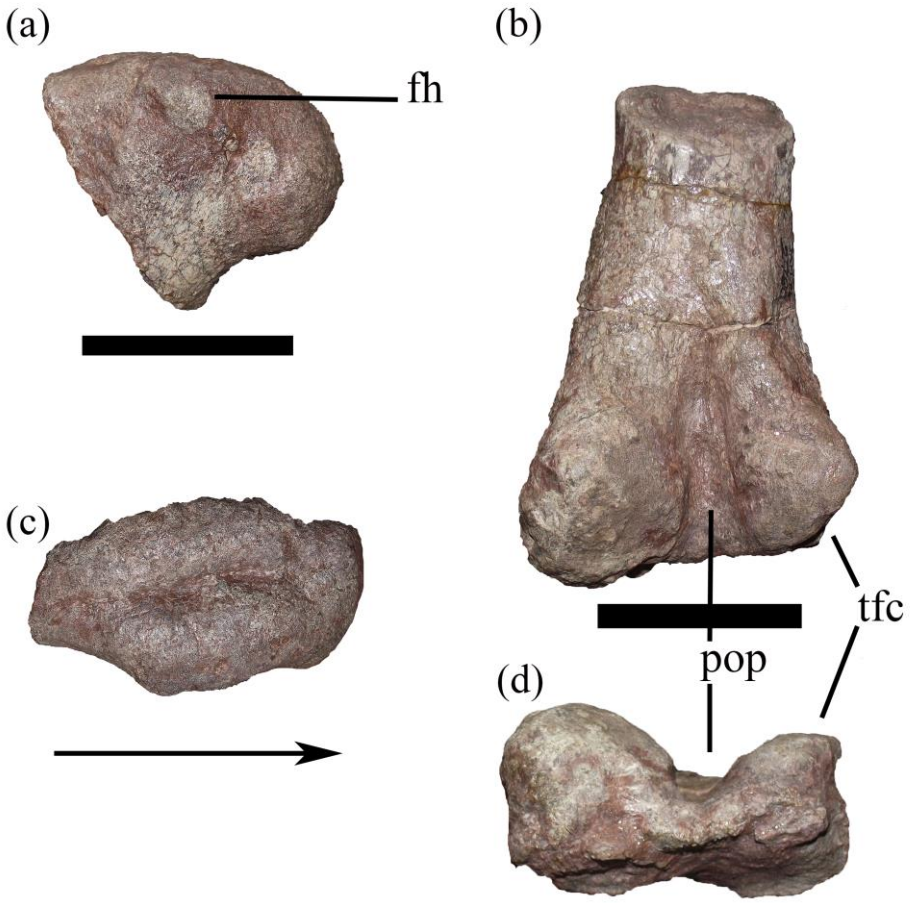

Figure 17. SAM PK 2780. A) Proximal portion of left femur in posterior view. B) Distal end of right femur in posterior view. C) Proximal portion of left femur in proximal view. D) Distal end of right femur in distal view. Arrow indicates medial direction. fh, femoral head; pop, popliteal fossa; tfc, tibiofibular crest **Scale = 10mm.**

Tibia

A relatively complete left tibia is present, only missing the anterolateral corner of the distal end. As no complete femur is present, we are unable to compare tibia-femur length ratio. This tibia is 40mm shorter in length than SAM PK 3341.

In general, this tibia is similar to SAM PK 3341 in that it also a shaft that is elliptical in cross-section below the cnemial

crest - with the long axis conforming to that of the proximal surface (i.e. in an anteroposterior direction), midway down the shaft the anterior surface begins to expand transversely, resulting in a more triangular cross-section of the shaft with the apex on the posterior side. It is also relatively slender compared to that of *Antetonitrus*, but similar in shape,

It differs in that the ratio between the length of the tibia and its anteroposterior depth at mid-length is smaller than SAM PK 3341 (6.52 versus 7.32). This condition is also seen in *Adeopapposaurus, Riojasaurus* and *Mussaurus*.

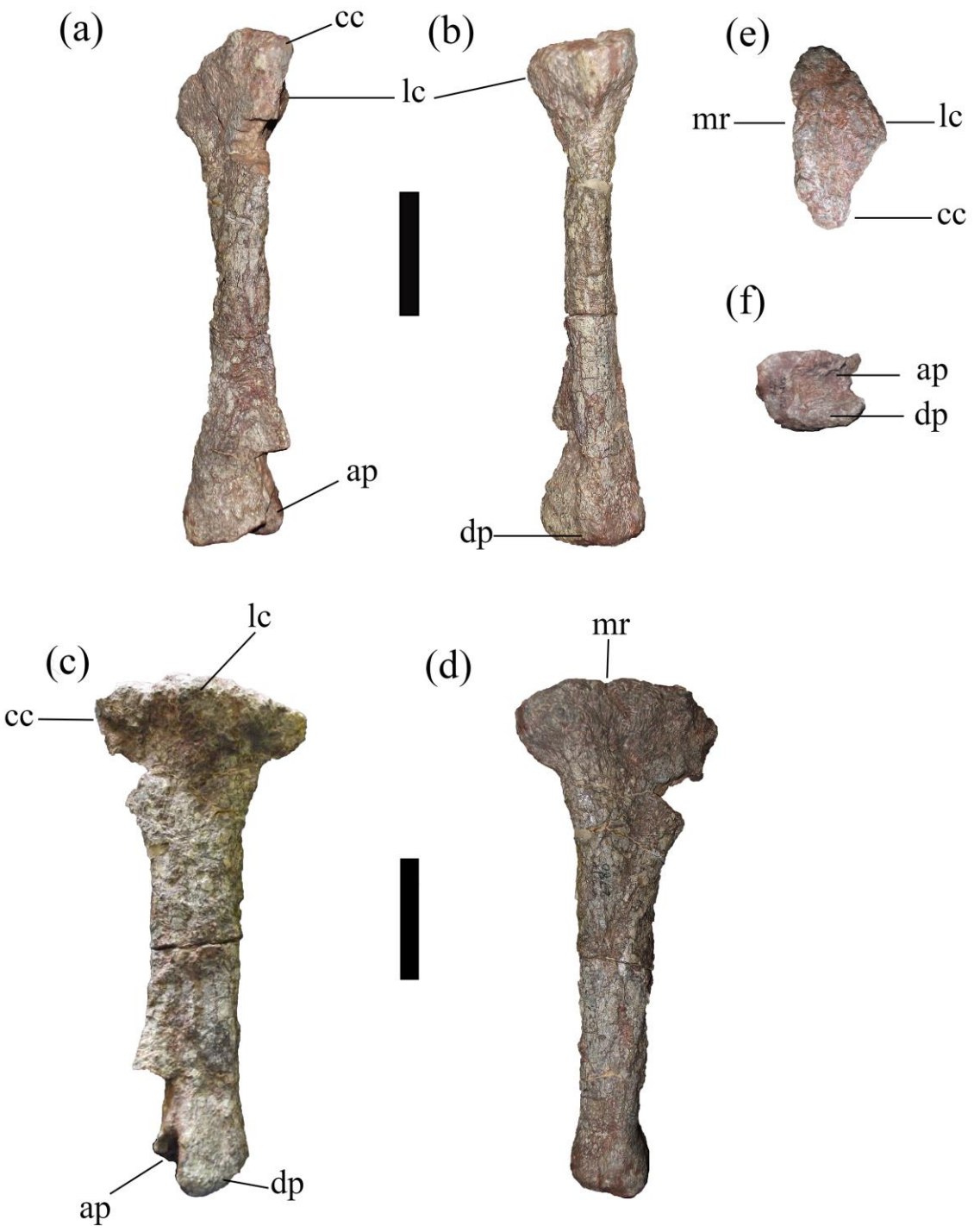

Figure 18. SAM PK 2780. Left tibia. A) anterior view, B) posterior view, C) lateral view, D) medial view, E) proximal view, F) distal view.ap, ascending process (ascending articular facet); cc, cnemial crest; dp, descending process; lc, lateral condyle; mr, medial ridge. Scale =10mm.

Phylogenetic Relationships

In Yate's (2003b) initial phylogenetic analysis, the Kromme Spruit material described in Van Heerden (1979) (SAM PK 2241-3356,3602-3607-9) was included in a single operational taxonomic unit (OTU) as "*Euskelosaurus*" and he found weak support for this OTU as a basal sauropod (Yates,2003a, b).

The data matrix included 76 taxa scored across 402 characters. The new lectotypic material from *Plateosauravus* was analysed. The initial heuristic search resulted in 70 most parsimonious trees (MPTs) of 1532 steps found in 8 out of 1000 replicates. A further round of TBR branch swapping of these 70 trees resulted in 3 744 MPTs of the same tree length (CI=0.307, RI= 0.671).

The strict consensus tree exhibits several polytomies (see Appendix 2). This is due to the instability of seven taxa due to character conflict and missing data identified using the IterPCR procedure (Pol & Escapa, 2009): *Blikanasaurus*, *Chromogisaurus*, *Glacialasaurus*, *Ingentia*, NMQR 1334, *Meroktenos,* and PULR 136.

After these unstable taxa were excluded from the consensus a posterioriori, *Plateosauravus* was recovered in a reduced strict consensus summary (Fig. 19) of all the MPTs as a Massopondylid taxon in a polytomy with *Leyesaurus* and *Adeopapposaurus*, as sister taxa to [*Massospondylus carinatus*+ [*Coloradisaurus*+ [*Massospondylus kaalae* + *Pradhania*]]].

(*Plateosauravus* + More Derived Sauropodomorphs [MDS]) form the immediate outgroup to Riojasauridae. The position of *Plateosauravus* within Massospondylidae is considerably more

derived than where *Plateosauravus* has historically been recovered as a non-Plateosaurian basal sauropodomorph in Yates (2003a) based phylogenies. This differs from the results found in previous analyses both the initial Yates (2010) and Yates et al. (2011) analyses, however it differs starkly from that of Yates (2003b) where weak support was found for this material falling within Sauropoda. Basal to the node Massospondylidae now lies *Anchisaurus*, while the highly labile LEF taxon, *Arcurusaurus* still retains a very basal position just below Nambalia in a polytomy with *Pantydraco* and *Thecodontosaurus*.

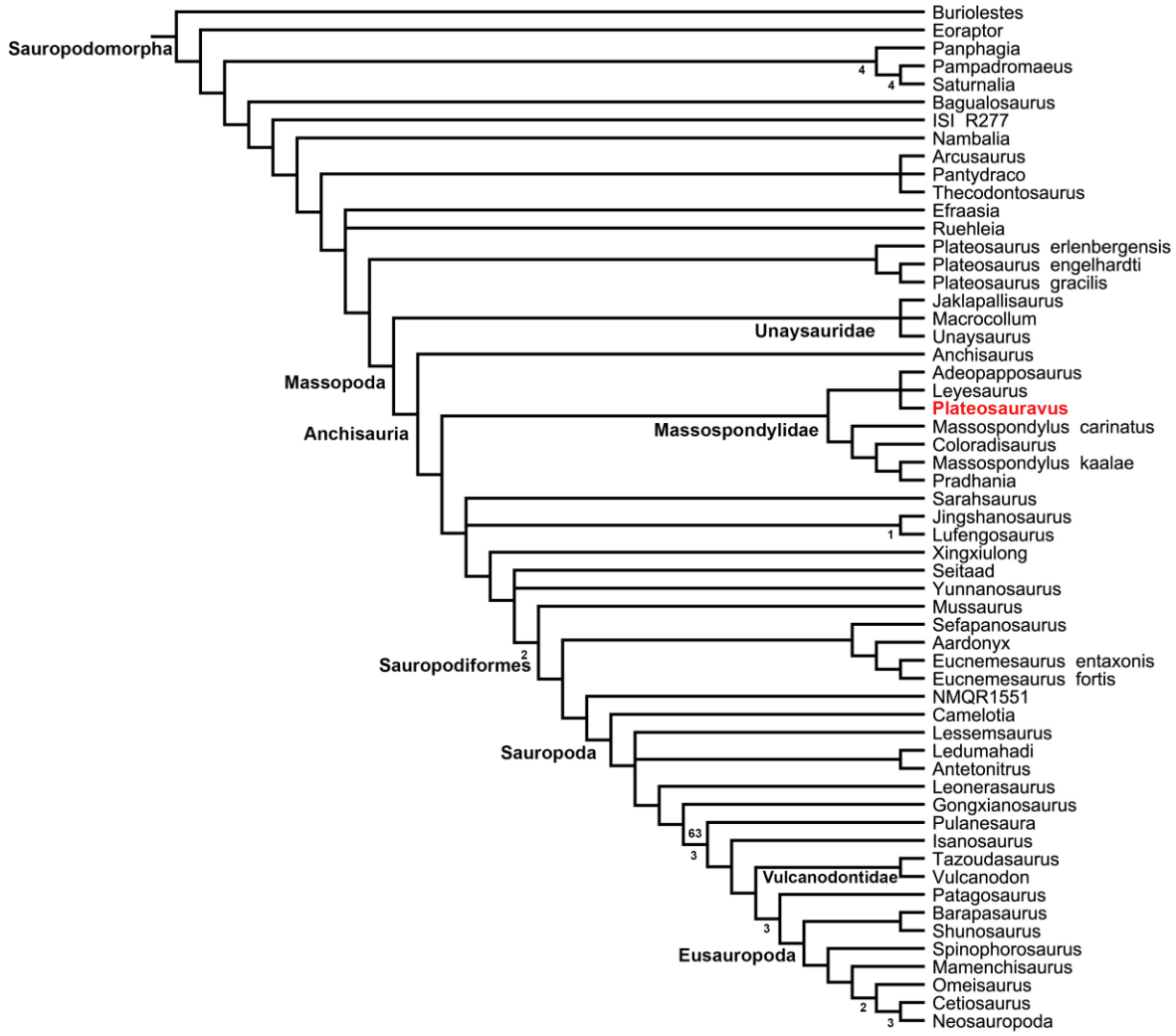

Figure 19. Reduced Strict Consensus summary. 3,744 Most Parsimonious Trees (MPTs) with a best score of 1532 (CI= 0.307, RI = 0.671), after seven unstable taxa: *Blikanasaurus*, Chromogisaurus, *Glacialasaurus*, *Ingentia*, NMQR 1334, *Meroktenos,* and PULR 136 were excluded from the consensus. Numbers below the branches represent bremer support and above the branches bootstrap values. Only sauropodomorph taxa are shown (for the complete strict consensus tree, including all taxa, see Appendix 2).

Conclusions

Plateosauravus, represented by the Kromme Spruit B material appears to be a valid taxon based a unique combination of characters not present in any other taxon. However, there are no uniquely autapomorphic characters present in this taxon. The results of the phylogenetic analysis indicate that *Plateosauravus* is less “primitive” than previously thought, being recovered as a massospondylid, it is recovered as less derived than the *Eucnemesaurus* spp.

However due to paucity of material comprising the new *Plateosauravus* (SAM PK 3341-3344,3346-3349,3356) lectotype, it is readily apparent that more material is needed to provide a more accurate assessment of this taxons phylogenetic position and provide a more robust taxonomic diagnosis. Future work on this taxon will hinge around finding more referable specimens and comparison with the host of material assigned to *Massosopondylus* in order to determine if any of that material may actually belong to *Plateosauravus*.

Chapter 3

The taxonomic affinity of the "Maphutseng Dinosaur" (NMQR 1705)

Introduction

Antetonitrus ingenipes represents the most complete and earliest definitive sauropod (*sensu* Yates, 2007) from the Early Jurassic (Hettangian) Upper Elliot Formation (UEF) of South Africa (McPhee et al., 2017 *contra* Yates & Kitching, 2003), the holotype of which was recently described in detail - providing important information on the anatomy of this basal-most sauropod (see McPhee et al., 2014). *Antetonitrus* has been interpreted as the sister taxon of a similar basal sauropod, *Lessemsaurus sauropoides,* from the Norian–Rhaetian upper section of the Los Colorados Formation in Argentina based on multiple derived features (Pol & Powell, 2007).

During the 1950's a large assemblage of sauropodomorph material of indeterminate taxonomic identity was excavated from Maphutseng in Lesotho (Ellenberger & Ellenberger, 1956; Charig et al., 1965; Gauffre, 1993). Ellenberger & Ellenberger (1956) stated that the material was probably either a large plateosaurid or a melanorosaurid. The material collected was split between the MNHN and Iziko, South African Museum and is currently catalogued at the NMQR collection (NMQR 1705). Gauffre (1993) studied part of this material but focused solely on the specimens housed at the MNHN reported by Ellenberger & Ginsburg (1966). Both Ellenberger & Ginsburg (1966) and Gauffre (1993) assigned the Maphutseng material to "*Euskelosaurus browni*", a taxon that is currently considered a *nomen dubium* (Yates & Kitching, 2003).

The materials described here (NMQR 1705) comprise postcranial remains of at least five individuals. Here we focus on the elements that are absent in the holotype of *Antetonitrus ingenipes* (Yates and Kitching, 2003; McPhee et al., 2014), which shed further light on the early evolution of sauropods. Furthermore, we re-evaluate the phylogenetic position of *Antetonitrus* based on previously referred specimens (i.e. from Yates & Kitching, 2003; McPhee et al., 2014) as well as new scorings derived from NMQR 1705.

Materials & Methods

NMQR 1705 is currently housed in the Department of Biological Science, University of Cape Town, South Africa but is accessioned in the National Museum, Bloemfontein, South Africa (NMB). The *Antetonitrus* holotype (BPI/1/4952a) and referred material (BPI/1/4952b, BPI/1/4952c and BPI/1/5091) are housed at the Bernard Price Institute, University of the Witwatersrand, Johannesburg (BPI). Additional referred material, NMQR 1545, is also housed at the NMB.

Anatomical terminology employed herein makes use of traditional or “Romerian” directional terms over veterinarian alternatives (e.g. anterior and posterior rather than cranial and caudal). Phylogenetic nomenclature for the clades mentioned in this chapter can be found in Table 1. The anatomical descriptions are based on first-hand observation of NMQR 1705. Comparisons made with other members of Sauropodomorpha are based both on first-hand observation of certain taxa and the literature, as specified in Table 2.

Institutional Abbreviations

BPI, Bernard Price Institute, Johannesburg, South Africa; **MACN**, Museo Argentino Ciencias Naturales “Bernardino Rivadavia”, Buenos Aires, Argentina; **MLP**, Museo de La Plata, La Plata, Argentina; **MPEF**, Museo Paleontologico “Egidio Feruglio”, Trelew, Chubut, Argentina; **NMB**, National Museum Bloemfontein, South Africa; **PVL**, Instituto “Miguel Lillo”, Tucumán, Argentina; **SAM**, South African Museum, Cape Town, South Africa.

Cladistic Analysis

Antetonitrus was re-scored, incorporating data from NMQR 1705, in a modified version of the Müller (2018) data matrix, which is a modified version of the data set originally published by Yates (2007). It includes the same characters employed in the McPhee et al. (2014) analysis of the *Antetonitrus* holotype plus additional characters (244, 277 and 402) and taxa (*Ledumahadi*) drawn from McPhee et al (2018). Forty-four characters were treated as ordered following Müller (2018). The dataset includes some sauropodomorph outgroups, reaching a total of 76 taxa and 402 characters (see Appendices 1-3 for character list, character-taxon matrix and for details of phylogenetic analysis). The data matrix was created using Mesquite 3.51 (Maddison & Maddison, 2018) and analysed using TNT Version 1.1 (Goloboff et al., 2008).

Systematic Palaeontology

Saurischia Seeley 1888

Sauropodomorpha Von Huene 1932

Massopoda Yates 2007

Anchisauria Galton & Upchurch, 2004

Sauropodiformes Sereno 2007

Sauropoda Marsh 1878

Genus *Antetonitrus* Yates & Kitching 2003

Type species. *Antetonitrus ingenipes* (Yates & Kitching 2003)
Diagnosis. As for type and only species.
Antetonitrus ingenipes Yates & Kitching 2003

Holotype. BPI/1/4952. Yates & Kitching (2003) designated as the holotype disarticulated postcranial material that was found closely associated *in situ*. They assumed that the fossils belonged to a single individual due to the fact that they are all from a large robust sauropodomorph representing most skeletal regions with no duplication of elements. However, as recently noted by McPhee et al. (2014) and confirmed by a re-examination of the material, there are two right second metacarpals and two left scapulae, rather than left and right pairs as initially described. This indicates that the holotype is composed of more than one individual. Despite the duplication of the scapulae and second metacarpals, there is no reason to doubt that these elements belong to the same taxon as they exhibit the same morphology. McPhee et al (2014) separated the smaller scapula and metacarpal II from the holotype, referring these two elements as BPI/1/4952c (see below). Furthermore, the materials as described by Yates & Kitching (2003) as the left radius, metacarpal I, and manual phalanx I.1 are in fact from the right side. The material catalogued under BPI/1/4952 also includes a cervical centrum, four dorsal vertebrae, sacral vertebra, caudal vertebrae, dorsal ribs, chevrons, right humerus, both ulnae, two? manual unguals, left pubis, left femur, left tibia, left fibula, left metatarsal I, right metatarsal II, left metatarsal III, right metatarsal V, two pedal phalanges, right pedal ungual I, right pedal ungual? III.

Referred Material.
BPI/1/4952b.This material was found at the same site and originally referred to *Antetonitrus ingenipes* by Yates & Kitching (2003) based on similarity to the holotype material, it is

approximately 80% of the size of the holotype material. It includes a right scapula, right humerus (with a deep sulcus on the lateral distal margin of the deltopectoral crest), left ulna, left fibula, and a right metatarsal II.

BPI/1/4952c. Right scapula and right metacarpal II. This material was found *in situ* with the disarticulated holotype material (Yates & Kitching, 2003). The additional scapula is slightly smaller than BPI/1/4952a (92% of the length of the larger scapula). The additional metacarpal II is almost exactly the same size as BPI/1/4952 but has not been figured by Yates & Kitching (2003). These elements belong to an individual (or individuals) of similar size (92% based on the right scapula and the same size based on the metacarpal II) to the holotype (McPhee et al., 2014).

BPI/1/5091. This material was collected from the *Antetonitrus* holotype locality two years after the collection of BPI/1/4952 and includes a sacral neural arch from one of the primordial sacral vertebrae, a partial caudosacral neural arch and a potential dorsosacral centrum (McPhee et al., 2014).

NMQR 1545. An assemblage of elements that includes a large right humerus; two small right ulnae; left and right ilia; two femora including a heavily damaged large left and a large right; three tibiae, a small (incomplete) right element, and two large, subequal sized left (complete) and right (incomplete) elements; three fibulae, a large right and two subequal sized, smaller elements of both sides (McPhee et al., 2014). The material represents two distinct size classes containing approximately three individuals (McPhee et al, 2014). Although in poorer condition than BPI/1/4952, NMQR 1545 displays the same diagnostic criteria and basic morphology as that listed above for BP/1/4952 and was referred to *Antetonitrus* by McPhee at al. (2014). McPhee et al. (2014) note that due to differential preservation amongst the elements NMQR 1545 may not

represent an associated assemblage of bones, but may be composed of a mix of ‘float’ from the surrounding area, as well as *in situ* material.

NMQR 1705. These materials comprise postcranial remains from several individuals found at Maphutseng and are referred here to *Antetonitrus ingenipes*. Unfortunately, due to lack of data on collection it is impossible to associate any elements together besides the articulated right pes with absolute certainty. NMQR 1705 includes elements from at least five individuals (minimum number of individuals based on presence of five right femora and five right fibulae) of different ontogenetic sizes, comprising 254 postcranial elements that represent almost all appendicular and axial skeletal components. This material includes: a single tooth; numerous cervical, dorsal and caudal vertebrae; an articulated sacrum; three scapulae; two right and one left coracoids; three humeri; three radii, six ulnae; metacarpals I and II; assorted manual phalanges; ribs and gastralia; three ilia; three ischia; two corresponding pubes; eight femora; six tibiae; eight fibulae; two astragali; a complete right pes; assorted metatarsals and pedal phalanges.

Comments on NMQR 1705.

The monospecificity of NMQR 1705 is supported by the lack of any noticeable difference in morphology amongst duplicated elements (i.e. femora, tibia, humeri, fibulae, radii, ulna, metatarsals, metacarpals, and vertebrae). The femora differ from non-sauropod sauropodomorphs known from the Elliot Formation (i.e., *Massospondylus*, *Plateosauravus* and *Eucnemasaurus)* in that the shaft is elliptical in cross-section, (rather than circular), possesses a medially located fourth trochanter, is straight in posterior view and the lesser trochanter is placed close to the lateral margin. The ulna exhibits an incipient radial fossa and is

tri-radiate, as in sauropods (see Bonnan, 2003; Yates & Kitching, 2003).

The following autapomorphies (indicated by *) and unique combination of characters found in *Antetonitrus* (identified by Yates & Kitching, 2003 and McPhee et al., 2014) are present in NMQR 1705 and are the basis for referring the material to this taxon: dorsal neural spines flared transversely at their distal end*; dorsal vertebrae with broad, triangular hyposphenes (in caudal view)*; high dorsal neural spines comprising more than half the total height of the neural arch*; a single articular facet on the proximal chevrons*; deep sulcus adjacent to the lateral distal margin of the deltopectoral crest*; the head of the humerus is vaulted and expanded posteriorly; the medial tuberosity of the humeral head is reduced and slightly medially inturned*; a medial deflection of the anterior process of the proximal ulna*; an incipient radial fossa on the proximal ulna; an extremely short, broad metacarpal I*; a distinct bifurcated tubercle on the ventrolateral edge of the shaft of the second metacarpal; the femoral shaft is elliptical in cross-section and reduced in lateral sinuosity; the fourth trochanter is located on the medial edge of the mid-shaft of the femur; the anteroposterior length of the proximal surface of the tibia is over twice its transverse width and roughly level with the horizontal plane; the descending process of the distal tibia is compressed laterally so that the anterior ascending process is visible in posterior view; and a robust, entaxonically spreading pes. As the hyposphenes of the caudal vertebrae are not preserved we cannot determine whether the NMQR 1705 also possessed a ventral ridge on the caudal hyposphenes.

In contrast to the holotype and previously referred material, we have identified slight differences present in NMQR 1705. The scapular blade is not broadly expanded dorsally, but both

anterior and posterior dorsal margins are broken. The dorsal neural arches do not exceed twice the dorsoventral height of centra as in the holotype, but their ratio is remarkably similar, ranging between 1.83 – 1.97 times the central height. There is no evidence of pneumatic subfossae in posterior infradiapophyseal fossae of the mid-posterior dorsal neural arch. The deltopectoral crest of the humerus is slightly more sinuous than in the holotype (BPI/1/4952) and it is less than half the length of the humerus. The lesser trochanter is not visible in posterior view of femur, although the anterolateral margin of the lesser trochanter is slightly worn in NMQR 1705. The first pedal ungual is shorter than the first metatarsal by 10mm, but the tip of the ungual is broken.

While these differences exist, most of them are ascribable to poor preservation, whereas others are minor differences that could be related to intraspecific or ontogenetic variations. Considering this and the largely identical morphology of the *Antetonitrus* holotype (BPI/1/4952a) and NMQR 1705 in most elements (see Table 3).

Locality and horizon. BPI/1/4952, BPI/1/4952b, BPI/1/4952c and BPI/1/5091 were collected in strata belonging to the lowest level of the Early Jurassic Upper Elliot Formation (Hettangian), at the saddle between the farms Welbedacht 611 and Edelweiss 698, Ladybrand District, Free State, South Africa (29.1° S, 27.2° E) (Yates & Kitching, 2003; McPhee et al., 2014; McPhee et al., 2017).

NMQR 1545 was collected from the Excelsior District of the Free State, South Africa (McPhee et al, 2014). No stratigraphic data is available for this element.

Ellenberger (1956) noted that this material was found in a bone

Holotype (from Yates & Kitching, 2003; McPhee et al, 2014)	**Referred material (according to McPhee et al, 2014)**				**Maphutseng material not represented in holotype (BPI/1/4952a)**
BPI/1/4952a	*BPI/1/4952b*	*BPI/1/4952c*	*BP/1/5091*	*NM QR1545*	*NM QR1705*
cervical centrum	posterior dorsal neural arch	left scapula	primordial sacral neural arch (uncertain which one)	right humerus	articulated sacrum comprising ?dorsal, dorsosacral , primordial sacral 1 and primordial sacral 2
three dorsal neural arches	?two caudal vertebrae	left metacarpal 2	partial ?caudosacral neural arch	two right ulnae	complete right pes
four dorsal centra	right scapulae		centra from ?dorsosacral vertebra	left and right ilia	two fragmentary right ilia and one smaller almost complete right ilium
?caudosacral neural arch	right humerus			left and right femora	two conjoined ischia and one partial right ischium
?ten caudal vertebrae	right ulna			three tibia (2 right and 1 left)	two fragmentary right coracoids and one almost complete left.
two dorsal ribs	right radius			three fibulae (2 right and 1 left)	two astragali, complete right and partial left
chevrons	right fibula				single fragmentary tooth
left scapula					
right humerus					
both ulnae					
right radius					
right metacarpal 1					
left metacarpal 2					
right manual phalanx 1.1					
left pubis					
left femur					
left tibia					
left fibula					
left metatarsal 1					
right metatarsal 2					
left metatarsal 3					
right metatarsal 5					
two pedal phalanges					
right pedal ungual 1					
right pedal ungual ?3					

Table 3. Elements present in *Antetonitrus* holotype (BPI/1/4952a), previously referred material (BPI/1/4952a, b, c; BPI/1/5091; NMQR 1545) and Maphutseng material (NMQR 1705).

NMQR 1705 was collected from Maphutseng, Mohale's Hook District, Lesotho 30.2° S, 27.5° E (see Fig. 20). Ellenberger & bearing lens, exceeding 1 hectare, at the base of the "Red Beds" situated at the foot of a hill, at the base of the LEF (Ellenberger & Ellenberger, 1956; Ellenberger, 1970; Gauffre, 1993). Ellenberger & Ellenberger (1956) describe the depositional environment as lacustrine, corresponding to our current understanding of the LEF as a fluvio-lacustrine in origin (see Bordy et al., 2004).

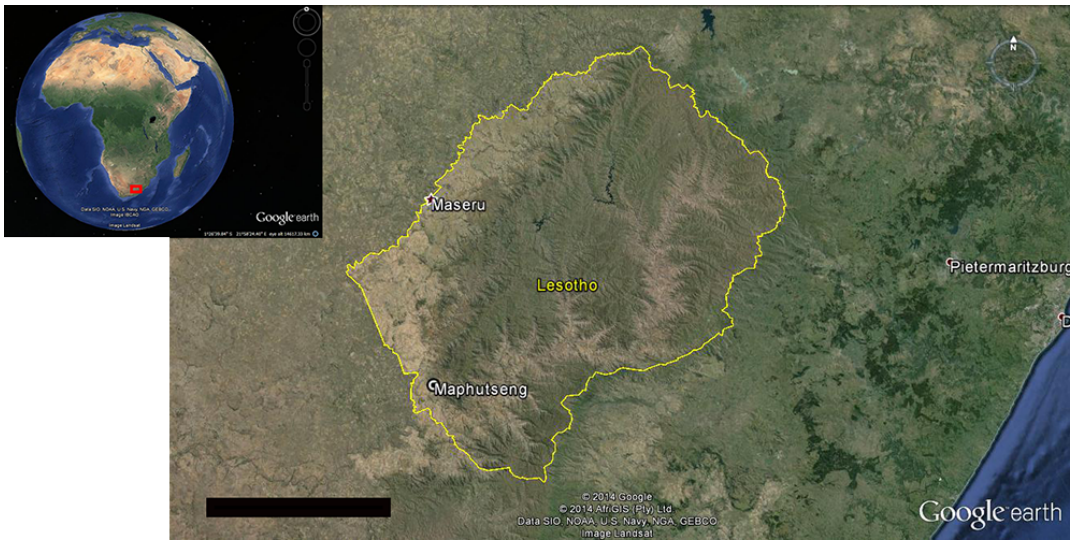

Figure 20. The Maphutseng locality. Scale = 100km. Google Earth (2014a, b).

All NMQR 1705 material comes from the Late Triassic Lower Elliot Formation (LEF), corresponding to the biostratigraphic "*Euskelosaurus* Range Zone" (Kitching & Raath, 1984; Gauffre, 1993; Bordy et al, 2004). The LEF was considered Norian in age (Lucas & Hancox, 2001; Yates & Kitching, 2003), with the possibility that the upper strata may even be Rhaetian in age (Bordy et al., 2004, 2005; McPhee et al., 2014;). If we accept Bordy et al's (2005) interpretation of the Elliot-Molteno contact as an abrupt unconformity, with an ending date of ~215 Ma (see McPhee et al., 2014), the LEF is actually bracketed between the mid-Norian and Early Rhaetian in age.

Revised Diagnosis. The following unique combination of characters and autapomorphies(designated by *) diagnoses this taxon (which adds one autapomorphy to the revised diagnosis recently provided by McPhee et al., 2014): dorsal neural spines flared transversely at their distal end* (present to a lesser extent in *Lessemsaurus*);high dorsal neural spines comprising more than half the total height of the neural arch*; dorsal neural arches more than twice as tall as associated centra*; pneumatic subfossae in the posterior infradiapophyseal fossae of the mid-posterior dorsal neural arch; dorsal vertebrae with broad, triangular hyposphenes (in caudal view)*; ventral ridge on the hyposphenes of the posterior dorsal vertebrae*; lateral surface of dorsosacral rib is hourglass-shaped in profile* (new autapomorphy); presence of a caudosacral vertebrae; single articular facet on proximal chevrons*; broadly expanded dorsal scapular blade; head of humerus vaulted and expanded posteriorly; medial tuberosity of the humeral head reduced and slightly medially inturned*; delicate, non-sinuous deltopectoral crest; deep sulcus adjacent to the lateral distal margin of the deltopectoral crest*; medial deflection of the anterior process of the proximal ulna*; incipient radial fossa on the proximal ulna; extremely short and broad metacarpal I*; distinct bifurcated tubercle on the ventrolateral edge of the shaft of metacarpal II; femoral shaft elliptical in cross-section and reduced in lateral sinuosity; laterally displaced lesser trochanter of the femur visible in posterior view; fourth trochanter located on the medial edge of the mid-shaft of the femur; anteroposterior length of the proximal surface of the tibia over twice its transverse width and roughly level with the horizontal plane; descending process of the distal tibia compressed laterally so that the anterior ascending process is visible in posterior aspect; robust, entaxonically spreading pes; metatarsal III less than 40% length of tibia; length of pedal ungual I greater than metatarsal I.

Antetonitrus resembles *Lessemsaurus* (Bonaparte 1999) and *Blikanasaurus* (Galton & Van Heerden 1985) most closely. However, the new pedal material of *A. ingenipes* (and that of *Lessemsaurus*) differs from *Blikanasaurus* in the following features: a horizontal shelf forming part of the fibular facet of the astragalus; the minimum transverse shaft diameters of metatarsal III and metatarsal IV are less than 60% of the minimum shaft diameter of metatarsal II and all non-terminal pedal phalanges as wide, if not wider, than long. Furthermore, differing from *Antetonitrus*, *Blikanasaurus* also has a much more robust pes and a marked cranial extension of the proximal articular surface of metatarsal II (Yates & Kitching, 2003). *Antetonitrus* also lacks a sharp medial margin around the depression posterior to the ascending process of the astragalus.

New features that distinguish *Antetonitrus* from *Lessemsaurus* include an astragalus that is kidney shaped in ventral view, as opposed to the more rectangular outline in *Lessemsaurus,* and an ilium lacking a brevis crest. It also possesses a more elongate, pointed postacetabular process (based primarily on NMQR 1545 as the postacetabular process in NMQR 1705/5091 is largely reconstructed with plaster), although Pol & Powell (2007) do point out that the blunted postacetabular process in *Lessemsaurus* may be due to preservational causes.

Description

Tooth

One isolated tooth (NMQR 1705/028) is present, part of the crown and the upper part of the root are preserved (Fig. 21), although there is an impression of the apical tip of the crown on the surrounding matrix allowing us to gauge the full height of the crown. It is in a very poor state of preservation, with small

patches of the outer enamel surface preserved, the mesial and distal carinae are not preserved, rendering it impossible to determine whether or not the tooth possessed denticles as in most basal sauropodomorphs, *Leonerasaurus* and certain gravisaurian sauropods such as *Tazoudasaurus* (Pol et al., 2011; Allain & Aquesbi, 2008).

Figure 21. Isolated tooth (NMQR 1705). Buccal view. Scale = 5mm

The tooth crown is elongate and lanceolate in shape, similar in morphology to that of the basal sauropodiform *Melanorosaurus* (Yates, 2007a) and the basal sauropod *Chinshakiangosaurus* (Upchurch et al., 2007), rather than the strongly spatulate condition present from *Pulanesaura*, *Gonxianosaurus* and more derived forms (He et al., 1998; Carballido & Pol, 2010; Upchurch, 2007, McPhee et al., 2015). It also lacks the lingual concavity that results in a spoon-shaped crown incipiently present in *Leonerasaurus* and basal sauropods such as *Pulanesaura*, *Chinshakiangosaurus* (Pol et al., 2011; Upchurch, 2007, McPhee et al., 2015).

The crown has a slenderness index of between 2.58 – 2.7 (the ratio of crown height to maximum crown width [Upchurch, 1998]), based on where we assume outer enamel surface of the crown terminates. This exceeds the ratio of 2.13 found in *Melanorosaurus* (Yates, 2007a) and 1.3 found in *Leonerasaurus* (Pol et al., 2011). It should be noted that Chure et al. (2010) give a SI value of 1.84 for *Melanorosaurus*, however this value seems dubious as measurements of the maxillary teeth of NMQR

3314 (taken from Text-Fig. 1 - Yates, 2007a) regularly yield a SI exceeding 2, thus we retain the value of 2.13 given by Yates (2007a) as being more realistic.

As in *Melanorosaurus* and *Jingshanosaurus* (Yates, 2007a) there is a mild mesiodistal expansion a short distance above the base of the crown. This differs from the condition observed in *Leonerasaurus* where the juncture between the root and crown is separated by a marked constriction (Pol et al., 2011). The crown is mesiodistally symmetrical and mildly convex in both labial and lingual aspects, in contrast to the asymmetrical condition present in *Leonerasaurus* (Pol et al., 2011). It is elliptical in cross-section differing from the D-shaped cross-section present in *Melanorosaurus* and *Pulanesaura,* but similar to *Jingshanosaurus xinwaensis* in this regard (Yates, 2007a; McPhee et al., 2015).

There are numerous, fine grooves running apicobasally on the small portion of enamel preserved on the tooth crown, similar to the “fluting” described in *Melanorosaurus* and *Jingshanosaurus* (Yates, 2007a), although less pronounced than in *Pulanesaura* (McPhee et al., 2015). This “fluting” may be homologous to the sulci described by Carballido & Pol (2010) for the basal sauropod *Amygdaladon patagonicus*. Based on the portion of enamel preserved they would have been more numerous than the four per face found in *Melanorosaurus* (Yates, 2007a). These grooves are much finer and distinct from the deep lingual and labial grooves described by Upchurch (1998) that occur (incipiently) in some basal sauropods and eusauropods (Pol et al., 2011).

The preserved portion of the outer enamel surface provides no evidence of the more coarsely wrinkled enamel synapomorphic of eusauropod teeth (Wilson & Sereno, 1998; Upchurch, 2007; Pol et al., 2011). It is not possible to determine if the

discontinuous, finely “wrinkled” enamel found in *Anchisaurus* (Galton & Upchurch, 2004; Yates, 2004), *Leonerasaurus* (Pol et al., 2011) and *Pulanesaura* (McPhee et al., 2015), is present in NMQR 1705 until it is examined under scanning electron microscopy. The tooth root is sub-circular in cross-section as in *Chinshakiangosaurus* (Upchurch, 2007).

The isolated tooth is most similar to that of *Melanorosaurus* and *Jingshanosaurus* (see Yates, 2007a). The teeth of *Melanorosaurus* can be distinguished based on a few differences including: less elongate crown that is D-shaped in cross-section, and the presence of denticles on the mesial and distal carinae.

Coracoids

A left coracoid, NMQR 1705/655 (Fig. 22) is the best preserved and forms the basis of the description. As in most sauropodomorphs, the mediolateral thickness of the coracoid ranges from very thin along the anteroventral half to a thick posteroventral region that encompasses the glenoid, the transversely expanded glenoid region is 3.2 times the thickness of the anteroventral margin.

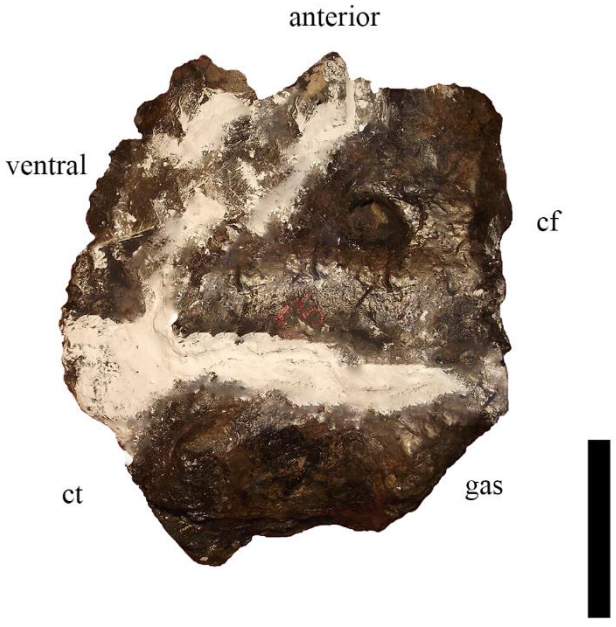

(Above) Figure 22. Left coracoid (NMQR 1705/655) in lateral view. ct, coracoid tubercle; cf, coracoid foramen; gas, glenoid articulatory surface.

The coracoid is laterally mildly convex and much more drastically medially concave. On the anterior margin there is a subtle notch situated just ventral to the glenoid. The coracoid foramen is situated near the contact with the scapula, approximately midway between the anterior and posterior margins. The prominent coracoid tubercle is located ventral to the glenoid and projects laterally (Fig. 22).

It is not possible to determine what angle the glenoid articular surface of the coracoid lies relative to the glenoid articular surface of the scapula, as none of the coracoids can be associated with a scapula due to poor preservation of the scapula-coracoid sutural region on both bones. Likewise, it is not possible to compare the size of the coracoid to the ventral expansion of the scapula due to lack of definite association.

As preserved the coracoid approaches the sauropod condition of a sub-circular outline rather than the more dorsoventrally compressed, sub-oval outline seen in most basal sauropodomorphs. However, this element is incomplete and its exact dimensions cannot be adequately determined. The anterior and ventral margins appear to merge into one another and do not meet at an abrupt angle as in more derived sauropods such as *Apatosaurus*.

Posterior-most dorsal vertebra?

Four vertebrae are preserved in articulation, the posteriormost three are identified as a dorsosacral and two primordial sacral vertebrae. However, the anterior-most articulated vertebrae in the series is represented by a centrum with the ventral-most portion of the neural arch still fused to it. The anterodorsal part of the centrum and a portion of the neural arch comprising the

beginning of the prezygapophyses, postzygapophyses and base of the neural spine are dislocated from the centrum and have been pushed posterodorsally onto the anterodorsal region of the following vertebra (dorsosacral), thereby deforming and covering the prezygapophyses of the dorsosacral, as well as destroying the anterior articular facet. No hyposphene is preserved on the posterior aspect of the neural arch.

As in the ensuing vertebrae, the centrum posseses a subcircular and slightly dorsoventrally compressed posterior articular facet. The centrum is mediolaterally constricted at its midpoint and tapers ventrally. There are depressions on the lateral surfaces at the suture between the neural arch and the centrum. Like the sacral centra, this element also possesses neither a ventral keel nor shallow groove, but does exhibit slight degree of mediolateral compression ventrally.

Since the anterodorsal margin of the centrum is not well preserved, nor is there any information on the morphology of the transverse process, we cannot definitively determine whether this element represents an additional dorsosacral as interpreted for *Melanorosaurus* (Yates, 2007a). Therefore, assignation of this element as the posterior-most dorsal is made on the absence of firm evidence to the contrary.

Sacral Vertebrae

Three sacral vertebrae and a fourth anterior vertebra (? posterior dorsal) were found in articulation among the preserved material (NMQR 1705/30; Fig. 23). All sacral centra have subcircular and slightly dorsoventrally compressed articular facets. As in *Leonerasaurus* (Pol et al., 2011) their ventral surface is smooth and lacks both a true keel and a shallow groove, however the ventral surface of the centra does become more mediolaterally compressed. The only well-preserved ilium

of NMQR 1705 belongs to a much smaller individual and the articulation facets on the medial side are not visible, thus it is difficult to draw conclusions about the articulation of the sacral ribs with the ilium.

The two posterior most sacral vertebrae are identified as the primordial sacrals, as they are the only sacrals that have fused their centra through their articular facets and based on the morphology of the sacral ribs (see Pol et al, 2011; Wilson & Sereno, 1998; Yates, 2007). The preceding vertebra is interpreted as a dorsosacral.

The first vertebra, the dorsosacral, retains the prezygapophyses (which have been pushed posteriorly due to the dislocation of the preceding vertebra's neural arch) along with the ventral portion of the neural arch, the dorsosacral rib complex is preserved on the left side. The neural spine and postzygapophyses are missing. However, the base of the neural spine is transversely wider than in the two primordial sacrals. As with the preceding vertebra the centrum is mediolaterally constricted between the two articular surfaces.

The posterior articular surface of the dorsosacral centrum was glued at an offset to the left, thus the ribs of the dorsosacral are not in line with that of the first primordial along the transverse axis. However, it is apparent that the posterior ventral portion of the dorsosacral rib would definitely have contacted the anterior ventral portion of the first primordial sacral rib complex when articulated correctly, however they do not seem to have fused. Dorsoventrally, the dorsosacral rib is in line with the first and second primordial ribs, indicating that they would all have contacted the ilium at approximately the same level.

Therefore, based on the similar height compared to the first primordial rib it is evident that the dorsosacral rib would have attached to the ilium directly anterior to the first primordial sacral rib as in more derived sauropods, rather than more dorsally as seen in *Melanorosaurus* (NMQR 1551), *Mussaurus* (MLP-61-III-20-23) and *Leonerasaurus* (see Pol et al., 2011).

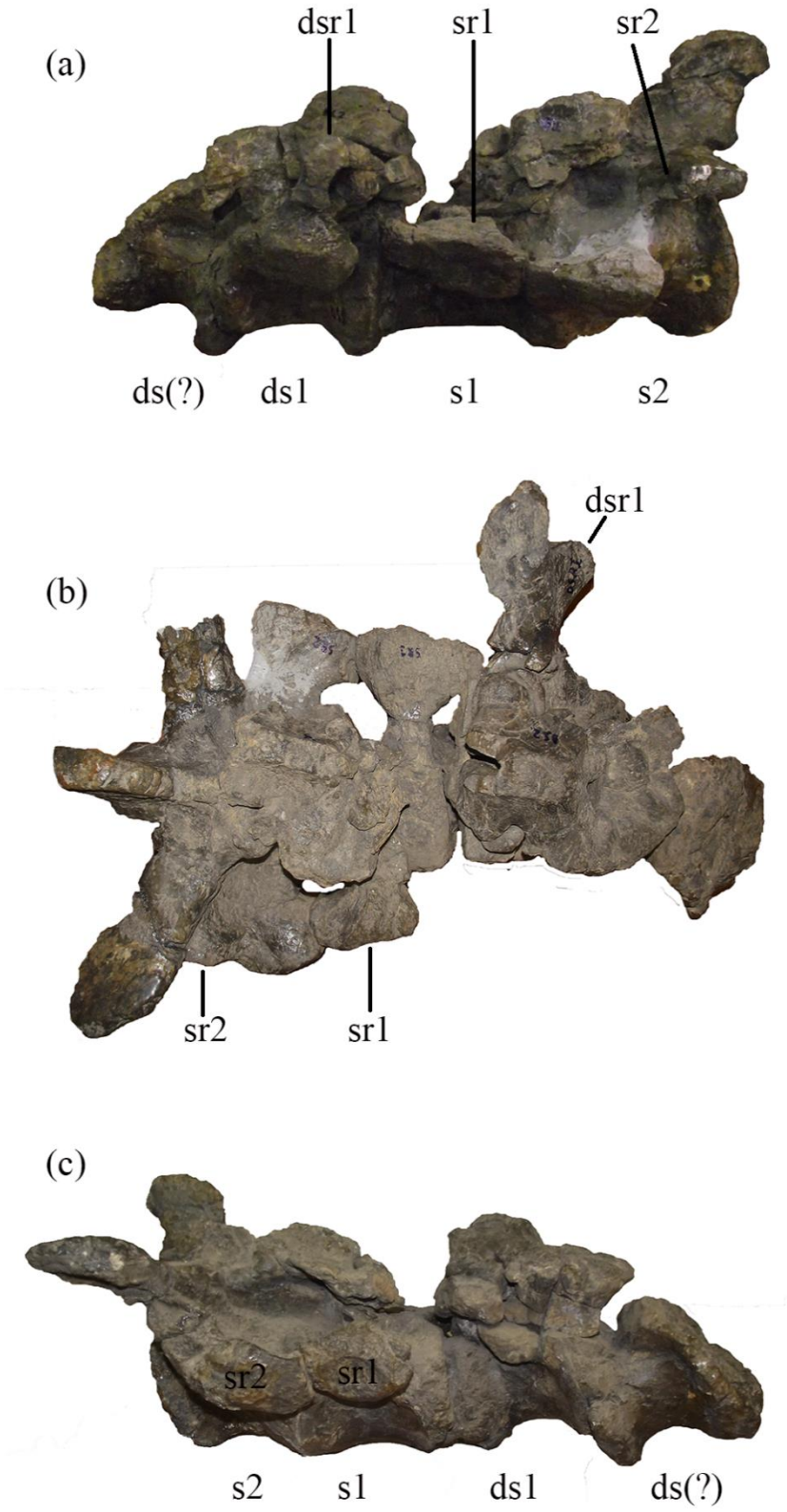

Figure 23. **Articulated sacrum (NMQR 1705).** (a) left lateral view (b) dorsal view (c) right lateral view. ?ds, potential dorsosacral ; ds1, first dorsosacral; dsr, dorsosacral rib; s1, first primordial sacral; s2, second primordial sacral; sr1, first primordial sacral rib; sr2, second primordial sacral rib. Scale = 5cm.

Dorsosacral

When aligned correctly it appears that an incipient sacro-costal yoke is formed by the rib of the dorsosacral and the two fused primordial ribs. While a sacro-costal yoke has been suggested as derived feature only found in eusauropods (Wilson & Sereno, 1998), a yoke-like structure is also present in the near-sauropod *Melanorosaurus*, *Massospondylus* (BPI/1/4934), *Jingshanosaurus*, and *Yimenosaurus* (Galton & Upchurch, 2004). However, the “yokes” of the latter four taxa do not form a medial extension to the acetabular surface as seen in sauropods such as *Barapasaurus* and appears to be present only in very large individuals (Wilson & Sereno, 1998; Galton & Upchurch, 2004; Galton et al., 2005).

The sacrocostal yoke present in NMQR 1705/30 bears a greater resemblance to these more basal forms in that it does not form a medial extension of the acetabular surface, but rather represents a fusion of the lateral margins of the sacral ribs. However, the posterior and anterior ends of the first and second primordial sacral rib iliac articular facets are slightly concave, but lacking an articulated ilium we cannot determine whether this mild concavity contributed to the rim of the acetabulum.

The dorsal and ventral parts of the dorsosacral rib are fused together dorsally, forming a single dorsosacral rib complex. In between the dorsal and ventral extent of the sacral rib complex, a laterally placed triangular fenestra is visible in anterior and posterior view, however this is not a feature and it is clearly visible that this is the result a missing piece of bone. The origin of the dorsosacral rib complex on the lateral surface of the centrum is extensive and starts at the middle (dorsoventrally) of the anterior margin of the centrum and proceeds posterodorsally for 60 % of the anteroposterior length of the centrum - in contrast this figure for *Melanorosaurus* (NMQR 1551), *Mussaurus* and

Leonerasaurus is approximately 50% (Galton et al, 2005; Pol et al., 2011; Otero & Pol, 2013).

The position of the dorsosacral rib is similar to the condition observed in *Melanorosaurus* (NMQR 1551) which occupies the anterior portion of the centrum laterally, projecting anteriorly past the anterior margin of the centrum - except for the more ventral placement of the dorsosacral rib. In *Mussaurus*, it also appears that the sacral rib would have originated on the anterior end of the centrum, however as the anterior portion of the centrum is not preserved, we cannot determine its dorsoventral position. In contrast, *Leonerasaurus* possesses a sacral rib that rises from the posterior end of the centrum (Pol et al., 2011), rather than the anterior end.

In terms of orientation, the dorsosacral rib extends acutely in an anteroventral to posterodorsal direction and expands as it approaches the ilium as a substantial dorsoventrally wide process. In *Melanorosaurus* (NM 1551), this feature is also angled acutely along its lateral articular surface. In contrast, *Leonerasaurus* possesses an obliquely oriented (anterodorsal to posteroventral) dorsosacral rib (Pol et al, 2011). This region is not preserved in *Mussaurus* (MLP-III-20-23).

In lateral profile, the dorsosacral rib is similar to the *en echelon* shape seen in the second primordial rib (see below), being composed of an anteroposteriorly expanded ventral (sacral rib) component, supplanted by a vertical lamina that is anteroposteriorly expanded dorsally, roofing a posterior concavity and a much smaller anterior concavity, resulting in an hourglass-shape in lateral view - which we identify as an autapomorphy of *Antetonitrus* (see Fig.23). This morphology does not conform to that seen in more basal sauropodomorphs (e.g. *Massospondylus, Adeopapposaurus, Riojasaurus,*

Jingshanosaurus, Leonerasaurus, and *Melanorosaurus).* It differs from the ovoid anteroventral-posterodorsal oriented dorsosacral rib seen in *Massospondylus* and *Jinghshanosaurus*; the distinctly laterally bifurcated dorsosacral rib morphology seen in *Riojasaurus* and *Adeopapposaurus* (with a prominent rectangular ventral portion of the rib, anteriorly projecting dorsal portion and posterior concavity); as well as the anterodorsal to posteroventral oriented lamina form seen in *Leonerasaurus*.

While the dorsosacral rib of NMQR 1705/30 does resemble the C- shaped morphology present in *Melanorosaurus* (NMQR 1551) most, it can be distinguished based on the anterior expansion of the dorsal part of the sacral rib complex, partly roofing a concavity on the anterior surface of the sacral rib and rendering the rib hourglass shaped in lateral view rather than strictly c-shaped. Furthermore, the ventral portion of the sacral rib does not extend beyond the anterior margin of the centrum.

First Primordial

The first primordial sacral preserves a portion of the neural arch but it is badly damaged, the neural arch remnant is dislocated posteriolaterally to the left, so that the base of the neural spine of the first primordial is not in-line with the neural spine or neural arch of the second primordial. The centrum and anteroposteriorly wide ventral portion of the rib complex is intact. The first primordial centrum is absolutely and relatively more constricted at its midpoint than the other sacral centra. NMQR 1705/30 lacks a geniculation at the posterior sutural contact between the sacral rib and the centrum of the first primordial sacral. Most sauropodomorphs, ranging from *Plateosaurus, Riojasaurus, Leonerasaurus, Mussaurus* to *Vulcanodon* also lack a geniculation at the sutural contact between the sacral rib and the centrum, however this feature is present in both of the primordial sacrals of *Melanorosaurus* (see

Yates, 2007a). Thus, while Moser (2003) has proposed that the presence of a geniculation at the costo-central suture is diagnostic of the second primordial sacral, *Melanorosaurus* proves the exception.

The first primordial's ventral portion of the sacral rib is fan-shaped in dorsal view, with concave anterior and posterior surfaces, as in most basal sauropodomorphs (e.g. *Riojasaurus*, *Massospondylus*, *Adeopapposaurus* & *Melanorosaurus*) and *Leonerasaurus* (Pol et al, 2011). It expands anteroposteriorly as it approaches the ilium. However, the dorsal portion of the sacral rib complex is not preserved, so we cannot make any conclusions about anteroposterior expansion of the dorsal portion and whether it roofs those concavities as in most basal sauropodomorphs.

In ventral view the medial area of attachment of the ventral portion of the sacral rib occupies the anterior half of the centrum, as in *Leonerasaurus* (Pol et al, 2011), *Mussaurus* (Otero & Pol, 2013) and *Melanorosaurus* (NMQR 1551) but is oriented at a slight angle posteroventrally to anterodorsally rather than in the opposite direction seen in *Massospondylus* (QG 1159), *Leonerasaurus*, *Mussaurus* or the horizontal orientation in *Melanorosaurus* (NMQR 1551). Based on the damaged neural arch it appears that the dorsal part of the sacral rib complex originated as an anteroposteriorly broad lamina, it was most likely fused to the ventral portion of the sacral rib as in the second primordial.

Second Primordial

The second primordial is the most intact vertebra of the sacrum and does not appear to be deformed. The centrum, neural arch, part of the neural spine and both sacral ribs are preserved. As in *Leonerasaurus, Mussaurus* and *Melanorosaurus*, the centrum

is absolutely and relatively broader and less mediolaterally constricted than the preceding centra, the posterior centrum articulatory surface is 120% wider than high.

The neural arch occupies the posterior two thirds of the centrum in contrast to *Leonerasaurus*, where it is placed anteriorly; or *Mussaurus* and *Melanorosaurus* (NMQR 1551), it occupies most of the anteroposterior length of the centrum. The neural spine is preserved, apart from the dorsal tip, and angled posterodorsally, together with the postzygapophyses, exceeding the posterior extent of the neural arch pedicles and posterior centrum margin. This differs from the condition observed in *Melanorosaurus* (NMQR 1551), where the neural spine does not exceed the posterior extent of the centrum margin. Only the ventral-most portion of the beginning of the neural spines of *Leonerasaurus* and *Mussaurus* are preserved, rendering a comparison impossible.

The neural spine occupies the majority of the dorsal surface of the neural arch, posterior to the prezygapophyses. Part of the prezygapophyses are preserved, but are under the dislocated neural arch of the first primordial. The position of the neural spine and prezygapophyses contrasts with the condition observed in *Leonerasaurus* and *Melanorosaurus* (NMQR 1551) where both the prezygapophyses and the neural spine project anteriorly, surpassing the anterior margin of the centrum (Pol et al, 2011). However, in *Mussaurus* it appears that the prezygapophyses do not exceed the anterior margin.

The postzygapophyses are incompletely preserved, but there seems to be evidence of a hyposphene underneath the base of the postzygapophyses. The neural canal is dorsoventrally narrow and measures 10mm in height. In *Melanorosaurus* (NMQR 1551) we can also observe a dorsoventrally narrow neural canal,

although there is no evidence of a hyposphene preserved. Due to the presence of caudosacral vertebrae in *Leonerasaurus* and *Mussaurus* we are unable to compare these features.

The second primordial sacral rib is fan-shaped in ventral view, expanding anteroposteriorly as it approaches the ilium, the area of attachment of the rib to the centrum is more extensive than in the preceding ribs, occupying 80% of the total centrum length, as opposed to 60% in *Leonerasaurus* (Pol et al., 2011), *Melanorosaurus* (NMQR 1551) and *Mussaurus*. In contrast to *Leonerasaurus* and *Mussaurus*, the area of attachment of the rib to the centrum occupies a more dorsal position, a trait shared with *Melanorosaurus* (NMQR 1551).

The ventral portion of the sacral rib extends anteriorly and contacts the posterior extension of the ventral portion of the first primordial sacral rib, they are in broad contact, laterally approaching the ilium it extends posteriorly to the midlength of the centrum and then slopes upwards posterodorsally at about 40 degrees and merges with the posteriolaterally swept dorsal part of the sacral rib complex (a characteristic of the second primordial [Yates, 2007]), rendering the entire sacral rib complex *en echelon* (inverted L-shaped with a posterior projection of the dorsal part of the sacral rib) in right lateral outline, rather than exactly L-shaped as in *Leonerasaurus*.

In more basal sauropodomorphs, (in right lateral view) the second primordial sacral rib complex ranges from L-shaped (e.g. *Leonerasaurus* [Pol et al, 2011]), to *en echelon* shaped as seen in *Melanorosaurus* (NMQR 1551), *Mussaurus* (MLP 61-III-20-23), *Riojasaurus* (PVL 3808), *Plateosaurus longiceps* and *Massospondylus* (Galton & Upchurch, 2004).In contrast to most of these basal forms, in NMQR 1705/30 there is no anterior concavity roofed by the anterior extent of the dorsal part of the

sacral rib (e.g. *Riojasaurus*, *Melanorosaurus*, *Leonerasaurus* or *Plateosaurus longiceps*). Barring the lack of an anterior expansion of the dorsal part of the sacral rib, the second primordial sacral rib complex of NMQR 1705/30 is most similar to that of *Melanorosaurus* (NMQR 1551) and *Mussaurus* (MLP 61-III-20-23).

Posteriorly, at the suture between the rib and centrum is a “geniculation” or step as mentioned by Moser (2003) that is diagnostic of the second primordial, this feature is present in a range of sauropodomorphs from *Plateosaurus, Massospondylus* (BPI/1/4257), *Riojasaurus, Leonerasaurus, Mussaurus* to *Vulcanodon* (Moser, 2003; pers. obs.). However, this geniculation is also present in the first primordial in *Melanorosaurus* (Yates, 2007a), rendering its use as a diagnostic feature of the second primordial uncertain.

The posterior aspect of the second primordial sacral rib of NMQR 1705/30 does not exhibit any evidence that a caudosacral rib was attached to it in contrast to the prominent scars on the dorsolateral corners of the posterior surface of the second primordial sacral rib of *Melanorosaurus* (Yates, 2007a). The lack of evidence of contact between the second primordial sacral rib and a caudosacral rib indicates that the caudosacral may have attached to both the ilium and second primordial, rather than exhibiting the condition hypothesised by Yates (2007a) for *Melanorosaurus* (NMQR 1551) - in which the caudosacral is wholly attached to the second primordial sacral.

While no caudosacral vertebrae has been preserved, McPhee et al (2014) have identified potential candidates amongst two neural arches BPI/1/4952 and BPI/1/5091.These neural arches appear to have sacral rib articular surfaces, discounting the likelihood that they are simply anterior caudal neural arches

(McPhee et al, 2014) and do not appear to belong to any of the neural arches preserved in the NMQR 1705/30 sacrum. Based on this material, it appears that *Antetonitrus* would have possessed a caudosacral vertebra - indicating that the sacrum of *Antetonitrus* would have consisted of at least a dorsosacral, two primordial sacrals and a caudosacral (DS+S1+S2+CS).

Ilia

While McPhee et al. (2014) have identified an ilium pertaining to *Antetonitrus* (NMQR 1545), its ischial peduncle and supracetabular crest are reconstructed with plaster and the pubic peduncle is lacking. Three right ilia are included in NMQR 1705: two very fragmentary partial ilia (NMQR 1705/011 and NMQR 1705/214) and one much smaller almost complete right ilium (NMQR 1705/591). There is a considerable size-difference among the preserved ilia of NMQR 1705. Although both the anterior-most and posterior-most portions of NMQR 1705/011 are broken, the distance from anterior most point of preacetabular process to posterior-most point of postacetabular process is a minimum of 420mm compared to 319mm in NMQR 1705/591.

Given NMQR 1705/591 is almost complete the description will be based primarily on this smaller ilium (Fig. 24). The general morphology is congruent with that of non-eusauropod sauropodomorphs. The iliac blade is dorsoventrally low above the acetabulum and anteroposteriorly long in relation. The dorsal margin of the ilium in lateral view is slightly convex. In dorsal view it curves slightly laterally anteriorly and posteriorly, thus being weakly convex above the acetabulum region and sub-parallel to the sagittal axis, a similar morphology as in *Lessemsaurus* and other basal sauropodomorphs.

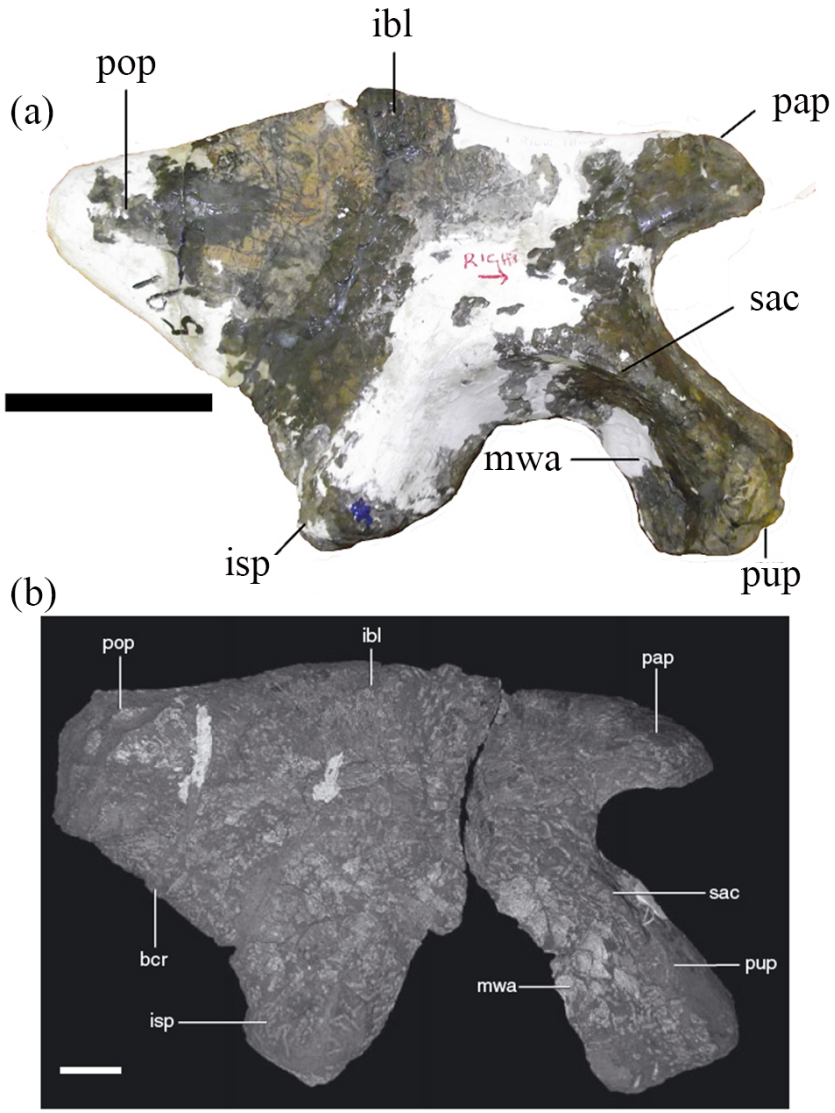

Figure 24. Right ilia. (a) right ilium (NMQR 1705/591) in lateral view. ibl, iliac blade; isp, ischial peduncle; mwa, medial wall; pap, preacetabular process; pop, postacetabular process; pup, pubic peduncle. Scale = 10cm (b) right ilium of *Lessemsaurus* in lateral view from Pol & Powel, 2007. Scale = 5cm.

The anterior extent of the preacetabular process does not extend further forward than the anterior end of the pubic process, contrasting with the anteriorly projected preacetabular process of *Anchisaurus* and *Leonerasaurus*. The preacetabular process is short and triangular with its apex directed anteriorly and dorsoventrally low relative to the iliac blade above the acetabulum as in *Lessemsaurus*, *Leonerasaurus,* and all non-eusauropod sauropodomorphs (Pol & Powell, 2007). The

preacetabular process is not anteriorly expanded as in *Anchisaurus polyzelus*, *Melanorosaurus readi* (NMQR 3314) and eusauropods (Pol et al., 2011). It forms an angle of approximately 70 degrees with the pubic process. It is not clear whether the dorsal margin of the preacetabular process is continuous with the dorsal margin of the iliac blade (Pol & Powell, 2007), as the dorsal margin between the preacetabular process and the iliac blade is not preserved and reconstructed with plaster. However, based on the left ilium of NMQR 1545 it would appear that this taxon did not possess a stepped margin as in some non-eusauropod sauropodomorphs (Pol & Powell, 2007; Galton et al, 2005; McPhee et al., 2014).

The ilium lacks the thick buttress at the base of the preacetabular process which contacts the supraacetabular crest ventrally that is present in basal dinosauriformes and the basal sauropodomorph *Chromogisaurus* (Ezcurra, 2010). The medial wall of the acetabulum circumscribes a fully open acetabulum as in most sauropodmorphs more derived than *Saturnalia*. Although the distal surface of the pubic peduncle is eroded, its preserved length (126mm) is slightly less than twice the anteroposterior width of its distal end as preserved (138mm).

As in all basal sauropodomorphs the anterior portion of the supracetabular crest is more developed than the posterior portion. The supracetabular crest extends along the entire pubic peduncle as a moderate ridge, resembling the intermediate condition found in *Lessemsaurus* (but slightly more pronounced), between the laterally directed broad shelf seen in *Chromogisaurus* and other basal sauropodomorphs and the lack of a large supracetabular crest seen in eusauropods (Ezcurra, 2010; Pol & Powell, 2007).

There is no posteriorly projecting heel at the distal end of the ischial peduncle, differing from the presence of this process in *Plateosaurus*, *Riojasaurus*, *Lufengosaurus*, *Coloradisaurus*, *Pantydraco*, and *Ruehleia*. The ischial peduncle is shorter than the pubic peduncle, resembling the condition seen in *Lessemsaurus*, *Leonerasaurus*, and *Plateosaurus* (Pol & Powell, 2007), although not as short as in *Kotasaurus*, *Vulcanodon* and eusauropods (e.g., *Shunosaurus*; Pol & Powell, 2007; Carrano, 2005).

The length of the postacetabular process is 79% of the distance between the pubic and ischial peduncles. This ratio may be higher, as the posterior-most tip of the postacetabular process is not preserved and reconstructed with plaster. Unlike *Lessemsaurus*, the dorsal margin of the postacetabular process is not mildly concave, but straight and runs anterodorsally at an angle of approximately 20 degrees to the longitudinal plane.

The dorsal half of the posteroventral margin and the posterior tip of the postacetabular process are not preserved and reconstructed with plaster. However, the preserved portion of the posteroventral margin lacks any signs of a brevis fossa and shelf, a condition also present in the specimen NMQR 1545 and that represents the derived sauropod condition (Upchurch et al, 2004). A thin brevis crest is present in NM 1545 (McPhee et al., 2014), however this part is not preserved in NMQR 1705/591. Based on NMQR 1545 it appears that the ‘brevis crest’ morphology described by Pol & Powell (2007) for *Lessemsaurus*, was present in *Antetonitrus* as well, although to a lesser degree.

The postacetabular process is not completely preserved, but based on the portion preserved in NMQR 1545 McPhee et al. (2014) noted it appears that it would have been bluntly rounded to subrectangular. In contrast to *Melanorosaurus* and

Lessemsaurus, Antetonitrus appears to have the morphology seen in *Riojasaurus* of a pointed ventral corner with a rounded posterodorsal margin.

Ischia

Two partial conjoined ischia (NMQR 1705/233 and NMQR 1705/N213A) and a single right ischial shaft (NMQR 1705/007) have been preserved. NMQR 1705/233 is almost complete and will form the basis of the description, lacking only the proximal part of the right ischium and the proximoventral portion of the left obturator plate (reconstructed with plaster; see Fig. 25). The ischium is similar to that of other basal sauropodomorphs and *Pulanesaura*. There is no evidence of a notch separating the posteroventral end of the obturator plate from the shaft (e.g. *Plateosaurus*). An elongate interischial fenestra is absent and conforms to the general sauropodomorph condition. An ischial groove (dorsolateral sulcus) is present along the dorsolateral area of the proximal ischium, this feature is common to Saurischia (except *Herrerasaurus*, Yates 2003; Otero & Pol, 2013). The ischial shaft is long and rod-like (271.1), the typical dinosaurian condition. It is sub-triangular in cross section as in most basal sauropodomorphs and is distally dorsoventrally expanded. Thus, in distal view the conjoined ischia are V-shaped as in most basal sauropodomorphs (e.g. *Massospondylus, Plateosaurus, Coloradisaurus*, *and Mussaurus*).

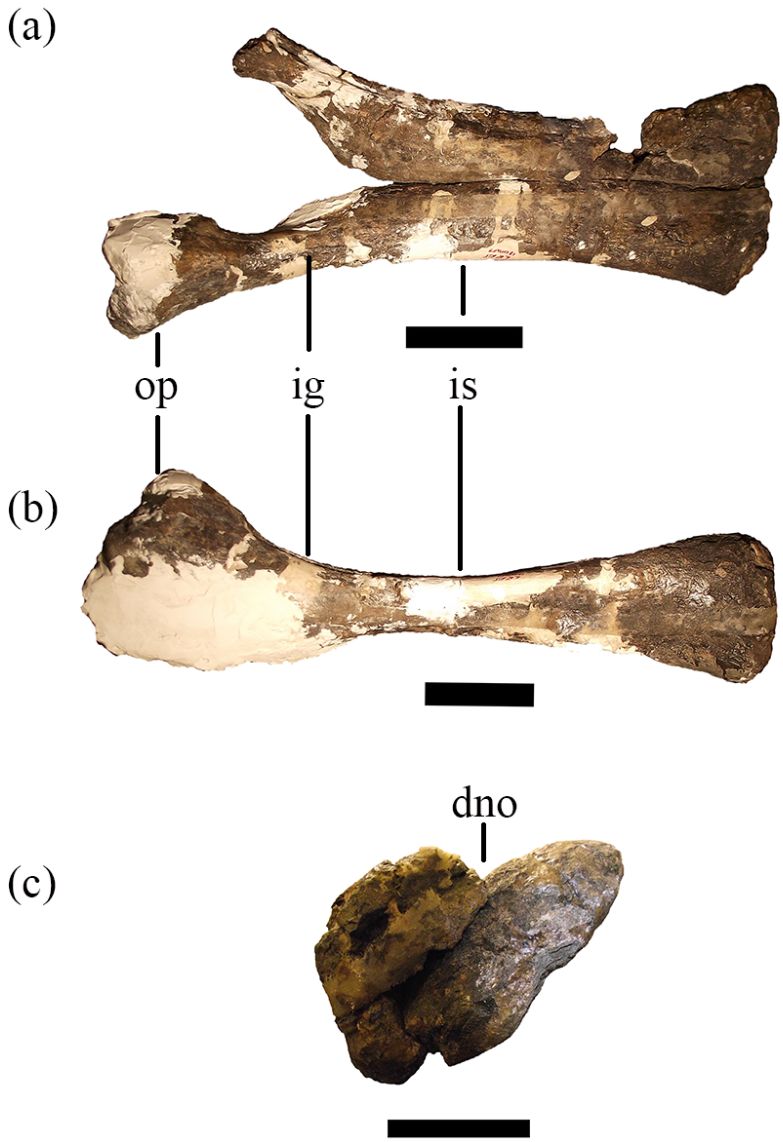

Figure 25. Conjoined ischia (NMQR 1705/233). (a) dorsal view (b) left lateral view (c) distal view. op, obturator plate; ig, ischial groove; ischial shaft; dno, dorsal notch. Scale = 10cm.

Astragalus

A right and left astragali are preserved, the right (NMQR 1705/633; Fig. 26) is complete, only missing the proximal tip of the ascending process, and forms the basis of this description. The long axis of the body runs mediolaterally. In dorsal view the

astragalus has a straight anterior margin, the medial margin gradually merges into the posterior margin, forming a rounded posteromedial region. The posterior margin continues parallel to the anterior margin after this. The posterolateral corner is slightly rounded, the lateral margin proper is almost perpendicular to the anterior margin.

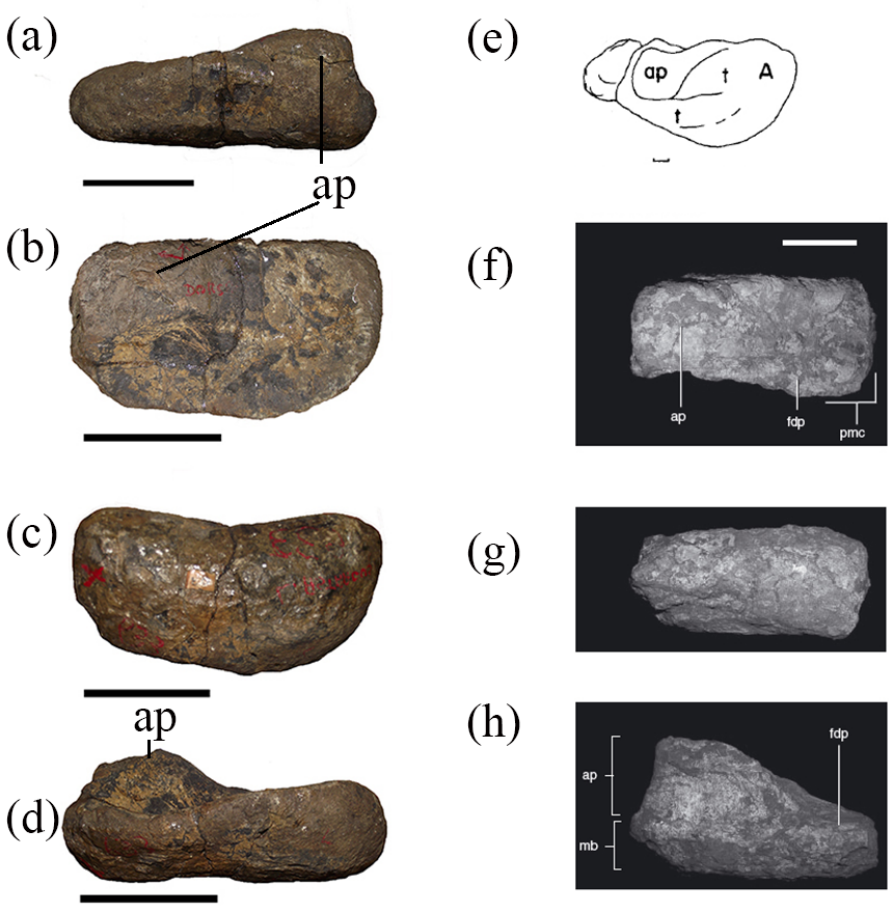

Figure 26. Astragali. (a) – (d) NMQR 1705/633 astragalus. (a) anterior (b)dorsal (c) ventral (d) posterior.Scale = 10cm. (e) *Blikanasaurus* astragalus in dorsal view from Galton & Van Heerden, 1998. Scale = 5cm. (f) – (h) *Lessemsaurus* astragalus from Pol & Powell, 2007. (f) dorsal (g) ventral (h) posterior. Scale = 5cm. ap, ascending process.

Bordering the dorsolateral edge is the fibular facet, which is largely vertical, except that ventrally it extends slightly laterally (where it would abut the calcaneum), NMQR 1705/633 does not possess a medioventral depression like *Blikanasaurus* (Galton & Van Heerden, 1998), but it is rather mediodorsally depressed

relative to a mild ventrolateral expansion, forming a mild concavity when viewed anteriorly (see Sereno, 1999). Thus, there is no ventromedial expansion of the calcaneum as in *Melanorosaurus* and *Blikanasaurus* (Galton & Van Heerden, 1998).

The astragalus contrasts with *Blikanasaurus* and *Lessemsaurus* in that in dorsal or ventral view the astragalus is approximately the same width anteroposteriorly on the lateral (100mm) and medial (98mm) sides as opposed to the lateral constriction present in the other two taxa (Galton & Van Heerden, 1998; Pol & Powell, 2007), thus it is more robust. It has a similar slope from the anterior, proximal, lateral side (including the ascending process) to the proximal anterior medial side of 83mm (versus 70mm in *Blikanasaurus*) to 54mm (versus 40mm) (Galton & Van Heerden, 1998).

Unlike *Blikanasaurus*, there is no anterior fossa of the ascending process evident. The ventral surface of the astragalus is convex to a similar degree of *Blikanasaurus'* 'rolling joint' (Galton & Van Heerden, 1998), in fact the convexity of the ventral surface is a feature also shared with *Lessemsaurus*, non-eusauropod sauropodomorphs and basal eusauropods (Pol & Powell, 2007). In ventral view the astragalus is oval, but with a straight anterior margin and a slight posteriorly directed indentation along this margin in the middle. In anterior view the proximodistal depth of the astragalar body is largely constant, as in *Lessemsaurus* (Pol & Powell, 2007). This represent the basal state rather than the wedge-shaped eusauropod state (Wilson & Sereno, 1998). The posteromedial margin of the astragalus in dorsal view is evenly rounded without the formation of a posteromedial corner (Wilson & Sereno, 1998), this is in contrast to the right angle seen in *Lessemsaurus* (Pol & Powell, 2007). There is no evidence of a pyramidal dorsal process on the posteromedial corner of the

astragalus, presence of this is a more derived sauropod condition (Yates 2007).

The ascending process of the astragalus is transversely wider than anteroposterior deep, it is a thick substantial process, transversely it occupies 46 percent of the mediolateral length and 50 percent of the anteroposterior width (anteriorly) of the body (see Yates 2007). This contrasts with *Lessemsaurus*, where the ascending process occupies 70 percent of the mediolateral and 83 percent the anteroposterior extent of the astragalar body (Pol & Powell, 2007). Thus, the posterior extent of the ascending process is located more anteriorly to the posterior margin of the astragalus than in *Lessemsaurus*, *Vulcanodon* and *Tazoudasaurus* (Wilson and Sereno, 1998; Pol & Powell, 2007), however none of these taxa possess a posterior extension of the ascending process approaching the condition seen in *Mamenchisaurus* and neosauropods (Pol & Powell, 2007)

There is an absence of a sharp medial margin around the depression posterior to the ascending process (Novas, 1996). There is no buttress dividing the posterior fossa and supporting the ascending process. (Wilson & Sereno, 1998). There is no evidence of a vascular foramina at the base of the ascending process in anterior view in contrast to in non-eusauropod sauropodomorphs, *Blikanasaurus* and *Lessemsaurus* (Galton & Van Heerden, 1998; Pol & Powell, 2007) – a trait shared with *Vulcanodon* and Eusauropoda (Pol & Powell,2007). There is also a lack of foramina posterior to the ascending process in dorsal view as in more derived sauropods (see Wilson & Sereno, 1998; Pol & Powell, 2007).

Pes

A complete right pes (Fig. 27) is preserved including all metatarsals and phalanges.

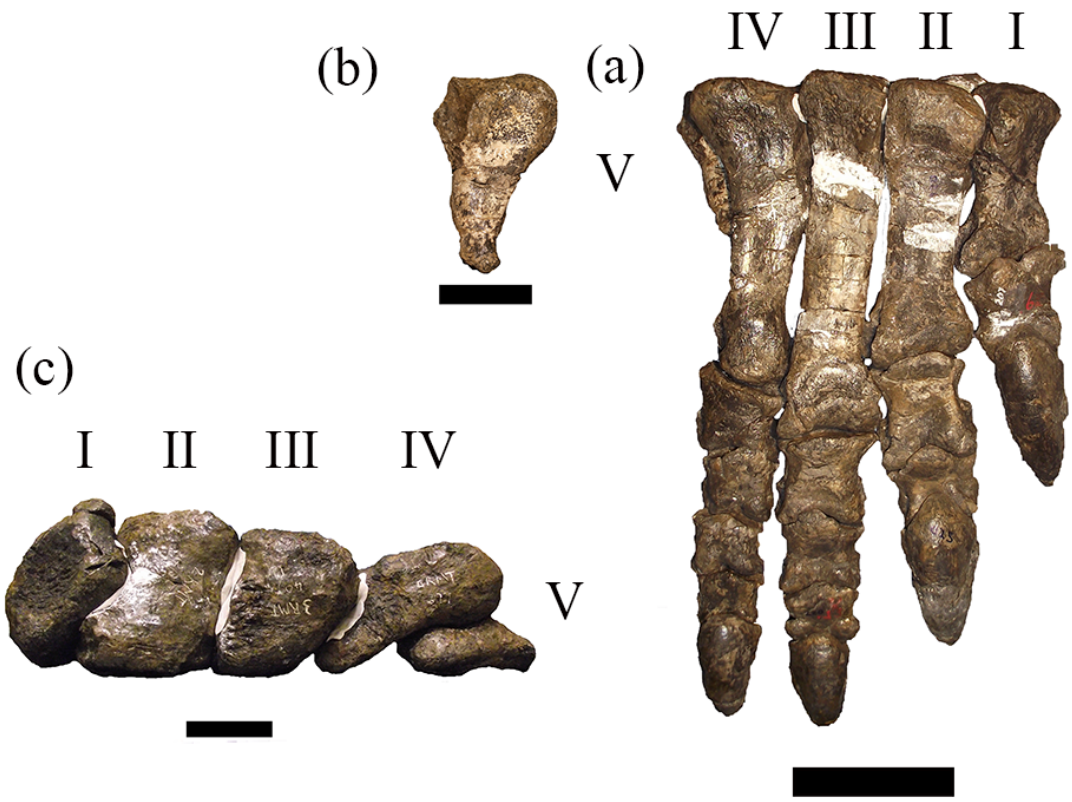

Figure 27. **NMQR 1705 articulated right pes.** (a) plantar view. Scale = 10cm. (b) metacarpal V in plantar view. Scale = 5cm (c) pes in proximal view. Scale = 5cm.

Metatarsals

Metatarsal I is short and robust. The proximal width of metatarsal I is slightly greater than that of metatarsal II (87 mm and 79mm respectively), this trait is shared with *Blikanasaurus*, *Melanorosaurus* and Neosauropoda. Orientation of the proximal articular surface of metatarsal I is horizontal as in most non-eusauropod sauropodomorphs. The transverse axis of the distal end of metatarsal I is angled proximomedially as in most sauropodomorphs. The medial distal condyle of metatarsal I is dorsoventrally smaller than the lateral distal condyle. The shaft of metatarsal I is only closely appressed to that of metatarsal II proximally, with space between them distally.

The medial margin of the proximal surface of metatarsal II is concave as in non-eusauropod sauropodomorphs and eusauropods, but not neosauropods. The lateral margin of the

proximal surface of metatarsal II is straight, in contrast to the more concave morphology seen in basal sauropodomorphs, *Blikanasaurus* and *Lessemsaurus*, but not more derived sauropods. The minimum transverse shaft diameters of the third and fourth metatarsals are greater than 60% of the minimum transverse shaft diameter of metatarsal II. This is generally the condition seen in all but the most derived sauropodomorphs (i.e. *Omeisaurus*, *Mamenchisaurus* and Neosauropoda) and interestingly *Blikanasaurus*. Indicating that *Blikanasaurus'* metatarsal II was more robust compared to metatarsal III and metatarsal IV. There appears to be no ventrolateral flange on the plantar surface of metatarsal II in proximal view as the lateral margin is straight in proximal view. A ventromedial flange on plantar surface of metatarsal II in proximal aspect is not present. Unlike in *Coloradisaurus*, *Lufengosaurus* and *Glacialasaurus*, there is a lack of a well-developed facet on the proximolateral corner of the plantar ventrolateral flange of metatarsal II for articulation with the medial distal tarsal.

The proximal outline of metatarsal III is subtriangular with an acute posterior border as in most sauropodomorphs.

In terms of the transverse width of the proximal end of metatarsal IV, it is greater than twice the anteroposterior depth of the proximal end, although the plantar tip is broken, the complete measurement would have to exceed 57mm in order for the transverse width to be less than twice the anteroposterior width. Metatarsal IV NMQR 1705/CS3 and NMQR 1705/N188 are less well preserved, but exhibit similar measurements. The transverse width of the distal articular surface of metatarsal IV is greater than the anteroposterior depth, this is generally the sauropodomorph condition (apart from more basal forms such as *Saturnalia*, *Jaklapallisaurus*, *Nambalia*, *Guibasaurus*, *Plateosaurus*, *Riojasaurus* and surprisingly more derived forms

such as *Melanorosaurus*, *Blikanasaurus* and *Lessemsaurus*). The angle formed by the anterior and anteromedial borders of Metatarsal IV is obtuse as in *Vulcanodon* in contrast to the condition seen in *Mussaurus*.

Metatarsal V is missing a small portion of its proximolateral corner. Despite this, the transverse width of the proximal end exceeds 50% of total length of metatarsal V by 13% (79mm versus 126mm). This trait is generally present in most members of Massopoda. It exhibits the non-eusauropod sauropodomorph condition of a reduced non-weight bearing form. The adaption towards a robust weight bearing morphology occurs from *Tazoudasaurus* onwards (see He et al., 1998; Allain & Aquesbi, 2008). Metatarsals IV and V appear to be plantar to metatarsals I-III as in more derived sauropods.

Discussion

Phylogenetic Relationships

The initial heuristic search resulted in 70 most parsimonious trees (MPTs) of 1532 steps found in 8 out of 1000 replicates. A further round of TBR branch swapping of these 70 trees resulted in 3 744 MPTs of the same tree length (CI=0.307, RI= 0.671).

The strict consensus tree exhibits several polytomies (see Appendix 2). This is due to the instability of seven taxa due to character conflict and missing data identified using the IterPCR procedure (Pol & Escapa, 2009): *Blikanasaurus*, *Chromogisaurus*, *Glacialasaurus*, *Ingentia*, NMQR 1334, *Meroktenos,* and PULR 136.

When the above-mentioned unstable taxa were excluded from the consensus a posteriori, *Antetonitrus* (recoded with NMQR 1705)

was recovered in a reduced strict consensus summary (Fig. 28) of all the MPTs, as a basal sauropod (*sensu* Yates, 2007) lying outside the clade containing (*Leonerasaurus* + More Derived Sauropods). It is the sister-taxon of *Ledumahadi*, that together, form a polytomy with *Lessemsaurus*.

The position of *Antetonitrus* largely corroborates the results found in both the initial Yates (2007) and McPhee et al. (2014) analyses as a basal sauropod, as well as all Yates (2007) based analyses in between (i.e. Ezcurra & Apaldetti, 2012; Otero & Pol, 2013, Müller et al, 2018; Apaldetti et al, 2018; McPhee et al, 2018). Due to the exclusion of *Ingentia* from the reduced strict consensus based on its instability, a monophyletic Lessemsauridae no longer exists, as *Lessemsaurus* and [*Antetonitrus*+*Ledumahadi*] form a polytomy, differing from a monophyletic Lessemsauridae found in McPhee et al. (2018) and Apaldetti et al. (2018). However, the relationship of *Antetonitrus* and *Ledumahadi* as sister-taxa is maintained when compared to McPhee et al. (2018). It is possible that with more character scores for *Ingentia* (see Appendix 2 for details), Lessemsauridae (sensu Apaldetti et al., 2018) may be resurrected. Nodes within Sauropodomorpha generally have a bremer support value no higher than 3, GC bootstrap values are extremely low and rarely >50.

Despite its fragmentary nature and frequent pruning from phylogenies, *Camelotia* is not identified as an unstable taxon and is resolved as the basal-most sauropod taxon. This result differs from that of McPhee et al. (2014) and Otero & Pol (2013) in that *Blikanasaurus* is no longer resolved as the basal-most sauropod, which now forms a polytomy with *Antetonitrus, Lessemsaurus, Ledumahadi, Sefapanosaurus* and several other taxa in the strict consensus tree (see Appendix 2). Nevertheless, the position of these taxa, still gives them primacy in terms of understanding

the origin of Sauropoda.

Melanorosaurus (NMQR 1551) forms the immediate outgroup to Sauropoda, while *Camelotia* has been excluded from most analyses, it was not identified as unstable in this analysis and retained. The position of *Melanorosaurus* is concomitant with that found in previous analyses (Yates, 2007; Pol et al, 2011; Ezcurra & Apaldetti, 2012; Otero & Pol, 2013; McPhee et al, 2014).

Basal to the node containing *Melanorosaurus* are the southern African basal sauropodiform (Sensu Sereno, 2007) taxa *Sefapanosaurus* and *Aardonyx*, which now form a clade with *Aardonyx* as the sister taxon to [*Eucnemesaurus entaxonis* + *Eucnemesaurus fortis*] and *Mussaurus* as the basal-most sauropodiform.

We retain the definition of Sauropodiformes *sensu* Sereno (2007) rather than adopt that of McPhee et al. (2014), as the latter definition points to the group almost identical in taxonomical composition to the one using the definition of Anchisauria used by several authors (Galton and Upchurch, 2004; Upchurch et al., 2007; Yates, 2007). Sauropodiformes *sensu* Sereno (2007) also has higher bremer support values, rendering it a better supported clade. Furthermore, the utilisation of the definition of Sauropodiformes given by McPhee et al. (2014) leaves us without a clade name to cluster the transitional taxa immediately outside Sauropoda (i.e. *Mussaurus, Sefapanosaurus, Aardonyx, Melanorosaurus* [NMQR 1551] and *Eucnemesaurus* spp.) along with sauropods. The redefinition of Sauropodiformes by McPhee et al. (2014) was based on the fact that the specifier taxon, *Mussaurus*, was only known from juvenile material at his stage of writing. However, Otero & Pol (2013) have since described a wealth of adult material pertaining to *Mussaurus* rendering this

a non-issue. Furthermore, Sauropodiformes (*sensu* Sereno, 2007) is much better supported compared to this novel definition of Sauropodiformes with a bremer support value of two as opposed to zero.

However, in the current analysis *Leonerasaurus* is no longer recovered as a basal sauropodiform, but rather is nested within Sauropoda and positioned as more derived than (*Antetonitrus* + *Ledumahadi*).

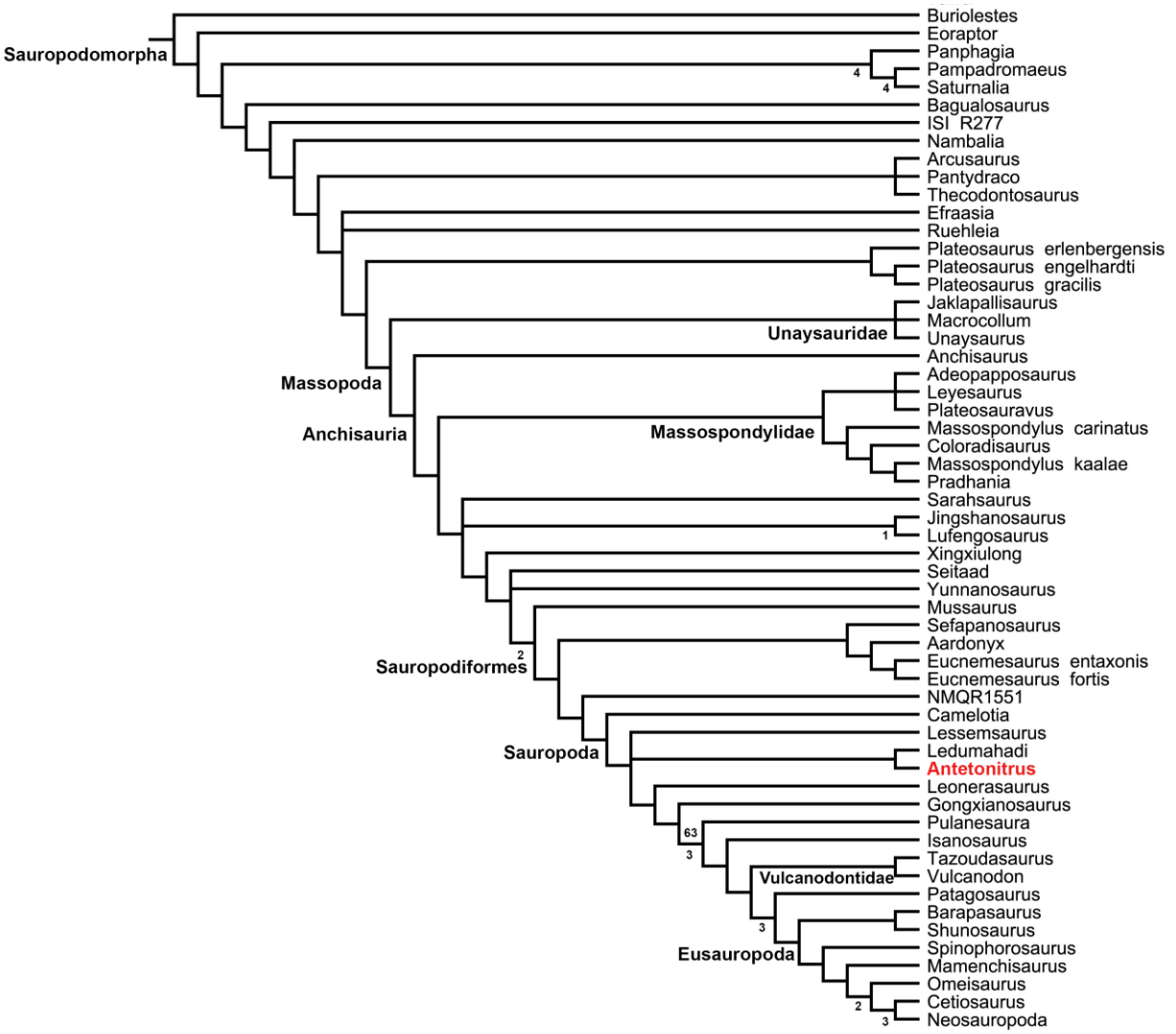

Figure 28. Reduced Strict Consensus summary. 3,744 Most Parsimonious Trees (MPTs) with a best score of 1532 (CI= 0.307, RI = 0.671), after seven unstable taxa: *Blikanasaurus*, Chromogisaurus, *Glacialasaurus*, *Ingentia*, NMQR 1334, *Meroktenos,* and PULR 136 were excluded from the consensus. Numbers below the branches represent bremer support and above the branches bootstrap values. Only sauropodomorph taxa are shown (for the complete consensus tree, including all taxa, see Appendix 2).

Leonerasaurus is united with more derived sauropods via a single unambiguous synapomorphy: the shape of the lateral margin of the proximal surface of the second metatarsal is straight (Character 377).

Antetonitrus: dental, pedal and sacrum evolution in basal/transitional sauropods

While poorly preserved, the single tooth (NMQR 1705/028) described here indicates that *Antetonitrus* exhibited a dentition morphology similar to basal sauropodomorphs rather than more derived sauropods. The SI range for basal sauropodomorphs is 1.56 -2.43 and for basal sauropods 1.16 – 2.42, indicating a substantial overlap in terms of tooth broadness (Chure et al., 2010). The SI value for the phylogenetically closest sauropod (bar *Leonerasaurus* in this study) is 1.45 for *Gonxianosaurus* (Chure et al., 2010). Including the SI data for NMQR 1705/028 into Chure et al's (2010) dataset would increase the SI range for basal sauropods to 1.16 – 2.7. Interestingly, an SI of 2.7 falls within the range given by Chure et al. (2010) for macronarians. This raises two possibilities, that the extremely slender tooth of NMQR 1705 is a retained primitive characteristic and the level of slenderness of basal sauropodomorphs is greater than previously thought or that the SI of NMQR 1705 is homoplastic with regard to more derived sauropods indicating that sauropod dental adaptations must have only occurred from *Gonxianosaurus* and more basal gravisaurian sauropods onwards (Allain & Aquesbi, 2008) (e.g. *Tazoudasaurus*).

While this new material provides evidence of a sauropod-type sacrum in *Antetonitrus*, it cannot be used as definite evidence for obligatory quadrupedalism. Pol et al. (2011) have shown that the presence of a sauropod-type sacrum in *Leonerasaurus*, a small non-sauropod sauropodiforme (according to their phylogeny), indicates that sacral configuration may be

decoupled from increases in body size and thus obligatory quadrupedalism. If the first vertebra in the sacral block is actually an additional dorsosacral, *Antetonitrus* would have had a five vertebrae sacrum, like *Melanorosaurus*, indicating that this would be the plesiomorphic state for sauropods. However, if the preserved four vertebrae state of NMQR 1705 reflects the actual sacral count in *Antetonitrus*, we see that the incorporation of dorsosacral vertebrae into the sacral block is plastic within (*Melanorosaurus* + Sauropoda), which contrasts with the stable presence of a caudosacral vertebra in these taxa. The presence of an incipient sacro-costal yoke in *Antetonitrus* needs to be viewed as a function of allometry primarily, due to its similarity to structures in large specimens of phylogenetically distant basal sauropodmorphs (i.e *Massospondylus*, *Jinghshanosaurus* and *Yimenosaurus*). It is likely that the presence of this feature in the basal sauropod lineage due to initial increases in size relative to more basal sauropodomorphs, provided the platform for the evolution of the proper sauropod sacro-costal yoke (which contributes to the rim of the acetabulum) seen in progressively larger more derived sauropod taxa. Thus, while in *Antetonitrus* (and *Melanorosaurus*) the presence of an incipient sacro-costal yoke can be viewed as a transitional feature en route to Sauropoda in this particular lineage, it is not always the case and does arise independently in phylogenetically distant sauropodomorphs.

When looking at the pelvic girdle, the ilium still shows a morphology very similar to basal sauropodomorphs (as is the case in *Lessemsaurus*), but with incipient morphological changes toward the sauropod condition, such as a shortening of the ischial peduncle and the lack of the brevis fossa and shelf. The lack of the latter is a key characteristic that indicates *Antetonitrus* was more derived than *Lessemsaurus* in this regard. Overall, the ischium of *Antetonitrus* and *Lessemsaurus* both still

reflect a morphology reminiscent of basal sauropodomorphs such as *Plateosaurus englehardti*.

In addition to the conservative morphology of the pelvic girdle, the oval/kidney-shaped morphology of the astragalus and more anterior termination of the posterior margin of the ascending process appears closer to that of basal sauropodomorphs than more derived sauropods such as *Vulcanodon* and *Shunosaurus*, where the element becomes wedge-shaped.

The morphology of the metatarsus also indicates that *Antetonitrus* possessed incipient adaptions towards the entaxonic sauropod stance, with the robust first metatarsal showing a shift in the distribution of weight on the metatarsus towards the medial side (Yates & Kitching, 2003). However, the initial nature of this shift must be emphasised as metatarsals III –V are still more than 65% the width of metatarsals I and II as opposed to the opposite condition seen in eusauropods (Wilson & Sereno, 1998).

Conclusions

While the holotypic material of *Antetonitrus* (BPI/1/4952) has recently been identified as coming from the Early Jurassic UEF (McPhee et al., 2017) as opposed to the Late Triassic LEF as previously held (Yates & Kitching, 2003), NMQR 1705 shows that this genus occurred across the Triassic-Jurassic boundary. The presence of *Antetonitrus* (NMQR 1705) in the Late Triassic LEF in addition to the UEF (BPI/1/4952) reduces the temporal gap (McPhee et al., 2017) between it and its sister taxon, *Lessemsaurus*.

The transitional nature of *Antetonitrus* is reinforced by the combination of sauropod-like sacrum and basal sauropodomorph-like pelvic girdle. Dorsosacral acquisition in

Sauropoda can no longer be considered linear and additive, but exhibits a degree of plasticity in terms of count. Furthermore, the presence of an incipient sacro-costal yoke is not necessarily a sauropod synapomorphy as initially assumed by Wilson & Sereno (1998), however in the case of *Antetonitrus* and *Melanorosaurus* we believe this structure to presage the more robust yoke seen in more derived sauropods. In terms of sacral rib morphology, we see a high degree of variation in terms of placement on the centrum body and shape. However as with the sacro-costal yoke, similarity in morphology is not strictly tied to phylogenetic affinity in taxa, suggesting that variation in morphology should be explained in terms of function rather than phylogeny for this feature.

This mosaic morphology of *Antetonitrus* is underscored by sauropod-type femora (i.e. elliptical in cross-section and straight in anterior view) coupled with a pes that is just starting to develop an entaxonic morphology. Based on NMQR 1705 it appears that morphological changes geared towards quadrupedality in the postcrania might have occurred prior to changes in dentition in basal sauropods Changes in the pelvic girdle and pes are very conservative compared to those in the sacrum and hindlimb. Considering the above, it is evident that *Antetonitrus* represents the clearest picture of the morphology of the earliest sauropods and the changes that occurred in the transition from basal sauropodomorph to the more derived sauropod condition.

Mef
Museo Paleontológico Egidio Feruglio

Trelew, February 7th, 2019

To whom it may correspond:

I declare that I agree that the article "The long bone histology of *Antetonitrus ingenipes*" may be included as a chapter in the PhD dissertation of Emil Krupandan. He has conducted this published work as part of this doctoral dissertation and successfully submitted the manuscript before the completion of his Ph.D.

Sincerely,

Diego Pol

CONICET – Museo Paleontológico E. Feruglio

Av. Fontana 140. (9100) Trelew, Chubut. **Patagonia Argentina.** Tel./ Fax: (54 2965) 432100. E-mail: info@mef.org.ar

Prof. Anusuya Chinsamy-Turan
Department of Biological Sciences
University of Cape Town
Private Bag X3, Rhodes Gift, 7701 South Africa
Tel: +27 (0) 21 650 4007 Fax: +27 (0) 21 650 3301
http://www.biologicalsciences.uct.ac.za
anusuya.chinsamy-turan@uct.ac.za

8 February 2019

TO WHOM IT MAY CONCERN

I confirm that the following published article was written by Emil Krupandan and that it forms a major part of his PhD research, which I co-supervised. As co-supervisor I basically read and commented on drafts of the manuscript.

Krupandan, E., Pol, D. and A. Chinsamy 2018. Long bone histology of the sauropodomorph *Antitonitris ingenipes*. Anatomical Record 301: 1506-1518.

I fully support that the content of this publication are acceptable as a chapter of Emil's thesis.

Yours sincerely,

Prof. Anusuya Chinsamy-Turan

Primary Supervisor

I support the inclusion of the above chapter (article) in Emil Krupandan's thesis.

Date: 8 February 2019

Prof. Muthama Muasya

Head of Biological sciences

Our Mission is to be an outstanding teaching and research university, educating for life and addressing the challenges facing our society."

Chapter 4

The long bone histology of *Antetonitrus ingenipes*

Published as: Krupandan, E., Chinsamy-Turan, A. & Pol, D. 2018. The long bone histology of the sauropodomorph, Antetonitrus ingenipes. *The Anatomical Record.* 301(9):1506-1518.

Introduction

Bone microstructure (osteohistology) provides a direct record of ontogenetic growth and provides a wealth of data on various aspects of dinosaur palaeobiology, such as, growth rates, ontogenetic stages and termination of growth (e.g. Chinsamy-Turan, 2005; Cerda et al., 2013). Studies of the bone histology of sauropodomorph bones have been conducted on several taxa, with particularly detailed work on the basal sauropodomorphs *Massospondylus carinatus* (Chinsamy, 1993a, b) and *Plateosaurus engelhardti* (Sander and Klein, 2005; Klein and Sander, 2007).

Recently the bones of sauropodiform taxa such as *Aardonyx celestae* (Yates et al., 2010), *Leonerasaurus taquetrensis* (Pol et al., 2011) and *Mussaurus patagonicus* (Cerda et al., 2014) have also been histologically examined, and have shed new light on the biology of these transitional forms *en route* to the sauropod bauplan. Although extensive studies on sauropod bone microstructure have been made over the past few years (Curry, 1999; Sander, 2000; Sander et al., 2004; Lehman and Woodward, 2008; Klein and Sander, 2008; Sander et al., 2011a; Curry Rogers et al., 2016), except for Sander et al. (2004) all of these studies have focused on neosauropod taxa.

The first (ostensibly) basal sauropod to be studied histologically is that of an unnamed taxon from the Late Early Jurassic (Pliensbachian - Toarcian) Upper Nam Phong

Formation of Thailand (Buffetaut et al., 2002; Sander et al., 2004; Laojumpon et al., 2017). Based on its size (comparable to that of *Apatosaurus louisae*) and location 1km away from the *Isanosaurus attavipachi* holotype site, it is possible that the remains pertain either to an adult specimen of *Isanosaurus* or to another unknown sauropod taxon (Buffetaut et al., 2002; Sander et al., 2004). Sander et al. (2004) found that this sauropod had uninterrupted laminar fibro-lamellar bone, which characterises later Jurassic sauropods (Sander et al., 2004, 2011a). At the time of publication *Isanosaurus* and the conferred material (see Sander et al., 2011a) represented the earliest sauropod remains discovered. Although the conferred material was found nearby, in the same formation, poor preservation and lack of skeletal element overlap with the holotype of *Isanosaurus*, prevents an actual diagnosis beyond Sauropoda indet. (Buffetaut et al., 2000, 2002.).

Bone histology studies of ontogenetic series of the basal sauropodomorph *Massospondylus carinatus* (Chinsamy, 1993a, 1993b; Chinsamy-Turan, 2005) and *Plateosaurus engelhardti* (Sander and Klein, 2005; Klein and Sander, 2007; Hurum et al., 2006) show that basal sauropodomorphs are characterised by zonal bone (sensu Reid, 1981) which is composed of fibrolamellar bone (FLB) tissue interrupted by growth marks (Lines of Arrested Growth [LAGs] or annuli). In the case of *Plateosaurus* termination of growth is recorded in the subperiosteal margin (Klein and Sander, 2007), while even the largest individual of *Massospondylus* does not show the closely spaced rest lines indicative of attainment of skeletal maturity (Cerda et al., 2017). Extensive studies of *Plateosaurus* have shown a marked degree of developmental plasticity (Sander and Klein, 2005), indicated by different sized elements possessing similar numbers of growth rings.

Based on samples taken from the scapula and rib, the sauropodiform taxon, *Aardonyx* appears to exhibit cortical bone tissue that is zonal and similar to that of the basal sauropodomorphs (Yates et al., 2010). The rib histology of *Leonerasaurus* also has zonal bone tissue (Pol et al., 2011), although the fibrolamellar bone is less vascularised in this taxon.

Recent studies on *Mussaurus* showed that it had a faster growth rate than *Massospondylus* [Cerda et al., 2014], with a much higher proportion of vascularisation, as compared to *Aardonyx* and *Leonerasaurus*. Furthermore, the pattern of vascularisation varies between laminar, plexiform and reticular FLB (Cerda et al., 2014). The lack of growth lines in juvenile *Mussaurus* material indicates a phase of rapid continuous growth during early ontogeny, similar to that experienced by sauropods throughout most of their lives. In adult *Mussaurus* individuals, there is evidence of the presence of growth marks restricted to the outer third of the of the cortex (Cerda et al. 2014; Cerda et al., 2017). Thus, it appears that *Mussaurus* possesses the “typical” sauropod growth pattern (see below), however Cerda et al. (2017) ascribe this to homoplasy rather than being a synapomorphic character for basal Sauropodomorpha and Sauropoda based on the results of character optimisation.

In contrast to the more basal sauropodomorphs, sauropods appear to have a highly vascularised fibrolamellar bone tissue, with LAGs being scarce and only occurring towards the subperiosteal margin (referred to as an external fundamental system by Klein and Sander [2008] or outer circumferential layer by Chinsamy-Turan [2005]), indicating rapid uninterrupted growth followed by a slowing down in deposition rates (Sander et al., 2004; Chinsamy-Turan 2005; Sander et

al., 2011a, b). However, it should be noted that there are exceptions to this trend. Based on material now identifiable as belonging to the titanosauriform *Lapparentosaurus* (de Ricqlès, 1983; Rimblot-Baly et al., 1995; Sander, 2000; Mannion, 2010), BMNH R9472 - an undescribed Middle Jurassic sauropod (Reid, 1981), *Europasaurus* and *Lessemsaurus* (Cerda et al., 2017), there is clear evidence of cyclical growth marks in the inner cortex of sauropod bones. As early as 1983, De Ricqlès pointed out that these cyclical growth rates may be more prevalent in sauropods than previously thought.

While the holotype of *Antetonitrus ingenipes* (Yates and Kitching, 2003) is now established as being from the Early Jurassic UEF (McPhee et al., 2017), the newly referred material (NMQR 1705) is from the Late Triassic LEF of South Africa. Therefore, *Antetonitrus* is both geologically older than the Thai basal sauropod - and according to recent analyses (Apaldetti et al., 2013; Otero and Pol, 2013; McPhee et al., 2014) is even more phylogenetically basal than *Isanosaurus.* Thus, *Antetonitrus* is now considered to be the earliest sauropod (*sensu* Yates, 2007a).

In addition to the holotype material (BPI/1/4952), the same unique combination of characters and autapomorphies (indicated with *) for *Antetonitrus*, identified by Yates and Kitching (2003) and expanded upon by McPhee et al. (2014), are present in NMQR 1705 (see Chapter 3 for detailed description thereof).

Here an osteohistological study of *Antetonitrus* (BPI/1/4952 and NMQR 1705) is undertaken to assess whether it had a growth strategy more similar to basal sauropodomorphs, or to its more derived relatives or whether instead it exhibited a

completely different growth. Furthermore, different sized femora, tibia and humeri are studied to deduce histological variation in long bone histology, and to assess how they grew through ontogeny.

Institutional Abbreviations

BMNH, British Museum of Natural History; **BPI**, Evolutionary Studies Institute, Johannesburg, South Africa; **NMQR (NMB)**, National Museum, Bloemfontein, South Africa.

Materials and methods

Samples for histological analyses were taken from the long bone elements (femora, humeri and tibiae) of NMQR 1705, a mono-specific, multi-individual assemblage collected from the Late Triassic, Lower Elliot Formation (LEF) site of Maphutseng, Lesotho (Ellenberger and Ellenberger, 1956; Charig et al., 1965; Gauffre, 1993; Van Gen et al., 2015; Krupandan personal observation, 2014). In addition to this, a core from the femur of the holotype (BPI/1/4952) was also included in the analysis. No data on association between elements for NMQR 1705 was available as this material was excavated during the 1950's and accessioned at NMQR as disarticulated material without any field notes. While some NMQR 1705 elements clearly articulate with each other (e.g. pedal phalanges), it cannot be accurately determined whether the long bones sampled belong to the same individuals as the only way to associate material would be based on ratios taken from the holotypic material (BPI/1/4952) – the results of which are equivocal at best due to some elements being incomplete.

The diaphyseal samples were taken from the femoral, tibial and humeral midshaft regions (identified by Chinsamy [1993b] and Klein and Sander [2007] as being neutral regions of growth with

the least remodelling). To ensure that the best possible record of growth was analysed, full cross-sections were sampled of the femora and tibia in order to determine the best region for core sampling (Stein and Sander, 2009). Due to the poor preservation of the humeri, only one was cored, partial segments of the bone wall of the other two were sampled. As far as possible, cores were taken from comparable regions. Specimens were cored using a drill with a diamond encrusted coring bit or cut using a Dremel Precision Tool. After samples were removed from the bone the area was infilled with plaster to retain the original shape of the bone. In the case of full cross-sections, casts of the removed slices were made with epoxy and inserted into the missing regions of the bones.

Eight femora (NMQR 1705/252, 1705/20, 1705/801, 1705/163, 1705/325, 1705/15, 1705/600, and BPI/1/4952) representing a size range of 435mm to 885mm in length were sampled. A thin section of the complete cross-section of the bone wall of NMQR 1705/163 permitted the determination that the posteromedial side of the midshaft was the thickest part of the bone wall and therefore held the best record of ontogenetic growth. All other femora were cored in this region. The exception to this was that the holotype femur (BPI/1/4952) was sampled from the posterior side of the distal femur, just proximal to the lateral and medial condyles, this core was taken before rules governing destructive sampling of South African holotypic material came into effect and subsequently no further sampling was permitted.

Six tibiae ranging in size from 322mm to 565mm in length were sampled for histological analyses. A complete cross-section of tibia NMQR 1705/235 indicated that the best location for core sampling was from the anteromedial or posterior sides of

the midshaft of the tibia. The remaining five tibiae were sampled (1705/304, 1705/561, 1705/100, 1705/354 and 1705/009) in this region. Three humeri (NMQR 1705/801, 1705/028 and 1705/359), ranging in size from 570mm to 620mm in length were sampled in the anterolateral half of the midshaft. Specimens were prepared for thin sections based on the methodology outlined in Chinsamy and Raath (1992). Cores/samples were embedded in resin (Struers Epofix), mounted on frosted glass slides and thin-sectioned using a Struers Accutom-50. The preparation of the histological sections was carried out at the University of Cape Town, South Africa. All sections were studied using a Nikon E200 microscope. Photomicrographs were captured using NIS D 3.0 Software and edited in Adobe Photoshop CC 2014. Nomenclature and definitions of structures used in this study are sensu Chinsamy-Turan (2005).

Comparative material includes published data on the following basal sauropodomorphs; *Massospondylus* (Chinsamy, 1993b, 1994), *Plateosaurus* (Sander and Klein, 2005; Klein and Sander, 2007) and the basal sauropodiforms, *Aardonyx* (Yates et al, 2010), *Leonerasaurus* (Pol et al, 2011) and *Mussaurus* (Cerda et al., 2014, 2017). BMNH R9472 (Reid, 1981), *Lapparentosaurus* (see de Ricqlès 1984, Rimblot-Baly et al. 1995, Mannion 2010), the Nam Phong sauropod (Sander et al., 2004), *Apatosaurus* (Curry, 1999) and the Tendaguru sauropods (Sander, 2000) were used as examples of derived Sauropoda.

Results

Detailed Histology of the Femora

All eight midshaft femoral samples exhibit well-vascularised, primary FLB tissue throughout the cortex. The vascular organisation of the FLB is generally characterised by an irregular, reticular arrangement of the vascular channels in the inner-most cortex and a change in arrangement of the channels to a plexiform (composed of radial and circumferential channels) arrangement in the subperiosteal cortex. Secondary osteons are present in all femora, except the smallest - NMQR/1705/252 (435mm length). While NMQR/1705/020 (756mm length) shows the change from reticular to plexiform FLB seen in most of the sampled bones, a thin band of avascular tissue (? annulus) is evident below the three LAGs that are present near the outer region of the cortex (Fig. 29).

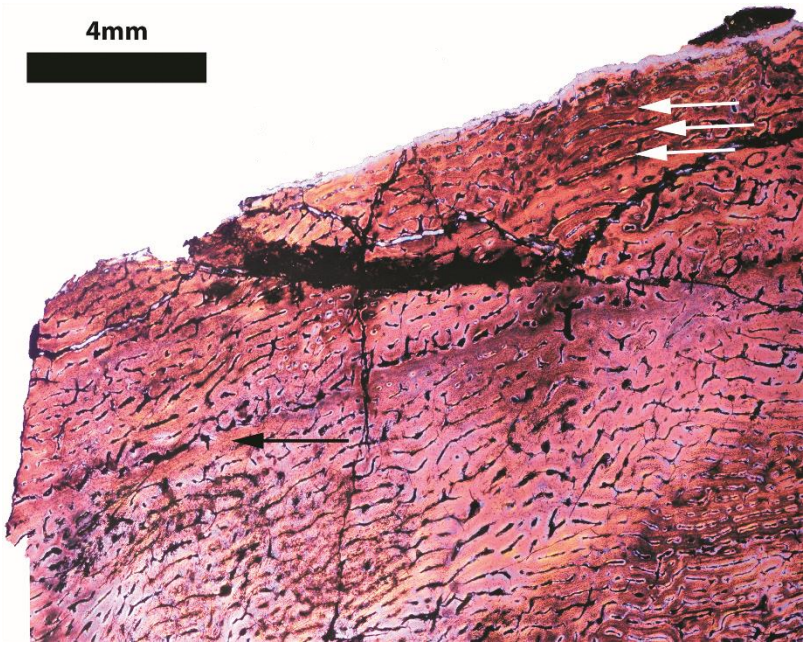

Figure 29. Right femur, NMQR 1705/020. Polarised light. Black arrow indicates thin band of avascular tissue/annulus. White arrows show LAGs.

In contrast to this general pattern, NMQR/1705/801 (760mm length) exhibits only reticular FLB, except for a small patch of plexiform tissue in middle of the cortex (Fig. 30).

NMQR/1705/163 (Fig. 31), the 5th largest femur (770mm length), shows a four-stage change in vascular orientation from outer cortex to the medullary region: in the outermost region there is a thin layer of less vascularised FLB with a vascular organisation composed of a combination of plexiform tissue, but with significant number of irregular channels as well (Fig. 31B), below which is a thicker region of less organised reticular FLB (Fig. 31C),

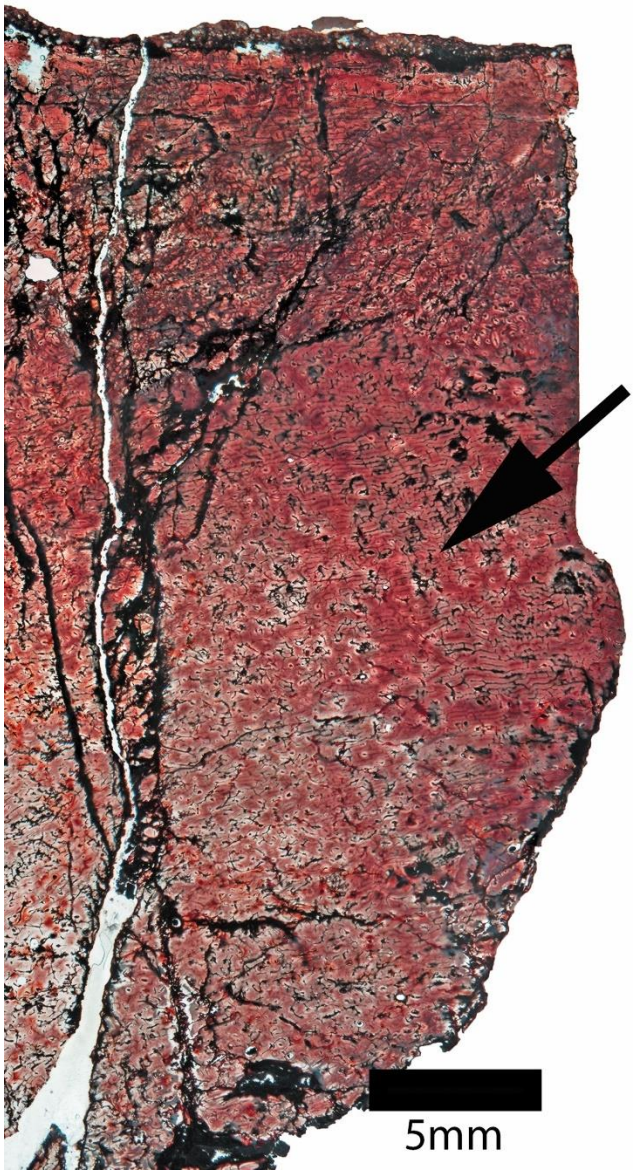

Figure 30. Left femur, NMQR 1705/801. Isolated patch of plexiform FLB showing localised change in vascularisation indicated by black arrow.

followed by a thinner layer of plexiform tissue (Fig. 31D), which overlies reticular FLB (with large amounts of secondary osteons) that occurs throughout the rest of the compacta (Fig. 31E). The less vascularised outermost cortical region possesses multiple (six) closely spaced LAGs (Fig. 31B). Below these LAGs, there is a band of two closely spaced LAGs, followed by an annulus towards the inner cortex (Fig. 31B). While this *less* vascularised outermost cortical region bears the hallmarks of an external fundamental system (EFS *sensu* Klein and Sander, 2008, Sander et al., 2011b), it is not completely avascular and most likely represents the beginning of an EFS.

The largest femur NMQR 1705/600 (885mm length) also shows growth marks in the inner cortex, three LAGs are present in the mid-cortical region, followed by five more LAGs towards the outer cortical region. However, it lacks the modulation in vascular channels as seen in NMQR/1705/163, exhibiting the usual change from reticular to plexiform FLB from the inner to outer cortex.

In all femora with LAGs, there is a distinct lack of change in tissue type preceding and anteceding these growth lines in contrast to the zonal bone condition seen in less derived sauropodomorphs.

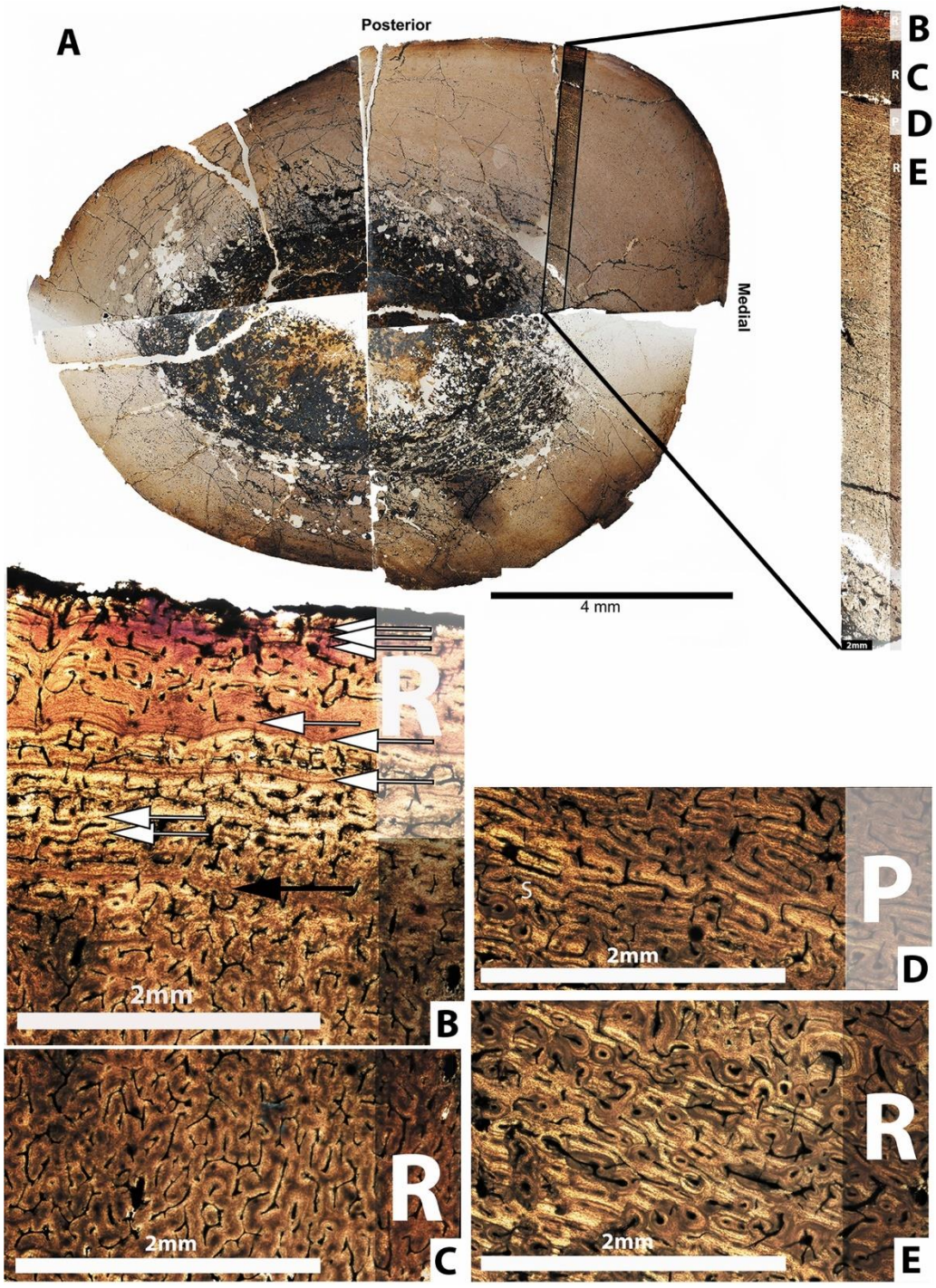

Figure 31. Right femur, NMQR 1705/163 A) view of overall cross-section. B) Outermost cortical layer showing change from plexiform to reticular FLB, note reduction in vascularisation and presence of 8 LAGs (white arrows) and an annulus (black arrow) in outermost cortical margin. C) subsequent bone tissue below B), showing continuation of reticular FLB. D) Thin layer of plexiform FLB with some secondary osteons, E) Innermost cortical region composed of reticular FLB with abundant secondary osteons. R, reticular FLB; P, plexiform FLB; S, secondary osteons.

Detailed Histology of the Humeri

Growth lines in the form of LAGs are apparent throughout the cortex of the humeri, although apart from the actual lines there does not seem to be a change in the type of tissue abutting them. Humeri NMQR 1705/801 (570mm preserved length) and 359 (620 mm length) do exhibit sparse secondary osteons in the perimedullary region, although humerus NMQR 1705/028 (which is intermediate in size between the two at 615mm in length) does not.

Humeri NMQR/1705/801 and 359 show a change in vascular arrangement from reticular to plexiform from the inner to outer cortex. In NMQR/1705/801 sparse secondary osteons are present in the perimedullary region. Seven LAGs are evident towards the outer cortex, with the outer-most 3 being “double” LAGs, followed by a “triple” LAG, two closely spaced LAGs and approaching the inner cortical region a single LAG occurs (Fig. 32). These growth lines occur throughout the compacta, but there is no change in vascular arrangement (plexiform) of the surrounding FLB tissue.

The core sample from NMQR/1705/028 (Fig.33) differs in that it is composed almost exclusively of plexiform FLB, and lacks the change in orientation of FLB from reticular to plexiform seen in the other two humeri. There is however, a regional change to a less organised reticular arrangement of FLB midway up the cortex (Fig. 33A) and again just below a thin band of radial FLB tissue just above the second innermost LAG (Fig. 33B).

Above this radial band there are three more closely spaced LAGs in the subperiosteal cortex (Fig. 33C). However, this

outer region of the cortex does not exhibit a decrease in vascularisation or change in the arrangement of FLB that would be considered an EFS (*sensu* Sander et al, 2011b).

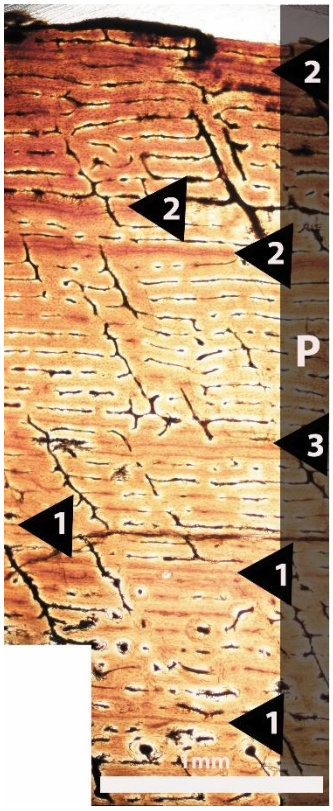

Figure 32. Right humerus, NMQR 1705/801.Black triangles with numbers indicate occurrence and number of LAGs, *i.e.* single, double or triple LAGs. P, plexiform FLB.

The band of localised radial FLB (Fig. 33B) is followed by the resumption of normal plexiform FLB. Secondary osteons are absent in this sample.

NMQR 1705/359 also exhibits growth lines in the form of seven LAGs approaching the outer cortex, five of which are closely spaced and are in the outermost fringe of the cortex, below these are 2 more closely spaced LAGs (Fig. 34). Note that these two LAGs are separated by a region of plexiform FLB, and thus, LAGs are not restricted only to the outermost cortical layer as in the more derived sauropods (Sander et al., 2004; 2011a).

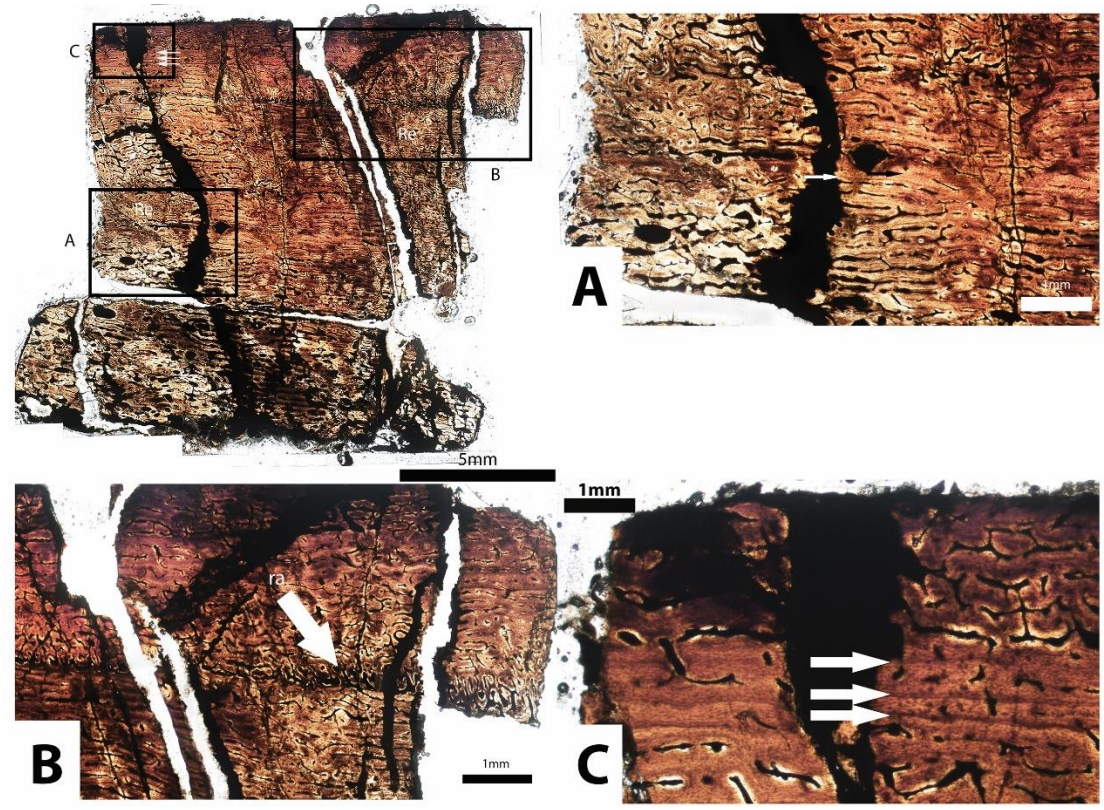

Figure 33. Right humerus, NMQR 1705/028.Composed almost exclusively of FLB. A)Mid-cortical area showing localised change to reticular FLB and LAG followed by annulus. B) Band of radial FLB tissue. C) Outermost cortical region with band of three LAGs. Horizontal white and black arrows indicate LAGs and annuli. Ra, radial FLB; Re, reticular FLB.

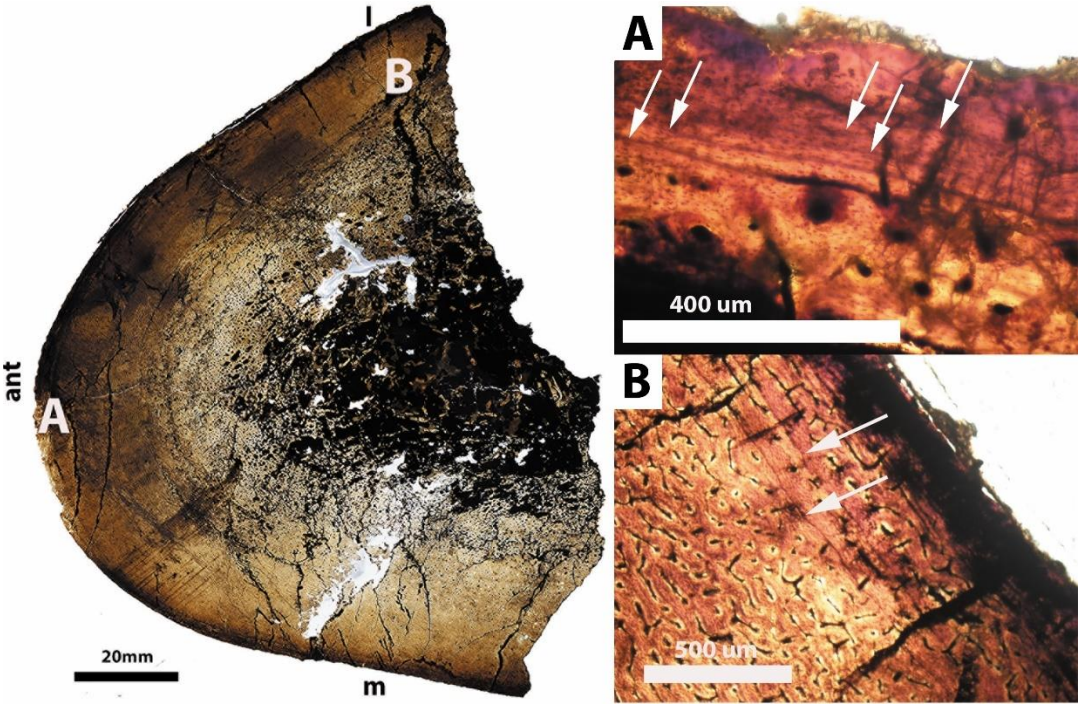

Figure 34. Left humerus, NMQR 1705/359. A) Outer-most cortical margin showing five closely spaced LAGs (white arrows), B) Two closely spaced LAGs (white arrows) deeper in the cortex. The edge of the bone

is not the periosteal surface, which has flaked off. ant, anterior; l, lateral; m, medial.

Detailed Histology of the Tibiae

The histology of the tibia generally conforms to the pattern seen in the femora and humeri having FLB with a vascular change from reticular to plexiform towards the outer-most cortex. Sparse secondary osteons are present in the perimedullary region (Fig. 35B). The smallest element, NMQR 1705/304 (322mm preserved length), does not exhibit any growth lines and shows uninterrupted deposition of FLB. The perimedullary region exhibits a reticular arrangement of FLB, with no secondary osteons.

Tibia NMQR 1705/561 (Fig. 36) (445mm preserved length) also exhibits exclusively FLB, but with a predominantly plexiform vascular arrangement. However, in the upper third of the cortex there is a band of radially oriented FLB (Fig. 36A)

(similar to that observed in humerus NMQR 1705/028, Fig. 5B).

Three LAGs are present in the innermost half of the cortex, followed by two closely spaced LAGs just below the band of radial FLB and, a single LAG above the radial FLB band followed by three closely spaced LAGs. As in NMQR 1705/028 resumption of normal growth occurs after the “event” that caused the radial deposition.

However, in Tibia NMQR 1705/235 (500mm length) there is a divergence from the general pattern seen amongst the tibia. It is composed almost exclusively of plexiform FLB tissue, apart from a small region of reticular FLB just above the medullary

region and two patches in the subperiosteal cortex. No growth marks are evident.

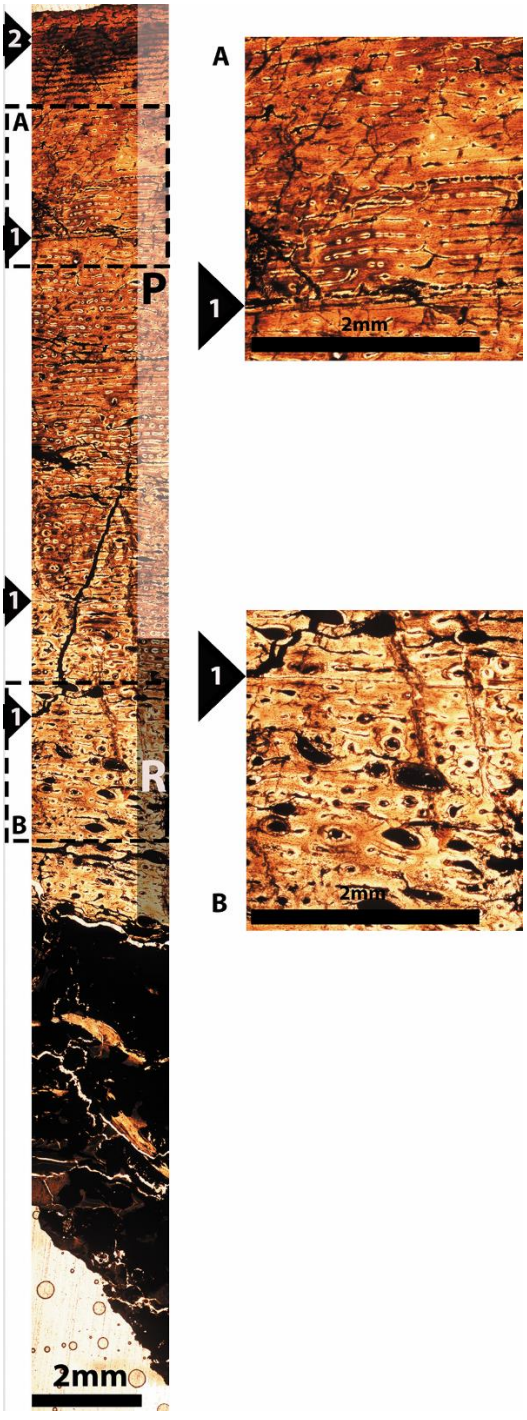

Figure 35. Right tibia, NMQR 1705/009. Textural shift from reticular A) to plexiform B) FLB. Black triangles with numbers indicate occurrence and amount of closely spaced LAGs, *i.e.* single or double LAGs. R, reticular; P, plexiform.

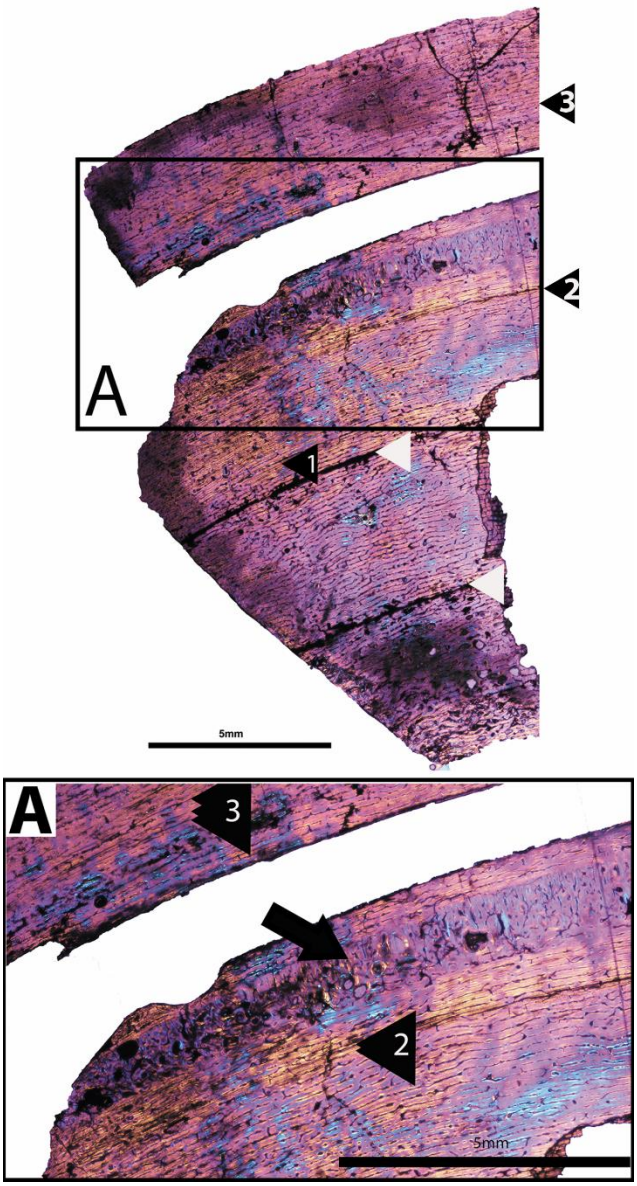

Figure 36. Right tibia, NMQR 1705/561. Polarised Light. Note preponderance of plexiform FLB. A) Region with band of radial FLB indicated by black arrow. Black triangles indicate LAGs; arrowheads indicate LAGs, and the numbers indicate single, double or triple LAGs. White triangles indicate fractures that may correspond to LAGs. ra, radial FLB.

Amongst the two largest tibia NMQR 1705/354 and NMQR 1705/009 (565mm as preserved), there is the characteristic change from reticular FLB in the perimedullary region to plexiform FLB towards the outer cortex. In the former, approaching the outer-most layer of the cortex there is a reduction in vascularisation, five LAGs are present in this region. It is similar to femur NMQR 1705/163, in terms of the

reduction in vascularisation and predominance of LAGs in the outer-most cortical layers. However, in contrast NMQR 1705/009 exhibits three LAGs spanning the cortex.

Discussion

General histological features

Samples taken from the midshaft of the diaphysis of the femora, tibia and humeri exclusively exhibit well vascularised, FLB tissue (see Table 1). The organisation of the vascular channels of the FLB is characterised by a reticular (irregular) arrangement in the inner cortex and a change in orientation to a more plexiform arrangement (laminar channels joined by radial anastomoses) towards the outer cortex (Fig. 35). Note however that this is a general trend and certain elements show combinations of reticular, plexiform and radial tissue, as well as changes in the degree of vascularisation in the outer cortical region. Primary osteons are present throughout the compacta and secondary osteons are present in the inner cortical regions of most bones, extending into the outer cortex in some (notably NMQR/1705/163). In femur NMQR/1705/163 Haversian reconstruction has progressed quite far, with several generations of secondary osteons present, however interstitial primary FLB is still present. In stark contrast femur NMQR 1705/252 exhibits no secondary osteons, with sparse occurrences of enlarged channels from the mid-cortex inwards.

Most of the long bones sampled show growth marks, which are predominately LAGs. Three femora (NMQR 1705/163, NMQR 1705/020 and BPI/1/4952) preserve annuli, while one humerus (NMQR 1705/028) preserves an annulus associated with a LAG. While a decrease in growth rate is apparent based on the reduction in vascularisation (of the FLB tissue) and a

concentration of LAGs in the subperiosteal margin of femur NMQR/1705/163 (Fig. 3A, 3B), LAGs are not restricted to this layer. Furthermore, there is no change in tissue type or vascular arrangement of the FLB *immediately* apical or basal to the growth lines in the inner compacta.

As with both the femora and humeri, generally the tibiae exhibit a change from reticular organisation of the FLB to a plexiform arrangement towards the outer cortex. In the case of tibia NMQR 1705/235 (500mm length), patches of reticular FLB are present in the subperiosteal cortex and there is no evidence of growth lines in the inner cortex. This contrasts with tibia NMQR 1705/354 (assumed to be from a juvenile based on length [322mm]), which has almost exclusively plexiform bone tissue and exhibits at least five LAGs in the outer region of the cortex.

Among the femora, the smallest specimen (NMQR 1705/252 [435mm]) shows no growth marks and is composed of uninterrupted FLB (see Fig. 9). However, there is a distinctive change in vascular orientation (modulation) from an earlier formed reticular bone to a later formed plexiform arrangement. The larger femora show a slight decrease in vascularisation in the outermost part of the cortex. This less vascularised outermost cortical region is also characterised by a prevalence of LAGs.

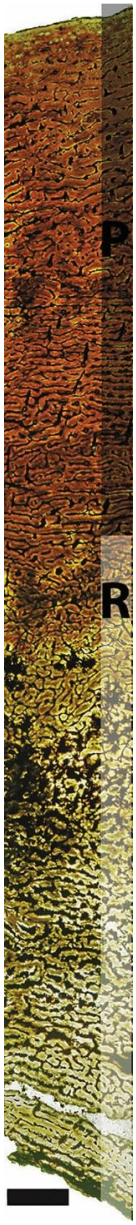

Figure 37. Left femur, NMQR 1705/252. Juvenile individual exhibiting uninterrupted FLB throughout the cortex. Note the lack of growth marks and secondary osteons. Note the textural shifts in FLB. P, plexiform FLB; R, reticular FLB.

Two of the humeri show the transition from reticular to plexiform FLB. However, humerus NMQR 1705/028 is composed almost exclusively of plexiform FLB with two patches (see Fig.5) showing a regional change to reticular FLB. Furthermore, close to the peripheral edge, there is a thin band of radially oriented FLB which resembles the sunburst pattern typical of periosteal reactive growth (Chinsamy and Tumarkin-Deratzian, 2009). A similar band of radial FLB is also present

in tibia NMQR 1705/561. In both elements, the radial FLB is followed by normal bone deposition.

When comparing similar sized humeri, femora and tibiae all are composed of FLB, with most showing modulations in vascular organisation from reticular to plexiform FLB (for exceptions to this pattern see Table 1). The presence of secondary osteons in similar sized elements is apparent in femora and tibia. However, in the humeri this is not the case, as humerus NMQR 1705/359 and NMQR 1705/028 are almost the same length (620mm and 615mm respectively) - yet secondary osteons are present in the former but not the latter. In terms of growth marks, there appears to be a large degree of variability in their occurrence amongst similar sized elements.

Growth Dynamics

Ontogenetic changes in the growth dynamics of *Antetonitrus* are evident based on the specimens studied. Early in ontogeny (as seen in femur NMQR 1705/252 and tibia NMQR 1705/304) it appears that *Antetonitrus* was characterised by rapid, uninterrupted growth, with deposition of reticular FLB, followed by a textural shift to plexiform FLB midway up the cortex. There is a total lack of growth marks or secondary osteons in these individuals. There is a large jump in size from these smallest elements (510mm and 322mm respectively) to the next longest complete elements in the sample of 256mm in the femora and 178mm in the tibia. While the larger bones are still composed of FLB and possess the textural shift from reticular to plexiform FLB these bones show evidence of intermittent growth marks throughout the cortex, as well as evidence of secondary remodelling. However, except for femur NMQR 1705/163 there is no evidence of termination of growth in the external cortex of the other bones yet, indicating that they are sub-adult. In

Accession No.	Element	Length (mm)	Sample Location	Primary Bone	Growth Marks	Bone Tissue from Medullary Region to Peripheral Edge	Sec. Osteons	Dense Haversian Bone	Maximum Cortical Thickness from midshaft segment sampled (mm)
NMQR 1705/252	F	435*†	Posteromedial	Fibrolamellar	-	Re, P	No	No	17.04
NMQR 1705/020	F	756	Posteromedial	Fibrolamellar	3,? Annulus	Re, P	Yes	No	43.13
NMQR 1705/801	F	760	Posteromedial	Fibrolamellar	No	Re	Yes	No	43.13
NMQR 1705/163	F	770	Cross-section, Posteromedial	Fibrolamellar	8 LAGS, Annulus	Re, P, Re, P	Yes	Incipient	44.00
BPI/1/4952a	F	770	Posterior	Fibrolamellar	Annulus, 3 LAGS	Re	No	No	20.00
NMQR 1705/325	F	793	Posteromedial	Fibrolamellar	2 LAGs	Re, P	Yes	No	31.48
NMQR 1705/15	F	795	Posteromedial	Fibrolamellar	No	Re,P	Yes	No	41.19
NMQR 1705/600	F	885	Posteromedial	Fibrolamellar	Yes, 5 LAGs	Re,P	Yes	No	41.10
NMQR 1705/801	H	570*	Anterolateral	Fibrolamellar	Yes, 7 LAGs	Re,P	Yes	No	26.15
NMQR 1705/359	H	620	Anterolateral	Fibrolamellar	Yes, 7 LAGs	Re,P	Yes	No	17.97
NMQR 1705/028	H	615	Anterolateral	Fibrolamellar	Yes, 5 LAGs, Annulus	P, Ra, P	No	No	14.10
NMQR 1705/304	T	322*	Anteromedial	Fibrolamellar	No	Re, P	No	No	15.47
NMQR 1705/561	T	445*	Posteromedial	Fibrolamellar	Yes, 6 LAGs	P, Ra, P	No	No	21.56
NMQR 1705/235	T	500	Posterior	Fibrolamellar	No	Re, P	No	No	22.55
NMQR 1705/100	T	520*	Posteromedial	Fibrolamellar	Yes, 2 LAGs	Re, P	Yes	No	23.22
NMQR 1705/354	T	565*	Posteromedial	Fibrolamellar	Yes, 5 LAGS	Re, P	Yes	No	23.23
NMQR 1705/009	T	565	Posteromedial	Fibrolamellar	Yes, 4 LAGS	Re, P	Yes	No	21.49

Table 4. List of specimens studied, including summary of histological features. F, femur; H, humerus; T, tibia; Re, reticular; P, plexiform; Ra, Radial. *Indicates incomplete/damaged bones. † While the proximal end of left femur NMQR 1705/252 is incomplete, the corresponding complete right femur NMQR 1705/304A is complete and its length of 510mm will be used in size comparisons.

femur NMQR 1705/163 a gradual decrease in vascularisation is evident in the outer cortical layer indicating that bone depositional rate had slowed down, however this region is not completely avascular. There is also a concentration of LAGs in this less well vascularised outer cortical region. This may correspond to the beginning of an EFS (*sensu* Klein and Sander, 2008). If this is the case, then *Antetonitrus* would have possessed a determinant growth strategy.

Based on bone length there is no association between size and number of growth lines (see Table 4), with larger individuals possessing fewer growth marks than smaller individuals in some cases: NMQR 1705/163 is the oldest femora based on growth marks and has an incipient EFS, but in terms of length, it is only the 5th largest femur. Considering the humeri, NMQR 1705/801 exhibits the most growth marks, despite being the smallest humerus. These findings suggest that the size of the element is not a good proxy for age. Furthermore, they suggest intra-specific differences that could be due to sexual dimorphism (which cannot be tested since the sample is too small) or perhaps to developmental plasticity as described for *Plateosaurus* (Sander and Klein, 2005). A third possibility is that the LAGs represent random periods of resource limitation similar to those occurring in large mammals seasonally (Köhler and Moyà-Solà, 2009; Köhler et al., 2012), although there is no published data to suggest that these occur non-annually.

In contrast to the dichotomy proposed by Sander et al. (2004) between growth patterns for basal Sauropodomorpha and Sauropoda, it appears that at least in early sauropods like *Antetonitrus*, growth lines are not restricted to the outer cortical layer and occur throughout ontogeny, albeit irregularly. Despite this, highly vascularised FLB predominates in the cortex - as in the Tendaguru neosauropods (Sander,

2000; Sander et al., 2004, 2011a). One femur (NMQR 1705/163) shows a reduction in vascularisation and concentration of LAGs in the outermost cortical layer, suggesting that its growth was slowing down or had virtually stopped. While growth marks occur throughout the cortex of most bones sampled, it should be noted that there is no associated change in degree or pattern of vascularisation prior to or after the growth marks in contrast to *Lessemsaurus* (Cerda et al., 2017).

The majority of the *Antetonitrus* bones also show modulations between reticular and plexiform FLB. This feature is also seen in the femoral histology of *Lessemsaurus* and *Volkheimeria* (Cerda et al. 2017). Such textural shifts (*sensu* Chinsamy et al. 2012) are reminiscent of those seen in temperate populations of *Edmontosaurus* and *Hypacrosaurus* (Chinsamy et al., 2012), reflecting periodic strains in resource acquisition. The lack of consistent cycles of vascular modulation in NMQR 1705 precludes seasonality as a factor, and is more similar to the inconsistent changes seen in temperate *Edmontosaurus* populations (Chinsamy et al., 2012). In most samples, there is only one textural shift from reticular to plexiform FLB tissue that occurs approximately halfway up the cortex. This may be evidence of a dietary change during ontogeny, but fails to explain the multiple textural shifts seen in the femur NMQR 1705/163, a feature which is also present in *Lessemsaurus* and *Volkheimeria* (Cerda et al., 2017). Based on the number of LAGs (eight) and the reduction in vascularisation in the outermost cortical layer of femur NMQR 1705/163 indicating that this femur belonged to the oldest individual, it seems more likely that multiple textural shifts are a function of increased age.

Phylogenetic context

When looking a range of sauropodomorphs spanning the transition from basal forms (i.e. *Massospondylus* and *Plateosaurus*), to more derived sauropodiforms (i.e. *Aardonyx*, *Leonerasaurus* and *Mussaurus*) to the most basal sauropod-*Antetonitrus*, there is a trend towards an increase in the deposition of highly vascularised FLB as the predominant cortical bone tissue. This trend starts with *Mussaurus* (see Cerda et al., 2014, 2017) and appears to continue in *Antetonitrus*.

Based on the juvenile material of *Antetonitrus* studied here and the juvenile *Mussaurus* material (Cerda et al. 2014), it appears that both taxa exhibited a phase of early uninterrupted rapid growth. The presence of growth marks in the outer cortical layers of adult *Mussaurus* specimens, may indicate that both taxa exhibited growth marks later in ontogeny after this rapid phase of growth, followed by a reduction in vascularisation and preponderance of growth marks in the outermost cortical layer (based on femur NMQR 1705/163), which likely correspond to an external fundamental system (*sensu* Klein and Sander, 2008). The similarity between the growth dynamics of the two species show remarkable convergence. However, Cerda et al (2017) hypothesise that the most parsimonious explanation for the occurrence of similar growth strategies in the basal sauropodiform, *Mussaurus* and in more derived sauropods is due to homoplastic convergence.

In *Antetonitrus* the absence of growth marks in the inner cortex seen in more derived neosauropod taxa (Curry, 1999; Sander, 2000; Sander et al., 2004, 2011a) and *Mussaurus* (Cerda et al., 2017) is lacking, however, this may be due to the material under study belonging to sub-adult individuals.

Occurrence of radial fibrolamellar tissue and pathology

The presence of radial FLB in the cortical region of a humerus and tibia may be periosteal reactive bone, indicative of pathological growth (Chinsamy and Tumarkin-Deratzian 2009). In the latter study, radial spicules radiated from the periosteal and endosteal margins of the bones. In contrast, the humerus and tibia belonging to NMQR 1705 the band of radial FLB is located within the cortex, indicating that after a period of trauma/illness, normal growth resumed. This pattern (and the lack of endosteal deposits) is more similar to that reported in *Psittacosaurus mongoliensis*, *Plateosaurus engelhardti*, and a Late Triassic dinosaur from Norway (Chinsamy et al., 2012), and may be related to hypertrophic osteopathy (see Lenehan and Fetter, 1985; Chinsamy et al., 2012). The ratio of the length of the humerus to tibia in the *Antetonitrus* holotype (BPI/1/4952) is 1.33, and for NMQR 1705 the humerus (NMQR 1705/028) and incomplete tibia (NMQR/1705/561) the ratio is 1.38. Since the length of the incomplete tibia is approximated, it is possible that the ratio would be less in reality. Given that both the aforementioned humerus and tibia of NMQR 1705 possess five LAGs each, and both have the anomalous radial fibrolamellar bone in the outermost part of their cortices, it is possible that these bones are from the same individual (see Sander, 2000). In lieu of other data on association between elements belonging to NMQR 1705, this is tentative proof that NMQR 1705/028 and NMQR 1705/561 belong to the same individual.

Conclusion

It appears that the growth strategies present in the earliest member of Sauropoda (*sensu* Yates, 2007a) are not a continuation of patterns first seen in the basal sauropodiform, *Mussaurus*, which are similar to more derived sauropods. This means that uninterrupted deposition of highly vascularised FLB

coupled with restriction of growth marks to the outer cortical margins is not a synapomorphy for Sauropodiformes. The presence of the “typical” sauropod growth pattern in both *Mussaurus* and derived sauropods, yet absence in *Antetonitrus* and *Lessemsaurus* suggests that the similarities between *Mussaurus* and more derived Sauropoda are the result of convergent evolution (see Cerda et al., 2017).

While there is an increase in the deposition of highly vascularised FLB in the cortex relative to basal sauropodomorphs, both *Antetonitrus* and *Lessemsaurus* exhibit evidence of growth marks throughout the compacta - although less regularly in *Antetonitrus*. Cerda et al. (2017) show that the basal sauropods *Lessemsaurus*, *Volkheimeria* and *Patagosaurus* exhibit subtle differences in growth patterns: cyclical growth in *Lessemsaurus* (reminiscent of basal sauropodomorphs) with marked textural shifts, poorly defined textural shifts in FLB in *Volkheimeria* and poorly formed annuli interspersing the FLB in *Patagosaurus* (Cerda et al., 2017). Compared to these three taxa, *Antetonitrus* appears to possess growth lines (although not quite as cyclical) and textural shifts as in *Lessemsaurus* (and to a lesser extent *Volkheimeria*).

However, ultimately *Antetonitrus* shows a unique bone depositional pattern. One unsurprisingly similar to its sister-taxon (*Lessemsaurus*) - but different in two key ways: 1) the regularity and cyclical frequency of growth marks in the cortex, and 2) lack of textural shifts from reticular to plexiform FLB presaging LAGs. Thus, changes in growth dynamics seen *en route* to Sauropoda appear to be confounded by homoplasy and high levels of plasticity. In the case of *Antetonitrus*, this suggests that there is no discrete “Sauropod pattern” in terms of growth dynamics and that changes in growth from basal

sauropodomorphs to derived sauropods does not occur along a continuum.

Despite this, *Antetonitrus* appears to follow the general trend, as seen in Sauropoda, of a rapid increase in growth rates during early ontogeny (as evidenced by the deposition of uninterrupted FLB). Termination of growth was not recorded, but one specimen exhibited a slowdown in growth in the outermost cortex (i.e. the beginning of an EFS) – indicating that we may still be dealing with somatically immature individuals. Furthermore, our study shows that the developmental plasticity seen in basal sauropodomorphs such as *Plateosaurus* is still present in more derived forms such as *Antetonitrus*. Infrequent modulations in vascularisation patterns indicate that the animals studied probably experienced periods of environmental stress (e.g. food shortages), although not on a regular, seasonal basis.

Addendum

While Chapter 4 was submitted for publication, new data on two new related Lessemsaurid taxa – *Ingentia prima* (Apaldetti et al, 2018) and *Ledumahadi mafube* (Mcphee et al, 2018) - and more data on *Lessemsaurus sauropides* become available that was not possible to include in the original publication. This addendum will incorporate this new data into our evaluation of the histological results of NMQR 1705.

Both *Lessemsaurus* and *Ingentia* exhibit well defined growth lines (LAGs) throughout the cortex of the femur and humerus (for *Lessemsaurus* and *Ingentia* respectively), that do not appear to impede the level of vascularisation of the preceeding or anteceding FLB bone (Apaldetti et al, 2018). They also share

with NMQR 1705 the modulations or textural shifts between thick sections of well vascularised plexiform and reticular FLB, indicating high rates of bone tissue formation despite the occurrence of growth lines. Indead, taking into account the same pattern of periods of high growth interspersed with erratic growth lines, we find further evidence of a uniquely Lessemsaurid growth strategy that allowed for the attainment of large body size despite retaining a relatively plesiomorphic bauplan in *Antetonitrus*.

Ledumahadi exhibits a similar growth pattern to the above taxa, characterised by high growth rates during early ontogeny, the appearance of growth lines later in ontogeny and as in *Antetonitrus* evidence of an OCL (McPhee et al., 2018). However, it differs from *Lessemsaurus*, *Ingentia* and *Antetonitrus* in that it lacks the textural shifts seen in these taxa from reticular to plexiform FLB.

Despite this, all these Lessemsaurid taxa share a unique growth strategy of cyclical growth, interspersed with periods of rapid bone deposition.

Chapter 5

Concluding Remarks and Scope for Future Research

The key findings of the current research on the problematic basal sauropodomorph material referred to *Plateosauravus* and "*Euskelosaurus*", and the description of material previously assigned to the latter (NMQR 1705) has led to much more clarity in terms of the taxonomic validity of both species, what material referred to them actually represents, their phylogenetic status, and histological insight into aspects of the biology southern African sauropodomorpha.

5.1 The taxonomic validity of *P. cullingworthi* (Haughton, 1924)

Hypotheses tested in this aspect of study:

Hypothesis 1 – *Plateosauravus* is a distinct/valid taxon.

Hypothesis 2 – *Plateosauravus* is a non-Massopodan taxon that lies outside Sauropodiformes.

This study finds that while there is a core assemblage of material pertaining to a Massopodan basal sauropodomorph, there exists material that should be excluded from this taxon based on doubtful provenance and association. Therefore **Hypothesis 1** is valid.

Despite the reduction in elements referable to *Plateosauravus*, we still find it to be a valid taxon that retains some of the unique combination of characteristics that Yates (2003) used to differentiate *Plateosauravus* from other taxa. Although it is phylogenetically unstable, in the current analysis it is

recovered as a basal Massopodan and is in a more derived position than Plateosauria. Based on the results of the phylogenetic analysis, Hypothesis **2** is partially invalid, as *Plateosauravus* does lie outside Sauropodiformes.

5.2 *Antetonitrus ingenipes*: A Step Towards the Acquisition of the Sauropod Bauplan

Hypotheses tested in this aspect of study:

Hypothesis 3 - The Maphutseng material is monospecific and represents a basal sauropod dinosaur.

Hypothesis 4 – Part of the current material assigned to *Euskelosaurus* corresponds to *Antetonitrus* and/or *Plateosauravus.*

Material from Maphutseng, Lesotho (NMQR 1705) was described and found to be referable to *Antetonitrus ingenipes*, supporting **Hypothesis 3 –** that the material in question is monospecific and belongs to a basal sauropod. **Hypothesis 4** is also partially supported, as this historically "Euskelosauran" material is in fact identiable as *Antetonitrus*. Elements not present in the *Antetonitrus* holotype (BPI/1/4952) include a tooth, articulated sacrum, coracoids, ischia, ilia, astragali and a complete right pes. These new elements reveal additional adaptations highlighting *Antetonitrus*' position as a transitional basal sauropod, exhibiting a mosaic of basal sauropomorph, incipient and derived sauropod characteristics. This includes a sauropod-type coracoid, the combination of sauropod-type sacrum and basal sauropodomorph-like pelvic girdle, coupled with a pes with a slightly developed entaxonic condition. The

sacrum shows that the acquisition of dorsosacral vertebrae in sauropods exhibits a degree of plasticity in contrast to the consistent acquisition of a caudosacral vertebra. The single tooth described suggests that locomotory changes associated with quadrupedality in the postcrania and large body size occurred prior to changes in dentition in the early evolution of Sauropoda. Our phylogenetic analysis corroborates the position of *Antetonitrus* as the sister taxon of *Lessemsaurus sauropoides,* but the new information from the pes places these taxa in a polytomy with *Blikanasaurus cromptoni*. With the addition of anatomical and histological information from the new skeletal material, *Antetonitrus* now provides the most complete example of a basal sauropod dinosaur for understanding the morphological adaptations that accompanied the transition from basal sauropodomorphs to the derived condition of basal sauropods.

5.3 The long bone histology of *Antetonitrus ingenipes*.

Hypotheses tested in this aspect of study:

Hypothesis 5 – As seen in Sauropod dinosaurs, the bone histology of the Maphutseng material will exhibit highly vascularised FLB, with LAGs only occurring late in ontogeny (in keeping with the general trend seen in sauropods). Therefore, early bone histology as determined from smaller femora and tibia will show the same azonal bone growth pattern seen in larger specimens with the exception of LAGs occurring in the OCL of the latter.

Hypothesis 6 – Similar to the condition found in basal sauropodmorphs such as *Massospondylus* and *Plateosauravus*, we expect a high degree of developmental plasticity in the

Maphutseng sample. Due to this, we do not expect a correlation between age and body size in this sample.

Hypothesis 7 – As continuous growth is a feature of taxa more closely related to Sauropoda than Massopoda, we expect NMQR 1705 to share this feature based on its phylogenetic proximity to Sauropoda.

Analysis of the long bone microstructure of *Antetonitrus ingenipes* fills a crucial gap in our understanding of the growth dynamics of sauropodomorph dinosaurs. The bone histology of basal Sauropodomorpha are often characterised by zonal tissue, and contrasts with that of more derived sauropod taxa which show a shift towards the deposition of uninterrupted fibrolamellar bone (with lines of growth being either absent or only present in the outer circumferential layer).

In *Antetonitrus*, growth patterns in the youngest individuals exhibit uninterrupted fibrolamellar bone without any growth marks. Sub-adult individuals, also exhibit highly vascularised fibrolamellar bone throughout the cortex, as in more derived Sauropods and *Mussaurus*, but growth lines occur intermittently (i.e. irregularly) throughout the cortex as in *Lessemsaurus*. The findings that NMQR 1705 exhibits highly vascularised FLB, but that LAGs are found throughout the cortex in addition to the EFS means that **Hypothesis 5** is largely unsupported. Younger individuals differ from sub-adult specimens in terms of the absence of growth marks. *Antetonitrus* does not exhibit the growth dynamics previously considered characteristic of Sauropoda. Although, the largest (and possibly the oldest femur, NMQR 1705/163) shows an

incipient external fundamental system (EFS), reminiscent of that seen in more derived sauropods.

The results of this histological investigation further suggest that growth marks are decoupled from bone size i.e., similar sized bones have different number of lags, which indicates a level of developmental plasticity in this taxon, supporting **Hypothesis 6**. Modulations or textural shifts in the pattern of vascular channel arrangements throughout the fibrolamellar bone in the cortex may be related to periods of resource limitations, although the lack of consistency of these modulations suggest that it is unlikely due to seasonal fluctuations. Localised bands of radial fibrolamellar bone, followed by resumption of normal growth in two samples are interpreted as evidence of infliction by a disease, and subsequent recovery thereof.

When taken as an example of a basal sauropod, we find that **Hypothesis 7** is supported. While not exhibiting a typically more derived sauropod pattern of azonal growth, we do see that the bones are highly vascularised, with no real cortical change preceding or anteceding LAGs, as well as evidence of an OCL in at least one sample. In summary, this basal sauropod, exhibits a histological profile more akin to (but not identical to) Sauropoda, rather than basal Massopodans.

5.4 Synthesis of findings

The results of the assessment of material assigned to *Plateosauruavus cullingworthi* indicate that it is a valid taxon, by virtue of lacking any of the autapomorphic features described for other southern African sauropodomorphs - besides an anterolateral sulcus on the deltopectoral crest, which is shared with *Antetonitrus*. However, it is not easily

distinguished from other basal sauropodomorphs due to the elements preserved presenting a morphology that is quite general and missing character data. It is not any unique features that distinguishes *Plateosauravus* from other taxa, rather a lack thereof.

Following this, we find that while valid, *Plateosauravus* cannot be used as “the next available taxon” for the collapsed taxon, “*Euskelosaurus*” for the reasons outlined below.

While material described as *Euskelosaurus africanus* was previously incorporated into *Plateosauravus* (Yates, 2003a), it is not unequivocal. Amongst material considered to represent “*Euskelosaurus*” from Maphutseng (NMQR 1705), we find that these elements are identifiable as belonging to *Antetonitrus*. Based on this, it is apparent that while some material referred to as *Euskelosaurus* could be *Plateosauruavus* - it isn’t necessarily the case due to the diversity and disparity in material that was “lumped” into this waste-basket taxon.

5.5 Scope for Future Study

While this study has identified that *Plateosauravus* is distinct from other EF sauropodomorphs, its morphology is relatively generically sauropodomorphan, more material is necessary to provide a better diagnosis and a more stable phylogenetic position. Contrary to Yates (2003) material previously assigned to “*Euskelosaurus*” cannot be subsumed under its mantle *en masse*.

It is possible that *some* material belonging to the latter may belong to *Plateosauravus*, but our analysis of “*Euskelosaurus*”

material from Maphutseng shows that in this case, the material is identifiable as belonging to *Antetonitrus*.

The implications of this are that while greater certainty has been brought to the hypodigm of *Plateosauravus* in terms of taxonomic validity of the genus and our knowledge of the anatomy and bone histology of *Antetonitrus* has vastly increased due to the new information presented, the question of what all the material accessioned and described as "*Euskelosaurus*" actually is, is still unanswered.

It is clearly evident that lumped together, under the now discredited label of "*Euskelosaurus*", are at least two different morphotypes of basal sauropodomorphs: a more basal gracile morph exemplified by *Plateosauravus* and a basal sauropodomorph (exemplified by *Antetonitrus*). It is imperative that further analysis be done on all material accessioned as "*Euskelosaurus*" from SAM, BPI and NMB on a case by case basis, to determine their true taxonomic identity as the current study has demonstrated that there is a degree of taxonomic diversity under this label.

Furthermore, other problematic genera such *Melanorosaurus* would benefit from the same test of taxonomic validity applied to *Plateosauravus* in this study. After certainty is obtained regarding the taxonomic identity of what the poorly and undescribed so called "*Euskelosaurus*" specimens are, histological analysis can then be performed in order to provide a better understanding of the growth dynamics of southern African Sauropodomorpha.

It is further proposed that histological studies on the immediate outgroup to Sauropoda (i.e. *Melanorosaurus*), the basal

sauropod *Blikanasaurus cromptoni* (Galton and Van Heerden, 1998), the non-eusauropod sauropod taxa *Gonxianosaurus shibeinsis* (He et al., 1998) and *Tazoudasaurus naimi* (Allain et al., 2004) will provide a more complete assessment of the changes in growth strategies during the transition from more basal sauropodiforms to true sauropods.

List of References

Allain R, Aquesbi N, Dejax J, Meyer C, Monbaron M, Montenat, C, Richir P, Rochdy M, Russell D, Taquet P. 2004. A basal sauropod dinosaur from the Early Jurassic of Morocco. *C R Palevol* 3:199-208.

Allain, R. & Aquesbi, N. 2008. Anatomy and phylogenetic relationships of Tazoudasaurus naimi (Dinosauria, Sauropoda) from the late Early Jurassic of Morocco. *Geodiversitas*. 30(2):345-424.

Apaldetti C, Pol D, Yates A. 2013. The postcranial anatomy of Coloradisaurus brevis (Dinosauria: Sauropodomorpha) from the late Triassic of Argentina and its phylogenetic implications. *Palaeontology* 56:277-301.

Apaldetti, C., Martínez, R.N., Cerda, I.A., Pol, D. & Alcober, O. 2018. An early trend towards gigantism in Triassic sauropodomorph dinosaurs. *Nature Ecology & Evolution*. 2(8):1227.

Bonaparte, J. F. 1999. Evolución de las vertebras presacras en Sauropodomorpha. *Ameghiniana* 36:115-187.

Bonaparte, J.F., Ferigolo, J. & Ribeiro, A.M. 1999. A new early Late Triassic saurischian dinosaur from Rio Grande do Sul state, Brazil. *National Science Museum Monographs.* 15:89-109.

Bonaparte, J.F., Brea, G., Schultz, C.L. & Martinelli, A.G. 2007. A new specimen of Guaibasaurus candelariensis (basal Saurischia) from the Late Triassic Caturrita Formation of southern Brazil. *Historical Biology*. 19(1):73-82.

Bonnan, M.F. 2003. Morphometric analysis of humerus and femur shape in Morrison sauropods: implications for functional morphology and paleobiology. *Paleobiology*, 30(3): 444-470

Bordy, E. M., P. J. Hancox, and B. S. Rubidge. 2004. Basin development during the deposition of the Elliot Formation (Late Triassic - Early Jurassic), Karoo Supergroup, South Africa. *South African Journal of Geology* 107:397-412.

Bordy, E.M., Hancox, P.J. & Rubidge, B.S. 2005. The contact of the Molteno and Elliot formations through the main Karoo Basin, South Africa: a second-order sequence boundary. *South African Journal of Geology*. 108(3):351-364.

Buffetaut E, Suteethorn V, Cuny G, Tong H, Le Loeuff J, Khansubha S, Jongautchariyakul S. 2000. The earliest known sauropod dinosaur. *Nature* 407:72-4.

Buffetaut E, Suteethorn V, Le Loeuff J, Cuny G, Tong H, Khansubha S. 2002. The first giant dinosaurs: A large sauropod from the Late Triassic of Thailand. *C R Palevol* 1:103-9.

Carballido, J.L. & Pol, D. 2010. The dentition of Amygdalodon patagonicus (Dinosauria: Sauropoda) and the dental evolution in basal sauropods. *Comptes Rendus Palevol*. 9(3):83-93.

Carrano, M.T. & Hutchinson, J.R. 2002. Pelvic and hindlimb musculature of Tyrannosaurus rex (Dinosauria: Theropoda). *Journal of Morphology*. 253(3):207-228.

Carrano, M. T. 2005. The Evolution of Sauropod Locomotion, pp. 229-250 in K. A. Curry Rogers and J. A. Wilson (eds.), *The Sauropods: Evolution and Paleobiology*. University of California Press.

Cerda IA, Pol D, Chinsamy A. 2013. Osteohistological insight into the early stages of growth in Mussaurus patagonicus (Dinosauria, Sauropodomorpha). *Hist Biol* 26:110-21.

Cerda IA, Chinsamy A, Pol D. 2014. Unusual endosteally formed bone tissue in a Patagonian basal sauropodomorph dinosaur. *Anat Rec* 297:1385-91.

Cerda I, Chinsamy A, Pol D, Apaldetti C, Otero A, Powell J, Martinez R. 2017. Novel insight into the origin of the growth dynamics of sauropod dinosaurs, and the attainment of gigantism. *PloS One 12*, e0179707.

Charig AJ, Attridge J, Crompton AW. 1965. On the origin of the sauropods and the classification of the Saurischia. *Proc Linn Soc Lond* 176:197-221.

Chinsamy A and Raath MA. 1992. Preparation of fossil bone for histological examination. *Palaeont Afr* 29:39-44.

Chinsamy A. 1993a. Image analysis and the physiological implications of the vascularization of femora in archosaurs. *Mod Geol* 19:101-8.

Chinsamy A. 1993b. Bone histology and growth trajectory of the prosauropod dinosaur Massospondylus carinatus Owen. *Mod Geol* 18:319-29.

Chinsamy A. 1994. Dinosaur bone histology: Implications and inferences. *Paleont Soc Spec Pub* 7:213-27.

Chinsamy A and Tumarkin-Deratzian A. 2009. Pathologic bone tissues in a turkey vulture and a nonavian dinosaur: Implications for interpreting endosteal bone and radial fibrolamellar bone in fossil dinosaurs. *Anat Rec* 292:1478-84.

Chinsamy A, Thomas DB, Tumarkin-Deratzian AR, Fiorillo AR. 2012. Hadrosaurs were perennial polar residents. *Anat Rec* 295:610-4.

Chinsamy-Turan A. 2005. *The microstructure of dinosaur bone*. Baltimore: Johns Hopkins University Press.

Chure, D., Britt, B.B., Whitlock, J.A. & Wilson, J.A. 2010. First complete sauropod dinosaur skull from the Cretaceous of the Americas and the evolution of sauropod dentition. *Naturwissenschaften*. 97(4):379-391.

Cooper, M.R. 1981. The prosauropod dinosaur Massospondylus carinatus Owen from Zimbabwe: its biology, mode of life and phylogenetic significance. *Occas.Pap. Natl.Monuments Rhod*. 6(10):690-840.

Cooper, M.R. 1984. A reassessment of Vulcanodon karibaensis Raath (Dinosauria: Saurischia) and the origin of the Sauropoda. *Palaeontology Africana*. 25: 203-231.

Curry KA. 1999. Ontogenetic histology of Apatosaurus (Dinosauria: Sauropoda): New insights on growth rates and longevity. *J Vert Paleont* 19:654-65.

Curry Rogers K, Whitney M, D'Emic M, Bagley B. 2016. Precocity in a tiny titanosaur from the Cretaceous of Madagascar. *Science* 352:450-3.

de Fabrègues, C.P. & Allain, R. 2016. New material and revision of Melanorosaurus thabanensis, a basal sauropodomorph from the Upper Triassic of Lesotho. *PeerJ*. 4:e1639.

De Ricqlès A. 1983. Cyclical growth in the long limb bones of a sauropod dinosaur. *Acta Palaeontol Pol* 28:1-2.

Ellenberger, F. and Ellenberger, P. 1956. Le gisement de Dinosauriens de Maphutseng (Basutoland, Afrique du Sud). *Compte Rendus de la Société Géologique de France*, 99-101.

Ellenberger and Ginsberg, 1966. Le gisement de Dinosauriens triasiques de Maphutseng (Basutoland) et l'origine des Sauropodes [The Triassic dinosaur locality of Maphutseng (Basutoland) and the origin of sauropods]. *Comptes Rendus de l'Académie des Sciences à Paris*, Série D. 262, 444-447.

Ellenberger, P. 1970. Les niveaux paléontologiques de première apparition des mammifères primordiaux en Afrique du Sud et leur ichnologie: établissement de zones stratigraphiques détaillées dans le Stormberg du Lesotho (Afrique du Sud) (Trias supérieur à Jurassique). IUGS, 2nd Symposium on Gondwana Stratigraphy and Palaeontology. *Council for Scientific and Industrial Research Pretoria*. 343-370.

Ezcurra, M.D., 2010. A new early dinosaur (Saurischia: Sauropodomorpha) from the Late Triassic of Argentina: a reassessment of dinosaur origin and phylogeny. *Journal of Systematic Palaeontology*. 8: 371–425.

Ezcurra, M.D. and Apaldetti, C. 2012. A robust sauropodomorph specimen from the Late Triassic of Argentina and insights on the diversity of the Los Colorados Formation. *Proceedings of the Geologists' Association*. 123: 155–164.

Galton, P.M. 1985. Notes on the Melanorosauridae, a family of large prosauropod dinosaurs (Saurischia: Sauropodomorpha). *Geobios*. 18(5):671-676.

Galton PM, Van Heerden J. 1998. Anatomy of the prosauropod dinosaur Blikanasaurus cromptoni (Upper Triassic, South Africa), with notes on the other tetrapods from the lower Elliot Formation. *J Paläontol* Z 72:163-177.

Galton, P.M. 2001. Prosauropod dinosaurs from the Upper Triassic of Germany. In Anonymous(eds.), *Actas de las I Jornadas internacionales sobre Paleontología de Dinosaurios y su Entorno*. Colectivo Arqueológico-Paleontológico de Salas (C. A. S.), Burgos, pp. 25-92.

Galton, P.M., Van Heerden, J. and Yates, A.M. 2004. Postcranial anatomy of referred specimens of the sauropodomorph dinosaur Melanorosaurus from the Late Triassic of South Africa. In K. Carpenter and V. Tidwell (eds.), *Thunder-Lizards: The Sauropodomorph Dinosaurs*. Indiana University Press, Bloomington, pp. 1-37.

Galton, PM and Upchurch, P. 2004. Prosauropoda. In D. B. Weishampel, P. Dodson, and H. Osmolska (eds.), *The Dinosauria (second edition).* University of California Press, Berkeley, pp. 232-258

Galton, P.M. 2005. Bones of large dinosaurs (Prosauropoda and Stegosauria) from the Thaetic Bone Bed (Upper Triassic of Aust Cliff, southwest England. *Revue De Paléobiologie*. 24(1):51.

Galton, P.M. & Kermack, D. 2010. The anatomy of Pantydraco caducus, a very basal sauropodomorph dinosaur from the Rhaetian (Upper Triassic) of South Wales, UK. *Revue De Paléobiologie*. 29:341-404.

Gauffre, F-X. 1993. Biochronostratigraphy of the lower Elliot Formation (southern Africa) and preliminary results on the Maphutseng dinosaur (Saurischia: Prosauropoda) from the same formation of Lesotho. In S. G. Lucas and M. Morales (eds.), The Nonmarine Triassic. New Mexico Museum of *Natural History and Science Bulletin*. 3: 147-149

Gilmore, C.W. 1936. Osteology of Apatosaurus, with Species Reference to Specimens in the Carnegie Museum. *Carnegie Institute*.

Goloboff, P. A., Farris, J. S. and Nixon, K. C. 2008. TNT, a free program for phylogenetic analysis. *Cladistics*, 24, 774–786.

Google Earth V7.1.2.2041. (October 04, 2013). Africa. 1°26’39.84’’S, 21°58’24.40’’ E, Eye alt 14617.33 km. SIO, NOAA, U.S. Navy, NGA, GEBCO. IBCAO 2014, Landsat 2014. http://www.earth.google.com [April 21, 2014a].

Google Earth V7.1.2.2041. (October 04, 2013). Maphutseng, Lesotho. 29°39’49.31’’S, 28°31’23.12’’E Eye alt 422.84 km. SIO, NOAA, U.S. Navy, NGA, GEBCO. Google 2014, AfriGIS (Pty) Ltd. 2014, Landsat 2014. http://www.earth.google.com [April 21, 2014b].

Haughton, S.H. 1924. The fauna and stratigraphy of the Stormberg Series. *Annals of the South African Museum*. 12(8):323-497.

Haughton, S.H. & Brink, A.S. 1954. A bibliographical list of Reptilia from the Karroo beds of Africa. *Die Afrikaanse Pers*

He X, Wang C, Liu S, Zhou F, Lui T, Cai K, Dai B. 1998. A new species of sauropod from the early Jurassic of Gongxian co., Sichuan. *Acta Geol Sich* 18:1-7.

Hurum JH, Bergan M, Muller R, Nystuen JP, Klein N. 2006. A Late Triassic dinosaur bone, offshore Norway. *Norsk Geol Tidsskr* 86:117.

Huxley, T.H. 1866. On some remains of large dinosaurian reptiles from the Stormberg mountains, South Africa. *Geological Society of London*.

Kitching, J. W., and M. A. Raath. 1984. Fossils from the Elliot and Clarens formations (Karoo sequence) of the northeastern Cape, Orange Free State and Lesotho, and a suggested biozonation based on tetrapods. *Palaeontologia africana* 25:111-125.

Klein N and Sander PM. 2007. Bone histology and growth of the prosauropod dinosaur Plateosaurus engelhardti Von Meyer, 1837 from the Norian bonebeds of Trossingen (Germany) and Frick (Switzerland). *Spec Pap Palaeontol* 77:169.

Klein N and Sander PM. 2008. Ontogenetic stages in the long bone histology of sauropod dinosaurs. *Paleobiology* 34:247-63.

Köhler M and Moyà-Solà S. 2009. Physiological and life history strategies of a fossil large mammal in a resource-limited environment. *Proc Natl Acad Sci* 106:20354-8.

Köhler M, Marín-Moratalla N, Jordana X, Aanes R. 2012. Seasonal bone growth and physiology in endotherms shed light on dinosaur physiology. *Nature* 487:358.

Laojumpon, C., Suteethorn, V., Chanthasit, P., Lauprasert, K. & Suteethorn, S. 2017. New Evidence of Sauropod Dinosaurs from the Early Jurassic Period of Thailand. *Acta Geologica Sinica-English Edition*. 91(4):1169-1178.

Langer, M.C. 2003. The pelvic and hind limb anatomy of the stem-sauropodomorph Saturnalia tupiniquim (Late Triassic, Brazil). *PaleoBios* 23(2):1-30.

Langer, M.C., Franca, M.A. & Gabriel, S. 2007. The pectoral girdle and forelimb anatomy of the stem-sauropodomorph Saturnalia tupiniquim (Upper Triassic, Brazil). *Special Papers in Palaeontology*. 77:113.

Lehman TM and Woodward HN. 2008. Modeling growth rates for sauropod dinosaurs. *Paleobiology* 34:264-81.

Lenehan TM and Fetter AW. 1985. Hypertrophic osteodystrophy. In: Newton CD and Nunamaker DM, editors. Textbook of small animal orthopedics. *Baltimore: Lippincott*. p 597.

Lucas, S. G., and J. P. Hancox. 2001. Tetrapod-based correlation of the nonmarine Upper Triassic of southern Africa. *Albertiana* 25:5-9.

Maddison, W. P. and D.R. Maddison. 2018. Mesquite: a modular system for evolutionary analysis. Version 3.51 http://www.mesquiteproject.org

Mallison, H. 2010a. The digital Plateosaurus I: body mass, mass distribution, and posture assessed using CAD and CAE on a digitally mounted complete skeleton. *Palaeontologia Electronica*. 13(2):8A.

Mallison, H. 2010b. The digital Plateosaurus II: an assessment of the range of motion of the limbs and vertebral column and of previous reconstructions using a digital skeletal mount. *Acta Palaeontologica Polonica*. 55(3):433-459.

Mannion PD. 2010. A revision of the sauropod dinosaur genus ‘Bothriospondylus’ with a redescription of the type material of the Middle Jurassic form ‘B. madagascariensis’. *Palaeontology* 53:277-96.

McPhee BW, Yates AM, Choiniere JN, Abdala F. 2014. The complete anatomy and phylogenetic relationships of Antetonitrus ingenipes (Sauropodiformes, Dinosauria): Implications for the origins of Sauropoda. *Zool J Linn Soc* 171:151-205.

McPhee, B. W., Bonnan, M. F., Yates, A. M., Neveling, J., & Choiniere, J. N. (2015). A new basal sauropod from the pre-Toarcian Jurassic of South Africa: evidence of niche-partitioning at the sauropodomorph–sauropod boundary? *Scientific Reports*. 5: 13224.

McPhee, B.W., Bordy, E.M., Sciscio, L. & Choiniere, J.N. 2017. The sauropodomorph biostratigraphy of the Elliot Formation of southern Africa: Tracking the evolution of Sauropodomorpha across the Triassic–Jurassic boundary. *Acta Palaeontologica Polonica*. 62(3):441-465.

McPhee, B.W., Benson, R.B., Botha-Brink, J., Bordy, E.M. and Choiniere, J.N., 2018. A giant dinosaur from the earliest Jurassic of South Africa and the transition to quadrupedality in early sauropodomorphs. *Current Biology*. 28(19):3143-3151. e7.

McPhee, B.W., Bittencourt, J.S., Langer, M.C., Apaldetti, C. & Da Rosa, ÁA. 2019. Reassessment of Unaysaurus tolentinoi (Dinosauria: Sauropodomorpha) from the Late Triassic (early Norian) of Brazil, with a consideration of the evidence for monophyly within non-sauropodan sauropodomorphs. *Journal of Systematic Palaeontology*. :1-35.

Moser, M. 2003. Plateosaurus engelhardti Meyer, 1837 (Dinosauria: Sauropodomorpha) aus dem Feuerletten (Mittelkeuper; Obertrias) von Bayern. *Zitteliana*. :3-186.

Müller, R.T., Langer, M.C. & Dias-da-Silva, S. 2018. An exceptionally preserved association of complete dinosaur skeletons reveals the oldest long-necked sauropodomorphs. *Biology Letters*. 14(11):20180633.

Nair, J. and Yates, A. 2014. Osteology of the type material of *Melanosaurus readi*, a 'near sauropod' (Dinosauria: Sauropodamorpha) from the Upper Triassic Lower Elliot Formation of South Africa, and the status of referred specimens. *Journal of Vertebrate Paleontology*, *Program and Abstracts*, 2014, pp. 193–194.

Novas, F. E. 1996. Dinosaur monophyly. *Journal of Vertebrate Paleontology* 16:723-741.

Novas, F.E., Ezcurra, M.D., Chatterjee, S., Kutty, T.S., 2011. New dinosaur species from the Late Triassic Upper Maleri and Lower Dharmaram formations of Central India. *Earth and Environmental Science Transactions of the Royal Society of Edinburgh*, 101: 333-349.

Otero, A. & Pol, D. 2013. Postcranial Anatomy and Phylogenetic relationships of Mussaurus patagonicus (Dinosauria, Sauropodomorpha). *Journal of Vertebrate Paleontology*,33 (5): 1138 -1168.

Otero, A., Krupandan, E., Pol, D., Chinsamy, A. & Choiniere, J. 2015. A new basal sauropodiform from South Africa and the phylogenetic relationships of basal sauropodomorphs. *Zoological Journal of the Linnean Society*. 174(3):589-634.

Peyre de Fabrègues C, Allain R. 2016. New material and revision of Melanorosaurus thabanensis, a basal

sauropodomorph from the Upper Triassic of Lesotho. *PeerJ* 4:e163

Pol, D. & Powell, J. E. 2007 New information on Lessemsaurus sauropoides (Dinosauria: Sauropodomorpha) from the Late Triassic of Argentina. *Special Papers in Palaeontology*, 77: 223–243.

Pol, D. & Escapa, I.H. 2009. Unstable taxa in cladistic analysis: identification and the assessment of relevant characters. *Cladistics*. 25(5):515-527.

Pol D, Garrido A, Cerda I .2011. A New Sauropodomorph Dinosaur from the Early Jurassic of Patagonia and the Origin and Evolution of the Sauropod type Sacrum. *PLoS ONE*, 6(1), e14572.

Reid R. 1981. Lamellar-zonal bone with zones and annuli in the pelvis of a sauropod dinosaur. *Nature* 292:49-51.

Rimblot-Baly F, de Ricqlès A, Zylberberg L. 1995. Analyse paléohistologique d'une série de croissance partielle chez Lapparentosaurus madagascariensis (Jurassique Moyen): Essai sur la dynamique de croissance d'un dinosaure sauropode. *Annls Paléont (Vert)* 81:49-86.

Sander PM. 2000. Longbone histology of the Tendaguru sauropods: Implications for growth and biology. *Paleobiology* 26:466-88.

Sander PM, Klein N, Buffetaut E, Cuny G, Suteethorn V, Le Loeuff J. 2004. Adaptive radiation in sauropod dinosaurs: Bone histology indicates rapid evolution of giant body size through acceleration. *Org Divers Evol* 4:165-73.

Sander PM and Klein N. 2005. Developmental plasticity in the life history of a prosauropod dinosaur. *Science* 310:1800-2.

Sander PM, Klein N, Stein K, Wings O. 2011a. Sauropod bone histology and its implications for sauropod biology. In: Gee CT, Klein N, Remes C, Sander PM, editors. *Biology of the Sauropod Dinosaurs: Understanding the Life of Giants*. Bloomington: Indiana University Press. p 276-302.

Sander PM, Christian A, Clauss M, Fechner R, Gee CT, Griebeler E, Gunga H, Hummel J, Mallison H, Perry SF. 2011b. Biology of the sauropod dinosaurs: The evolution of gigantism. *Biol Rev Camb Philos Soc*. 86:117-55.

Sereno, P.C. 1998. A rationale for phylogenetic definitions, with application to the higher-level taxonomy of Dinosauria. *Neues Jahrbuch Für Geologie Und Paläontologie-Abhandlungen.* 210:41-83.

Sereno, P.C. 1999. The evolution of dinosaurs. *Science*. 284(5423):2137-2147.

Sereno, P. C. 2007. Basal Sauropodomorpha: historical and recent phylogenetic hypothese, with comments on Ammosaurus major (Marsh, 1889). *Special Papers in Palaeontology* 77:261-289.

Smith, N.D. & Pol, D. 2007. Anatomy of a basal sauropodomorph dinosaur from the Early Jurassic Hanson Formation of Antarctica. *Acta Palaeontologica Polonica*. 52(4).

Stein K and Sander PM. 2009. Histological core drilling: A less destructive method for studying bone histology. In: Brown MA, Kane JF, Parker WG., editors. *Methods In Fossil Preparation: Proceedings of the First Annual Fossil Preparation and Collections Symposium.* Petrified Forest: University of Nebraska. pp. 69–80.

Upchurch, P. 1998. The phylogenetic relationships of sauropod dinosaurs. *Zoological Journal of the Linnean Society*. 124(1):43-103.

Upchurch, P., Barrett, P. M. & Dodson, P. 2004 Sauropoda. In D. B. Weishampel, P. Dodson & H. Osmolska (eds), *Dinosauria* (2nd edn). University of California Press, Berkeley, pp. 259–322.

Upchurch, P., Barrett, P.M., Xijin, Z. & Xing, X.U. 2007. A re-evaluation of Chinshakiangosaurus chunghoensis Ye vide Dong 1992 (Dinosauria, Sauropodomorpha): implications for cranial evolution in basal sauropod dinosaurs. *Geological Magazine*. 144(2):247-262.

Van Gen J, Bordy EM, Tucker R, McPhee, BW. 2015. Maphutseng fossil heritage: Stratigraphic context of the dinosaur trackways and bone bed in the Upper Triassic–Lower Jurassic Elliot Formation (Karoo Supergroup, Lesotho). *Proc Abstr/ I Int Congr Contl Ichnol*. 1:67.

Van Heerden, J. 1979. The morphology and taxonomy of Euskelosaurus (Reptilia: Saurischia: Late Triassic) from South Africa. *Navorsinge van die Nasionale Museum Bloemfontein*. 4: 21-84

von Huene, F. 1932. Die fossile Reptil-Ordnung Saurischia, ihre Entwicklung und Geschichte. *Monographien zur Geologie und Palaeontologie*, series 1:4, 361.

Wilhite, R. 2003. Biomechanical Reconstruction of the Appendicular Skeleton of Three North American Jurassic Sauropods. PhD Thesis. *Louisiana State University*.

Wilson, J. A., and P. C. Sereno. 1998. Early Evolution and Higher-Level Phylogeny of Sauropod Dinosaurs. *Memoir (Society of Vertebrate Paleontology)*. 5:1-68.

Yadagiri, P. 2001. The osteology of Kotasaurus yamanpalliensis, a sauropod dinosaur from the Early Jurassic Kota Formation of India. *Journal of Vertebrate Paleontology*. 21(2):242-252.

Yates, A.M. 2003a. A definite prosauropod dinosaur from the lower Elliot Formation (Norian: Upper Triassic) of South Africa. *Palaeontology Africana*. 39: 63-68.

Yates, A.M. 2003b. A new species of the primitive dinosaur Thecodontosaurus (Saurischia: Sauropodomorpha) and its implications for the systematics of early dinosaurs. *Journal of Systematic Palaeontology*. 1(1):1-42.

Yates, A.M. 2004. Anchisaurus polyzelus (Hitchcock): the smalles known Sauropod Dinosaur and the evolution of gigantism among Sauropodomorph Dinosaurs. *Peabody Museum of Natural History New Haven*.

Yates, A. M. 2007a.The first complete skull of the Triassic dinosaur Melanorosaurus Haughton (Sauropodomorpha: Anchisauria). *Special Papers in Palaeontology*, 77, 9–55.

Yates, A.M. 2007b. Solving a dinosaurian puzzle: the identity of Aliwalia rex Galton. *Historical Biology: An International Journal of Paleobiology*. 19(1): 93-123.

Yates, A. M. & Kitching, J. W. 2003 The earliest known sauropod dinosaur and the first steps towards sauropod locomotion. *Proceedings of the Royal Society B*. 270: 1753–1758.

Yates, A. M., M. F. Bonnan, J. Neveling, A. Chinsamy, and M. G. Blackbeard. 2010. A new transitional sauropodomorph dinosaur from the Early Jurassic of South Africa and the evolution of sauropod feeding and quadrupedalism. *Proceedings of the Royal Society B*. 277:787–794.

Yates, A.M., Bonnan, M.F. & Neveling, J. 2011. A new basal sauropodomorph dinosaur from the Early Jurassic of South Africa. *Journal of Vertebrate Paleontology*. 31(3):610-625.

Young, C. 1941. A Complete Osteology of Lufengosaurus Heunei Young (gen. et sp. nov.) from Lufeng, Yunnan, China. *Geol. Survey of China*.

Appendix 1: Character List

1. Skull to femur ratio: greater than 0.6 (0); less than 0.6 (1). (Yates 2007).

2. Lateral plates appressed to the labial side of the premaxillary, maxillary and dentary teeth: absent (0); present (1). (Yates 2007).

3. Relative height of the rostrum at the posterior margin of the naris: more than 0.6 the height of the skull at the middle of the orbit (0); less than 0.6 the height of the skull at the middle of the orbit (1). (Yates 2007).

4. Foramen on the lateral surface of the premaxillary body: absent (0); present (1). (Yates 2007).

5. Distal end of the dorsal premaxillary process: tapered (0); transversely expanded (1). (Yates 2007).

6. Profile of premaxilla: convex (0); with an inflection at the base of the dorsal process (1). (Yates 2007).

7. Size and position of the posterolateral process of premaxilla: large and lateral to the anterior process of the maxilla (0); small and medial to the anterior process of the maxilla (1). (Yates 2007).

8. Relationship between posterolateral process of the premaxilla and the anteroventral process of the nasal: broad sutured contact (0); point contact (1); separated by maxilla (2). Ordered. (Yates 2007).

9. Posteromedial process of the premaxilla: absent (0); present (1). (Yates 2007).

10. Shape of the anteromedial process of the maxilla: narrow, elongated and projecting anterior to lateral premaxilla-maxilla suture (0); short, broad and level with lateral premaxilla-maxilla suture (1). (Yates 2007).

11. Premaxilla, position of the first tooth: adjacent to rostral tip (0); retreated (1). (Pretto et al. 2018)

12. Development of external narial fossa: absent to weak (0); well-developed with sharp posterior and anteroventral rims (1). (Yates 2007).

13. Development of narial fossa on the anterior ramus of the maxilla: weak and orientated laterally to dorsolaterally (0);

well-developed and forming a horizontal shelf (1). (Yates 2007).

14. Size and position of subnarial foramen: absent (0); small (no larger than adjacent maxillary neurovascular foramina) and positioned outside of narial fossa (1); large and on the rim of, or inside, the narial fossa (2). Ordered. (Yates 2007).

15. Shape of subnarial foramen: rounded (0); slot-shaped (1). (Yates 2007).

16. Maxillary contribution to the margin of the narial fossa: absent (0); present (1). (Yates 2007).

17. Maxilla, dorsally open neurovascular canal on the floor of the antorbital fossa: absent (0); present (1). (Witmer 1997; Yates & Kitching 2003; Pretto et al. 2018).

18. Maxilla, promaxillary fenestra: (0) absent; (1) present. (Martínez et al. 2011).

19. Diameter of external naris: less than 0.5 of the orbital diameter (0); greater than 0.5 of the orbital diameter. (Yates 2007).

20. Shape of the external naris (in adults): rounded (0); subtriangular with an acute posteroventral corner (1). (Yates 2007).

21. Level of the anterior margin of the external naris: anterior to the midlength of the premaxillary body (0); posterior to the midlength of the premaxillary body (1). (Yates 2007).

22. Level of the posterior margin of external naris: anterior to, or level with the premaxilla-maxilla suture (0); posterior to the first maxillary alveolus (1); posterior to the midlength of the maxillary tooth row and the anterior margin of the antorbital fenestra (2). Ordered. (Yates 2007).

23. Dorsal profile of the snout: straight to gently convex (0); with a depression behind the naris (2). (Yates 2007).

24. Elongate median nasal depression: absent (0); present (1). (Yates 2007).

25. Width of anteroventral process of nasal at its base: less than the width of the anterodorsal process at its base (0);

greater than the width of the anterodorsal process at its base (1). (Yates 2007).

26. Nasal relationship with dorsal margin of antorbital fossa: not contributing to the margin of the antorbital fossa (0); lateral margin overhangs the antorbital fossa and forms its dorsal margin (1); overhang extensive, obscuring the dorsal lachrymal-maxilla contact in lateral view (2). Ordered. (Yates 2007).

27. Pointed caudolateral process of the nasal overlapping the lachrymal: absent (0); present (1). (Yates 2007).

28. Anterior profile of the maxilla: slopes continuously towards the rostral tip (0); with a strong inflection at the base of the ascending ramus, creating a rostral ramus with parallel dorsal and ventral margins (1). (Yates 2007).

29. Length of rostral ramus of the maxilla: less than its dorsoventral depth (0); greater than its dorsoventral depth (1). (Yates 2007).

30. Shape of the main body of the maxilla: tapering posteriorly (0); dorsal and ventral margins parallel for most of their length (1). (Yates 2007).

31. Shape of the ascending ramus of the maxilla in lateral view: tapering dorsally (0); with an anteroposterior expansion at the dorsal end (1). (Yates 2007).

32. Rostrocaudal length of the antorbital fossa: greater than that of the orbit (0); less than that of the orbit (1). (Yates 2007).

33. Posteroventral extent of medial wall of antorbital fossa: reaching the anterior tip of the jugal (0); terminating anterior to the anterior tip of the jugal (1).

34. Development of the antorbital fossa on the ascending ramus of the maxilla: deeply impressed and delimited by a sharp, scarp-like rim (0); weakly impressed and delimited by a rounded rim or a change in slope (1). (Yates 2007).

35. Shape of the antorbital fossa: crescentic with a strongly concave posterior margin that is roughly parallel to the anterior margin of the antorbital fossa (0); subtriangular with a straight to gently concave posterior margin (1); antorbital fossa absent (2). (Yates 2007).

36. Size of the neurovascular foramen at the posterior end of the lateral maxillary row: not larger than the others (0); distinctly larger than the others in the row (1). (Yates 2007).

37. Direction that the neurovascular foramen at the posterior end of the lateral maxillary row opens: posteriorly (0); anteriorly, ventrally, or laterally (1). (Yates 2007).

38. Arrangement of lateral maxillary neurovascular foramina: linear (0); irregular (1). (Yates 2007).

39. Longitudinal ridge on the posterior lateral surface of the maxilla: absent (0); present (1). (Yates 2007).

40. Dorsal exposure of the lachrymal: present (0); absent (1). (Yates 2007).

41. Shape of the lachrymal: dorsoventrally short and block shaped (0); dorsoventrally elongate and shaped like an inverted L (1). (Yates 2007).

42. Orientation of the lachrymal orbital margin: strongly sloping anterodorsally (0); erect and close to vertical (1). (Yates 2007).

43. Length of the anterior ramus of the lachrymal: greater than half the length of the ventral ramus (0); less than half the length of the ventral ramus (1); absent altogether (2). Ordered. (Yates 2007).

44. Web of bone spanning junction between anterior and ventral rami of lachrymal: absent and antorbital fossa laterally exposed (0); present, obscuring posterodorsal corner of antorbital fossa (1). (Yates 2007).

45. Extension of the antorbital fossa onto the ventral end of the lachrymal: present (0); absent (1). (Yates 2007).

46. Length of the posterior process of the prefrontal: short (0); elongated, so that total prefrontal length is equal to the anteroposterior diameter of the orbit (1). (Yates 2007).

47. Bone sheet between the rostral and ventral processes of the prefrontal: (0) absent; (1) present. (Müller et al. 2018).

48. Ventral process of prefrontal extending down the posteromedial side of the lachrymal: present (0); absent (1). (Yates 2007).

49. Maximum transverse width of the prefrontal: less than 0.25 of the skull width at that level (0); more than 0.25 of the skull width at that level (1). (Yates 2007).

50. Shape of the orbit: subcircular (0); ventrally constricted making the orbit subtriangular (1). (Yates 2007).

51. Slender anterior process of the frontal intruding between the prefrontal and the nasal: absent (0); present (1). (Yates 2007).

52. Jugal-lachrymal relationship: lachrymal overlapping lateral surface of jugal or abutting it dorsally (0); jugal overlapping lachrymal laterally (1). (Yates 2007).

53. Shape of the suborbital region of the jugal: an anteroposteriorly elongate bar (0); an anteroposteriorly shortened plate (1). (Yates 2007).

54. Jugal contribution to the antorbital fenestra: absent (0); present (1). (Yates 2007).

55. Angle between ascending process and caudal process of jugal: right or obtuse (0); acute, with an ascending process strongly dorsocaudally oriented (1). (Ezcurra 2006).

56. Dorsal process of the anterior jugal: present (0); absent (1). (Yates 2007).

57. Ratio of the minimum depth of the jugal below the orbit to the distance between the anterior end of the jugal and the anteroventral corner of the infratemporal fenestra: less than 0.2 (0); greater than 0.2 (1). (Yates 2007).

58. Transverse width of the ventral ramus of the postorbital: less than its anteroposterior width at midshaft (0); greater than its anteroposterior width at midshaft (1). (Yates 2007).

59. Postorbital, distal end of frontal ramus, distinct concave notch between parietal and frontal facets: (0) absent; (1) present. (Chapelle & Choiniere 2018).

60. Shape of the dorsal margin of postorbital in lateral view: straight to gently curved (0); with a distinct embayment between the anterior and posterior dorsal processes (1). (Yates 2007).

61. Height of the postorbital rim of the orbit: flush with the posterior lateral process of the postorbital (0); raised so that it projects laterally to the posterior dorsal process (1). (Yates 2007).

62. Postfrontal bone: present (0); absent (1). (Yates 2007).

63. Position of the anterior margin of the infratemporal fenestra: behind the orbit (0); extends under the rear half of the orbit (1); extends as far forward as the midlength of the orbit (2). Ordered. (Yates 2007).

64. Frontal contribution to the supratemporal fenestra: present (0); absent (1). (Yates 2007).

65. Orientation of the long axis of the supratemporal fenestra: longitudinal (0); transverse (1). (Yates 2007).

66. Medial margin of supratemporal fossa: simple smooth curve (0); with a projection at the frontal/postorbital-parietal suture producing a scalloped margin (1). (Yates 2007).

67. Length of the quadratojugal ramus of the squamosal relative to the width at its base: less than four times its width (0); greater than four times its width (1). (Yates 2007).

68. Proportion of infratemporal fenestra bordered by squamosal: more than 0.5 of the depth of the infratemporal fenestra (0); less than 0.5 of the depth of the infratemporal fenestra (1). (Yates 2007).

69. Squamosal-quadratojugal contact: present (0); absent (1). (Yates 2007).

70. Angle of divergence between jugal and squamosal rami of quadratojugal: close to 90 degrees (0); close to parallel (1). (Yates 2007).

71. Length of jugal ramus of quadratojugal: no longer than the squamosal ramus (0); longer than the squamosal ramus (1). (Yates 2007).

72. Shape of the rostral end of the jugal ramus of the quadratojugal: tapered (0); dorsoventrally expanded (1). (Yates 2007).

73. Relationship of quadratojugal to jugal: jugal overlaps the lateral surface of the quadratojugal (0); quadratojugal

overlaps the lateral surface of the jugal (1); quadratojugal sutures along the ventrolateral margin of the jugal (2). (Yates 2007).

74. Position of the quadrate foramen: on the quadrate-quadratojugal suture (0); deeply incised into, and partly encircled by, the quadrate (1); on the quadrate-squamosal suture, just below the quadrate head (2). (Yates 2007).

75. Shape of posterolateral margin of quadrate: sloping anterolaterally from posteromedial ridge (0); everted posteriorly creating a posteriorly facing fossa (1); posterior fossa deeply excavated, invading quadrate body (2). Ordered. (Yates 2007).

76. Exposure of the lateral surface of the quadrate head: absent, covered by lateral sheet of the squamosal (0); present (1). (Yates 2007).

77. Proportion of the length of the quadrate that is occupied by the pterygoid wing: at least 70 per cent (0); greater than 70 per cent (1). (Yates 2007).

78. Depth of the occipital wing of the parietal: less than 1.5 times the depth of the foramen magnum (0); more than 1.5 times the depth of the foramen magnum (1). (Yates 2007).

79. Position of foramina for mid-cerebral vein on occiput: between supraoccipital and parietal (0); on the supraoccipital (1). (Yates 2007).

80. Post-parietal fenestra between supraoccipital and parietals: absent (0); present (1). (Yates 2007).

81. Shape of the supraoccipital: diamond-shaped, at least as high as wide (0); semi-lunate and wider than high (1). (Yates 2007).

82. Orientation of the supraoccipital plate: erect to gently sloping (0); strongly sloping forward so that the dorsal tip lies level with the basipterygoid processes (1). (Yates 2007).

83. Orientation of the paroccipital processes in occipital view: slightly dorsolaterally directed to horizontal (0); ventrolaterally directed (1). (Yates 2007).

84. Orientation of the paroccipital processes in dorsal view: posterolateral forming a v-shaped occiput (0); lateral forming a flat occiput (1) (Yates 2007).

85. Size of the post-temporal fenestra: large fenestra (0); a small hole that is much less than half the depth of the paraoccipital process (1). (Yates 2007).

86. Exit of the mid-cerebral vein: through trigeminal foramen (0); through a separate foramen anterodorsal to trigeminal foramen (1). (Yates 2007).

87. Shape of the floor of the braincase in lateral view: relatively straight with the basal tuberae, basipterygoid processes and parasphenoid rostrum roughly aligned (0); bent with the basipterygoid processes and the parasphenoid rostrum below the level of the basioccipital condyle and the basal tuberae (1); bent with the basal tuberae lowered below the level of the basioccipital and the parasphenoid rostrum raised above it (2). (Yates 2007).

88. Basioccipital component of the basal tubera, medial component in relation to the parabasisphenoidal component: (0) present; (1) absent. (Yates 2007).

89. Length of the basipterygoid processes (from the top of the parasphenoid to the tip of the process): less than the height of the braincase (from the top of the parasphenoid to the top of the supraoccipital) (0); greater than the height of the braincase (from the top of the parasphenoid to the top of the supraoccipital) (1). (Yates 2007).

90. Basioccipital – basisphenoid junction on the ventral surface of the bones: (0) straight line; U/V shaped (1). (Bronzati & Rauhut 2017).

91. Subsellar recess: (0) maximum width equal or greater than the dorsoventral height; (1) maximum width smaller than the dorsoventral height. (Bronzati & Rauhut 2017).

92. Laminae/ridges extending from the basipterygoid process onto the parasphenoid rostrum: extend parallel until they fade into the ventral margin of the cultriform process (0); converge anteromedially on the ventral surface of the cultriform process (1). (Bronzati & Rauhut 2017).

93. Angle between basipterygoid process and cultriform process of the parabasisphenoid: < 90 degrees (0); 90 digress (1); > 90 degrees (2). (Bronzati et al. 2018)

94. Length of the basisphenoid (from the basipterygoid process to the basisphenoidal component of the basal tubera) in relation to the length of the basioccipital (from the basioccipital component of the basal tubera to posterior limit of the condyle): longer or equal (0); shorter (1). (Bronzati & Rauhut 2017).

95. Notch in the posterodorsal margin of the lateral portion of the parabasisphenoid: absent (0); present (1). (Bronzati & Rauhut 2017).

96. Number of foramina in the otoccipital between the exoccipital pillar (excluding the foramina for the hypoglossal nerve) posteriorly and fenestra ovalis anteriorly: one (0), two (1). (Bronzati & Rauhut 2017).

97. Unossified gap between the basioccipital and basisphenoidal component of the basal tubera and ventral ramus of the opistothic: absent (0); present (1). (Bronzati & Rauhut 2017).

98. Otosphenoidal crest: low and not projecting posterolaterally (i.e. does not cover the fenestra ovalis with the braincase in lateral view) (0); developed as a lamina projecting posterolaterally (i.e. cover the fenestra ovalis with the braincase in lateral view) (1). (Bronzati et al. 2018).

99. Frontal, anteroposterior length: approximately twice (0); or less than minimum transverse breadth (1). (Wilson 2002).

100. Parietal, distance separating supratemporal fenestrae: less than (0); or twice the long axis of supratemporal fenestra (1). (Wilson 2002).

101. Supratemporal region, anteroposterior length: temporal bar longer (0); or shorter anteroposteriorly than transversely (1). (Wilson 2002).

102. Dorsoventral depth of the parasphenoid rostrum: much less than the transverse width (0); about equal to the transverse width (1). (Yates 2007).

103. Shape of jugal process of ectopterygoid: gently curved (0); strongly recurved and hook-like (1). (Yates 2007).

104. Pneumatic fossa on the ventral surface of the ectopterygoid: present (0); absent (1). (Yates 2007).

105. Relationship of the ectopterygoid to the pterygoid: ectopterygoid overlapping the ventral surface of the pterygoid (0); ectopterygoid overlapping the dorsal surface of the pterygoid (1). (Yates 2007).

106. Position of the maxillary articular surface of the palatine: along the lateral margin of the bone (0); at the end of a narrow anterolateral process due to the absence of the posterolateral process (1). (Yates 2007).

107. Centrally located tubercle on the ventral surface of palatine: absent (0); present (1). (Yates 2007).

108. Medial process of the pterygoid forming a hook around the basipterygoid process: absent (0); flat and blunt-ended (1); bent upward and pointed (2). Ordered. (Yates 2007).

109. Length of the vomers: less than 0.25 of the total skull length (0); more than 0.25 of the total skull length (1). (Yates 2007).

110. Position of jaw joint: no lower than the level of the dorsal margin of the dentary (0); depressed, well below this level (1). (Yates 2007).

111. Shape of upper jaws in ventral view: narrow with an acute rostral apex (0); broad and U-shaped (1). (Yates 2007).

112. Length of the external mandibular fenestra: more than 0.1 of the length of the mandible (0); less than 0.1 of the length of the mandible (1). (Yates 2007).

113. Caudal end of dentary tooth row medially inset with a thick lateral ridge on the dentary forming a buccal emargination: absent (0); present (1). (Yates 2007).

114. Height: length ratio of the dentary: less than 0.2; greater than 0.2 (1). (Yates 2007).

115. Orientation of the symphyseal end of the dentary: in line with the long axis of the dentary (0); strongly curved ventrally (1). (Yates 2007).

116. Position of first dentary tooth: adjacent to symphysis (0); inset one tooth's width from the symphysis (1). (Yates 2007).

117. Dorsoventral expansion at the symphyseal end of the dentary: absent (0); present (1). (Yates 2007).

118. Splenial foramen: absent (0); present and enclosed (1); present and open anteriorly (2). Ordered. (Yates 2007).

119. Splenial-angular joint: flattened sutured contact (0); synovial joint surface between tongue-like process of angular fitting in groove of the splenial (1). (Yates 2007).

120. A stout, triangular, medial process of the articular, behind the glenoid: present (0); absent (1). (Yates 2007).

121. Length of the retroarticular process: less than the depth of the mandible below the glenoid (0); greater than the depth of the mandible below the glenoid (2). (Yates 2007).

122. Strong medial embayment behind glenoid of the articular in dorsal view: absent (0); present (1). (Yates 2007).

123. Number of premaxillary teeth: four (0); more than four (1). (Yates 2007).

124. Premaxilla, crown height of the first tooth: significantly lower than most teeth in the row (0); at least as high as the tallest maxillary tooth (1). (Pretto et al. 2018).

125. Premaxillary teeth, serration in the mesial margin: (0) present; (1) absent. (Rowe 1989).

126. Number of dentary teeth (in adults): less than 18 (0); 18 or more (1). (Yates 2007).

127. Arrangement of teeth within the jaws: linearly placed, crowns not overlapping (0); imbricated with distal side of tooth overlapping mesial side of the succeeding tooth (1).

128. Orientation of the maxillary tooth crowns: erect (0); procumbent (1). (Yates 2007).

129. Orientation of the dentary tooth crowns: erect (0); procumbent (1). (Yates 2007).

130. Teeth with basally constricted crowns: absent (0); present (1). (Yates 2007).

131. Tooth-tooth occlusal wear facets: absent (0); present (1). (Yates 2007).

132. Mesial and distal serrations of the teeth: fine and set at right angles to the margin of the tooth (0); coarse and

angled upwards at an angle of 45 degrees to the margin of the tooth (1). (Yates 2007).

133. Distribution of serrations on the maxillary and dentary teeth: present on both the mesial and distal carinae (0); absent on the posterior carinae (1); absent on both carinae (2). (Yates 2007).

134. Long axis of the tooth crowns distally recurved: present (0); absent (1). (Yates 2007).

135. Texture of the enamel surface: entirely smooth (0); finely wrinkled in some patches (1); extensively and coarsely wrinkled (2). Ordered. (Yates 2007).

136. Lingual concavities of the teeth: absent (0); present (1). (Yates 2007).

137. Longitudinal labial grooves on the teeth: absent (0); present (1). (Yates 2007).

138. Distribution of the serrations along the mesial and distal carinae of the tooth: extend along most of the length of the crown (0); restricted to the upper half of the crown (1). (Yates 2007).

139. Pterygoid teeth on palatal process: (0) present; (1) absent. (Rauhut 2003).

140. Number of cervical vertebrae: eight or fewer (0); 9-10 (1); 12-13 (2); more than 13 (3). Ordered. (Yates 2007).

141. Shallow, dorsally facing fossa on the atlantal neurapophysis bordered by a dorsally everted lateral margin: absent (0); present (1). (Yates 2007).

142. Width of axial intercentrum: less than width of axial centrum (0); greater than width of axial centrum (1). (Yates 2007).

143. Position of axial prezygapophyses: on the anterolateral surface of the neural arch (0); mounted on anteriorly projecting pedicels (1). (Yates 2007).

144. Posterior margin of the axial postzygapophyses: overhang the axial centrum (0); flush with the caudal face of the axial centrum (1). (Yates 2007).

145. Length of the axial centrum: less than three times the height of the centrum (0); at least three times the height of the centrum (1). (Yates 2007).

146. Axis, dorsal margin of the neural spine: (0) expanded caudodorsally; (1) arcs dorsally where the cranial portion height is equivalent to the caudal height. (Nesbitt 2011).

147. Length of the anterior cervical centra (cervicals 3-5): no more than the length of the axial centrum (0); greater than the length of the axial centrum (1). (Yates 2007).

148. Length of middle to posterior cervical centra (cervical 6-8): no more than the length of the axial centrum (0); greater than the length of the axial centrum (1). (Yates 2007).

149. Dorsal excavation of the cervical parapophyses: absent (0); present (1). (Yates 2007).

150. Lateral compression of the anterior cervical vertebrae: centra are no higher than they are wide (0); are approximately 1.25 times higher than wide (1). (Yates 2007).

151. Relative elongation of the anterior cervical centra (cervical 3-5): lengths of the centra are less than 2.5 times the height of their anterior faces (0); lengths are 2.5-4 times the height of their anterior faces (1); the length of at least cervical 4 or 5 exceeds 4 times the anterior centrum height (2). Ordered. (Yates 2007).

152. Ventral keels on cranial cervical centra: present (0); absent (1). (Yates 2007).

153. Height of the mid cervical neural arches: no more than the height of the posterior centrum face (0); greater than the height of the posterior centrum face (1). (Yates 2007).

154. Orientation of the anterior-to-middle cervical postzygapophyses: (0) planar (minimally offset) with respect to the prezygapophyses; (1) dorsally raised roughly 20° relative to the coronal plane; (2) and dorsally raised at least 30° or more relative to the coronal plane. Ordered. (McPhee & Choiniere 2017).

155. Cervical epipophyses on the dorsal surface of the postzygapophyses: absent (0); present on at least some cervical vertebrae (1). (Yates 2007).

156. Posterior ends of the anterior, postaxial epipophyses: with a free pointed tip (0); joined to the postzygapophysis along their entire length (1). (Yates 2007).

157. Shape of the epipophyses: tall ridges (0); flattened, horizontal plates (1). (Yates 2007).

158. Epipophyses overhanging the rear margin of the postzygapophyses: absent (0); present in at least some postaxial cervical vertebrae (1). (Yates 2007).

159. Anterior spur-like projections on mid-cervical neural spines: absent (0); present (1). (Yates 2007).

160. Shape of mid-cervical neural spines: less than twice as long as high (0); at least twice as long as high (1). (Yates 2007).

161. Cervical vertebrae, deep recesses on the cranial face of the neural arch lateral to the neural canal: (0) absent; (1) present. (Nesbitt 2011).

162. Cervical vertebrae, pneumatic features (=pleurocoels) in the anterior portion of the centrum: absent (0); present (1). (Nesbitt 2011).

163. Shape of cervical rib shafts: short and posteroventrally directed (0); longer than the length of their centra and extending parallel to cervical column (1). (Yates 2007).

164. Position of the base of the cervical rib shaft: level with, or higher than the ventral margin of the cervical centrum (0); located below the ventral margin due to a ventrally extended parapophysis (1). (Yates 2007).

165. Postzygodiapophyseal lamina in cervical neural arches 4-8: present (0); absent (1).

166. Laminae of the cervical neural arches 4-8: well-developed tall laminae (0); weakly developed low ridges (1). (Yates 2007).

167. Shape of anterior centrum face in cervical centra: concave (0); flat (1); convex (2). Ordered. (Yates 2007).

168. Ventral surface of the centra in the cervicodorsal transition: transversely rounded (0); with longitudinal keels (1). (Yates 2007).

169. Number of vertebrae between cervicodorsal transition and primordial sacral vertebrae: 15-16 (0); no more than 14 (1). (Yates 2007).

170. Lateral surfaces of the dorsal centra: with at most vague, shallow depressions (0); with deep fossae that approach the midline (1); with invasive, sharp-rimmed pleurocoels (2). Ordered. (Yates 2007).

171. Oblique ridge dividing pleural fossa of cervical vertebrae: absent (0); present (1). (Yates 2007).

172. Laterally expanded tables at the midlength of the dorsal surface of the neural spines: absent in all vertebrae (0); present on the pectoral vertebrae (1); present on the pectoral and cervical vertebrae (2). Ordered. (Yates 2007).

173. Dorsal centra: entirely amphicoelous to amphiplatyan (0); first two dorsals are opisthocoelous (1); cranial half of dorsal column is opisthocoelous (2). Ordered. (Yates 2007).

174. Shape of the posterior dorsal centra: relatively elongated for their size (0); strongly axially compressed for their size (1). (Yates 2007).

175. Laminae bounding triangular infradiapophyseal fossae (chonae) on dorsal neural arches: absent (0); present (1). (Yates 2007).

176. Location of parapophysis in first two dorsals: at the anterior end of the centrum (0); located at the mid-length of the centrum, within the middle chonos (1). (Yates 2007).

177. Parapophyses of the dorsal column completely shift from the centrum to the neural arch: anterior to the thirteenth presacral vertebra (0); posterior to the thirteenth presacral vertebra (1). (Yates 2007).

178. Orientation of the transverse processes of the dorsal vertebrae: most horizontally directed (0); all upwardly directed (1). (Yates 2007).

179. Contribution of the paradiapophyseal lamina to the margin of the anterior chonos in mid-dorsal vertebrae: present (0); prevented by high placement of parapophysis (1). (Yates 2007).

180. Hyposphenes in the dorsal vertebrae: absent (0); present but less than the height of the neural canal (1); present and equal to the height of the neural canal (2). Ordered. (Yates 2007).

181. Prezygodiapophyseal lamina and associated anterior triangular fossa (anterior infradiapophyseal fossa): present on all dorsals (0); absent in mid-dorsals (1). (Yates 2007).

182. Anterior centroparapophyseal lamina in dorsal vertebrae: absent (0); present (1). (Yates 2007).

183. Prezygoparapophyseal lamina in dorsal vertebrae: absent (0); present (1). (Yates 2007).

184. Accessory lamina dividing posterior chonos from postzygapophysis: absent (0); present (1). (Yates 2007).

185. Pneumatic excavation of the dorsal neural arches: absent (0); equivocal (e.g., no more than depressions within the infradiapophyseal chambers) (1); sharp-rimmed subfossae or foramina clearly invading bone surface (2). Ordered. (Yates 2007).

186. Separation of lateral surfaces of anterior dorsal neural arches under transverse processes: widely spaced (0); only separated by a thin midline septum (1). (Yates 2007).

187. Height of dorsal neural arches, from neurocentral suture to level of zygapophyseal facets: much less than height of centrum (0); subequal to or greater than height of centrum (1). (Yates 2007).

188. Form of anterior surface of neural arch: simple centroprezygopophyseal ridge (0); broad anteriorly facing surface bounded laterally by centroprezygopophyseal lamina (1). (Yates 2007).

189. Shape of posterior dorsal neural canal: subcircular (0); slit-shaped (1). (Yates 2007).

190. Height of middle dorsal neural spines: less than the length of the base (0); higher than the length of the base but less than 1.5 times the length of the base (1); greater than 1.5 times the length of the base (2). Ordered. (Yates 2007).

191. Shape of anterior dorsal neural spines: lateral margins parallel in anterior view (0); transversely expanding towards dorsal end (1). (Yates 2007).

192. Cross-sectional shape of dorsal neural spines: transversely compressed (0); broad and triangular (1); square-shaped in posterior vertebrae (2). Ordered. (Yates 2007).

193. Spinodiapophyseal lamina on dorsal vertebrae: absent (0); present and separated from spinopostzygapophyseal lamina (1); present and joining spinopostzygapophyseal lamina to create a composite posterolateral spinal lamina (2). Ordered. (Yates 2007).

194. Well-developed, sheet-like suprapostzygapophyseal laminae: absent (0); present on at least the caudal dorsal vertebrae (1). (Yates 2007).

195. Shape of the spinopostzygapophyseal lamina in middle and posterior dorsal vertebrae: singular (0); bifurcated at its distal end (1). (Yates 2007).

196. Shape of posterior margin of middle dorsal neural spines in lateral view: approximately straight (0); concave with a projecting posterodorsal corner (1). (Yates 2007).

197. Transversely expanded plate-like summits of posterior dorsal neural spines: absent (0); present (1). (Yates 2007).

198. Last presacral rib: free (0); fused to vertebra (1). (Yates 2007).

199. Number of dorsosacral vertebrae: none (0); one (1); two (2). Ordered. (Yates 2007).

200. Caudosacral vertebra: absent (0); present (1). (Yates 2007).

201. Shape of the iliac articular facets of the first primordial sacral rib: singular (0); divided into dorsal and ventral facets separated by a non-articulating gap (1). (Yates 2007).

202. Deep, medially-directed pit excavating the surface of the non-articulating gap of the first primordial sacral rib: absent (0); present (1). (Yates 2007).

203. Depth of the iliac articular surface of the primordial sacrals: less than 0.75 of the depth of the ilium (0); greater than 0.75 of the depth of the ilium (1). (Yates 2007).

204. Sacral ribs contributing to the rim of the acetabulum: absent (0); present (1). (Yates 2007).

205. Posterior and anterior expansion of the transverse processes of the first and second primordial sacral vertebrae, respectively, partly roofing the intercostal space: absent (0); present (1). (Yates 2007).

206. Length of first caudal centrum: longer anteroposteriorly than dorsoventrally tall (0); taller than long (1); highly compressed (dorsoventral height at least twice anteroposterior length) (2). Ordered. (Yates 2007).

207. Position of postzygapophyses in proximal caudal vertebrae: protruding with an interpostzygapophyseal notch visible in dorsal view (0); placed on either side of the caudal end of the base of the neural spine without any interpostzygapophyseal notch (1). (Yates 2007).

208. A hyposphenal ridge on caudal vertebrae: absent (0); present (1). (Yates 2007).

209. Prezygadiapophyseal laminae on anterior caudals: absent (0); present (1). (McPhee et al. 2015).

210. Depth of the bases of the proximal caudal transverse processes: shallow, restricted to the neural arches (0); deep, extending from the centrum to the neural arch (1). (Yates 2007).

211. Position of last caudal vertebra with a protruding transverse process: distal to caudal 16 (0); proximal to caudal 16 (1). (Yates 2007).

212. Orientation of posterior margin of proximal caudal neural spines: sloping posterodorsally (0); vertical (1). (Yates 2007).

213. Longitudinal ventral sulcus on proximal and middle caudal vertebrae: present (0); absent (1). (Yates 2007).

214. Length of midcaudal centra: greater than twice the height of their anterior faces (0); less than twice the height of their anterior faces (1). (Yates 2007).

215. Cross-sectional shape of the distal caudal centra: oval with rounded lateral and ventral sides (0); square-shaped with flattened lateral and ventral sides (1). (Yates 2007).

216. Length of distal caudal prezygapophyses: short, not overlapping the preceding centrum by more than a quarter (0); long and overlapping the preceding the centrum by more than a quarter (1). (Yates 2007).

217. Shape of the terminal caudal vertebrae: unfused, size decreasing toward tip (0); expanded and fused to form a club-shaped tail (1). (Yates 2007).

218. 'Weaponized' dermal spikes on tail: absent (0); present (1). (McPhee et al. 2015).

219. Length of the longest chevron: less than twice the length of the preceding centrum (0); greater than twice the length of the preceding centrum (1). (Yates 2007).

220. Anteroventral process on distal chevrons: absent (0); present (1). (Yates 2007).

221. Mid-caudal chevrons with a ventral slit: absent (0); present (1). (Yates 2007).

222. Longitudinal ridge on the dorsal surface of the sterna plate: absent (0); present (1). (Yates 2007).

223. Craniocaudal length of the acromion process of the scapula: less than 1.5 times the minimum width of the scapula blade (0); greater than 1.5 times the minimum width of the scapula blade (1). (Yates 2007).

224. Minimum width of the scapula: greater than 20 per cent of its length (0); less than 20 per cent of its length (1). (Yates 2007).

225. Caudal margin of the acromion process of the scapula: rises from the blade at angle that is less than 65 degrees from the long axis of the scapula, at its steepest point (0); rises from the blade at angle that is greater than 65 degrees from the long axis of the scapula, at its steepest point (1). (Yates 2007).

226. Ventromedial ridge of scapula: absent (0) or present (1). (Otero & Pol 2013).

227. Width of dorsal expansion of the scapula: less than the width of the ventral end of the scapula (0); equal to the width of the ventral end of the scapula (1). (Yates 2007).

228. Flat caudoventrally facing surface on the coracoids between glenoid and coracoid tubercle: absent (0); present (1). (Yates 2007).

229. Coracoid tubercle: present (0); absent (1). (Yates 2007).

230. Length of the humerus: less than 55 per cent of the length of the femur (0); 55-65 per cent of the length of the femur (1); 65-70 per cent of the length of the femur (2); more than 70 per cent of the length of the femur (3). Ordered. (Yates 2007).

231. Shape of the humeral head: weakly developed, rounded in anterior-posterior view but minimally expanded perpendicular to the latter axis (0); flat in anterior-posterior view with only a slightly expanded lateral component (1); domed, being convex/hemispherical in anterior-posterior view with a strong lateral incursion onto the humeral shaft (2). (McPhee et al. 2018).

232. Shape of the deltopectoral crest: subtriangular (0); subrectangular (1). (Yates 2007).

233. Length of the deltopectoral crest of the humerus: less than 30 per cent of the length of the humerus (0); 30-50 per cent of the length of the humerus (1); greater than 50 per cent of the length of the humerus (2). Ordered. (Yates 2007).

234. Shape of the anterolateral margin of the deltopectoral crest of the humerus: straight (0); strongly sinuous (1). (Yates 2007);

235. Rugose pit centrally located on the lateral surface of the deltopectoral crest: absent (0); present (1). (Yates 2007).

236. Well-defined fossa on the distal flexor surface of the humerus: present (0); absent (1). (Yates 2007).

237. Transverse width of the distal humerus: less than 33 per cent of the length of the humerus (0); greater than 33 per cent of the length of the humerus (1). (Yates 2007).

238. Shape of the entepicondyle of the distal humerus: rounded process (0): with a flat distomedially facing surface bounded by a sharp proximal margin (1). (Yates 2007).

239. Length of the radius: greater than 80 per cent of the humerus (0); less than 80 per cent of the humerus (1). (Yates 2007).

240. Radial fossa on the anterolateral corner of the proximal ulna: absent (0); present, but only shallowly defined (1); a well-defined recess, deeper than transverse width of the anterior end of the anterior process (2). Ordered (Yates 2007).

241. Caudodistal tubercle of the radius: absent (0) or present (1). (Otero et al. 2015).

242. Biceps tubercle of the radius: absent (0) or present (1). (Otero et al. 2015).

243. Olecranon process on proximal ulna: present (0); absent (1); greatly enlarged olecranon (2). (Yates 2007).

244. Anterior tip of anterior process of proximal ulna: no deflection or continues lateral curvature (0); medially deflected (1). (McPhee et al., 2018).

245. Maximum linear dimensions of the ulnare and radiale: exceed that of at least one of the first three distal carpals (0); less than any of the distal carpals (1). (Yates 2007).

246. Transverse width of the first distal carpal: less than 120 per cent of the transverse width of the second distal carpal (0); greater than 120 per cent of the transverse width of the second distal carpal (1). (Yates 2007).

247. Sulcus across the medial end of the first distal carpal: absent (0); present (1). (Yates 2007).

248. Lateral end of first distal carpal: abuts second distal carpal (0); overlaps second distal carpal (1). (Yates 2007).

249. Second distal carpal: completely covers the proximal end of the second metacarpal (0); does not completely cover the proximal end of the second metacarpal (1). (Yates 2007).

250. Ossification of the fifth distal carpal: present (0); absent (1). (Yates 2007).

251. Length of the manus: less than 38 per cent of the humerus + radius (0); 38-45 per cent of the humerus + radius (1); greater than 45 per cent of the humerus + radius (2). Ordered. (Yates 2007).

252. Shape of metacarpus: flattened to gently curved and spreading (0); a colonnade of subparallel metacarpals tightly curved into a U-shape (1). (Yates 2007).

253. Proximal width of first metacarpal: less than the proximal width of the second metacarpal (0); greater than the proximal width of the second metacarpal (1). (Yates 2007).

254. Minimum transverse shaft width of first metacarpal: less than twice the minimum transverse shaft width of second metacarpal (0); greater than twice the minimum transverse shaft width of second metacarpal (1). (Yates 2007).

255. Proximal end of first metacarpal: flush with other metacarpals (0); inset into the carpus (1). (Yates 2007).

256. Shape of the first metacarpal: proximal width less than 65 per cent of its length (0); proximal width 65-80 per cent of its length (1); proximal width 80-100 per cent of its length (2); greater than 100 per cent of its length (3). Ordered. (Yates 2007).

257. Ventromedial margin of first metacarpal: poorly concave (0) or deeply concave (1). (Otero et al. 2015).

258. Strong asymmetry in the lateral and medial distal condyles of the first metacarpal: absent (0); present (1). (Yates 2007).

259. Deep distal extensor pits on the second and third metacarpals: absent (0); present (1). (Yates 2007).

260. Shape of the distal ends of second and third metacarpals: subrectangular in distal view (0); trapezoidal with flexor rims of distal collateral ligament pits flaring beyond extensor rims (1). (Yates 2007).

261. Shape of the fifth metacarpal: longer than wide at the proximal end with a flat proximal surface (0); almost as wide as it is long with a strongly convex proximal articulation surface (1). (Yates 2007).

262. Length of the fifth metacarpal: less than 75 per cent of the length of the third metacarpal (0); greater than 75 per cent of the length of the third metacarpal (1). (Yates 2007).

263. Length of manual digit one: less than the length of manual digit two (0); greater than the length of manual digit two (1). (Yates 2007).

264. Ventrolateral twisting of the transverse axis of the distal end of the first phalanx of manual digit one relative to its proximal end: absent (0); present but much less than 60 degrees (1); 60 degrees (2). Ordered. (Yates 2007).

265. Length of the first phalanx of manual digit one: less than the length of the first metacarpal (0); greater than the length of the first metacarpal (1). (Yates 2007).

266. Length of first phalanx of manual digit 1: much greater than (0), subequal or equal to (1), or much less than (2), its mediolateral width at proximal end. (Otero et al. 2015).

267. Shape of the proximal articular surface of the first phalanx of manual digit one: rounded (0); with an embayment on the medial side (1). (Yates 2007).

268. Shape of the first phalanx of manual digit one: elongate and subcylindrical (0); strongly proximodistally compressed and wedge-shaped (1). (Yates 2007).

269. Length of the penultimate phalanx of manual digit two: less than the length of the second metacarpal (0); greater than the length of the second metacarpal (1). (Yates 2007).

270. Length of the penultimate phalanx of manual digit three: less than the length of the third metacarpal (0); greater than the length of the third metacarpal (1). (Yates 2007).

271. Shape of non-terminal phalanges of manual digits two and three: longer than wide (0); as long as wide (1). (Yates 2007).

272. Pronounced tubercle on the ventrolateral corner of the shaft of the non-first metacarpals, just below the proximal surface: absent (0); present (1). (McPhee et al., 2018).

273. Shape of the unguals of manual digits two and three: straight (0); strongly curved with tips projecting well below flexor margin of proximal articular surface (1). (Yates 2007).

274. Length of the ungual of manual digit two: greater than the length of the ungual of manual digit one (0); 75-100 per cent of the ungual of manual digit one (1); less than 75 per cent of the ungual of manual digit one (2); the ungual of manual digit two is absent (3). Ordered. (Yates 2007).

275. Phalangeal formula of manual digits two and three: three and four, respectively (0); with at least one phalanx missing from each digit (1). (Yates 2007).

276. Phalangeal formula of manual digits four and five: greater than 2-0, respectively (0); less than 2-0, respectively (1). (Yates 2007).

277. Strongly convex dorsal margin of the ilium: absent (0); present (1). (Yates 2007).

278. Cranial extent of preacetabular process of ilium: does not project further anterior than the anterior margin of the pubic peduncle (0); projects anterior to the cranial margin of the pubic peduncle (1). (Yates 2007).

279. Shape of the preacetabular process: blunt and rectangular (0); with a pointed, projecting anteroventral corner and a rounded dorsum (1). (Yates 2007).

280. Depth of the preacetabular process of the ilium: much less than the depth of the ilium above the acetabulum (0); subequal to the depth of the ilium above the acetabulum (1). (Yates 2007).

281. Length of preacetabular process of the ilium: less than twice its depth (0); greater than twice its depth (1). (Yates 2007).

282. Medial wall of acetabulum: fully closing acetabulum with a triangular ventral process between the pubic and ischial peduncles (0); partially open acetabulum with a straight ventral margin between the peduncles (1); partially open acetabulum with a concave ventral margin between the peduncles (2); fully open acetabulum with medial ventral margin closely approximating lateral rim of acetabulum (3). Ordered. (Yates 2007).

283. Length of the pubic peduncle of the ilium: less than twice the anteroposterior width of its distal end (0); greater than twice the anteroposterior width of its distal end (1). (Yates 2007).

284. Caudally projecting ‘heel’ at the distal end of the ischial peduncle: absent (0); present (1). (Yates 2007).

285. Length of the ischial peduncle of the ilium: similar to pubic peduncle (0); much shorter than pubic peduncle (1); virtually absent so that the chord connecting the distal end of the pubic peduncle with the ischial articular surface contacts the postacetabular process (2). Ordered. (Yates 2007).

286. Length of the postacetabular process of the ilium: between 40 and 100 per cent of the distance between the pubic and ischial peduncles (0); less than 40 per cent of the distance between the pubic and ischial peduncles (1); more than 100 per cent of the distance between the pubic and ischial peduncles (2). (Yates 2007).

287. Well-developed brevis fossa with sharp margins on the ventral surface of the postacetabular process of the ilium: absent (0); present, ventrally facing (1); present, lateroventrally facing (2). (Yates 2007).

288. Anterior end of ventrolateral ridge bounding brevis fossa: not connected to supracetabular crest (0); joining supracetabular crest (1). (Yates 2007).

289. Shape of the caudal margin of the postacetabular process of the ilium: rounded to bluntly pointed (0); square ended (1); with a pointed ventral corner and a rounded caudodorsal margin (2). (Yates 2007).

290. Width of the conjoined pubes: less than 75 per cent of their length (0); greater than 75 per cent of their length (1). (Yates 2007).

291. Pubic tubercle on the lateral surface of the proximal pubis: present (0); absent (1).

292. Proximal anterior profile of pubis: anterior margin of pubic apron smoothly confluent with anterior margin of iliac pedicel (0); iliac pedicel set anterior to the pubic apron creating a prominent inflection in the proximal anterior profile of the pubis (1). (Yates 2007).

293. Minimum transverse width of the pubic apron: much more than 40 per cent of the width across the iliac peduncles of the ilium (0); less than 40 per cent of the width across the iliac peduncles of the ilium (1). (Yates 2007).

294. Position of the obturator foramen of the pubis: at least partially occluded by the iliac pedicel in anterior view (0); completely visible in anterior view (1). (Yates 2007).

295. Lateral margins of the pubic apron in anterior view: straight (0); concave (1). (Yates 2007).

296. Anterior fossa on the proximal region of the pubic apron: absent (0) or present (1). (Apaldetti et al. 2013).

297. Orientation of distal third of the blades of the pubic apron: confluent with the proximal part of the pubic apron (0); twisted posterolaterally relative to proximal section so that the anterior surface turns to face laterally (1). (Yates 2007).

298. Orientation of the entire blades of the pubic apron: transverse (0); twisted posteromedially (1). (Yates 2007).

299. Anteroposterior expansion of the distal pubis: absent (0); less than 15 per cent of the length of the pubis (1); greater than 15 per cent of the length of the pubis (2). Ordered. (Yates 2007).

300. Elongate interischial fenestra: absent (0); present (1). (Yates 2007).

301. Longitudinal dorsolateral sulcus on proximal ischium: absent (0); present (1). (Yates 2007).

302. Shape of distal ischium: broad and plate-like, not distinct from obturator region (0); with a discrete rod-like distal shaft (1). (Yates 2007).

303. Length of ischium: less than that of the pubis (0); greater than that of the pubis (1). (Yates 2007).

304. Notch separating posteroventral end of the ischial obturator plate from the ischial shaft: present (0); absent (1). (Yates 2007).

305. Ischial component of acetabular rim: larger than the pubic component (0); equal to the pubic component (1) (Yates 2007).

306. Shape of the transverse section of the ischial shaft: ovoid to subrectangular (0); triangular (1). (Yates 2007).

307. Orientation of the long axes of the transverse section of the distal ischia: meet at an angle (0); are coplanar (1). (Yates 2007).

308. Depth of the transverse section of the ischial shaft: much less than the transverse width of the section (0); at least as great as the transverse width of the section (1). (Yates 2007).

309. Distal ischial expansion: absent (0); present (1). (Yates 2007).

310. Transverse width of the conjoined distal ischial expansions: greater than their sagittal depth (0); less than their sagittal depth (1). (Yates 2007).

311. Length of the hindlimb: greater than the length of the trunk (0); less than the length of the trunk (1). (Yates 2007).

312. Longitudinal axis of the femur in lateral view: strongly bent with an offset between the proximal and distal axes greater than 15 degrees (0); weakly bent with an offset of less than 10 degrees (1); straight (2). Ordered. (Yates 2007).

313. Shape of the cross-section of the mid-shaft of the femur: subcircular (0); strongly elliptical with the long axis orientated mediolaterally (1). (Yates 2007).

314. Angle between the long axis of the femoral head and the transverse axis of the distal femur: about 30 degrees (0); close to 0 degrees (1). (Yates 2007).

315. Shape of femoral head: roughly rectangular in profile with a sharp medial distal corner (0); roughly hemispherical with no sharp medial distal corner (1). This character only applies to taxa with a medially, or anteromedially protruding femoral head. It does not apply to outgroup taxa (*Euparkeria* or Crurotarsi) with proximally directed femoral heads and is coded as unknown in these taxa. (Yates 2007).

316. Posterior proximal tubercle on femur: well-developed (0); indistinct to absent (1). (Yates 2007).

317. Shape of the lesser trochanter: small rounded tubercle (0); proximodistally orientated, elongate ridge (1); absent (2). (Yates 2007).

318. Position of proximal tip of lesser trochanter: level with the femoral head (0); distal to the femoral head (1). (Yates 2007).

319. Projection of the lesser trochanter: just a scar upon the femoral surface (0); a raised process (1). (Yates 2007).

320. Transverse ridge extending laterally from the lesser trochanter: absent (0); present (1). (Yates 2007).

321. Height of the lesser trochanter in cross section: less than its basal width (0); at least as high as its basal width (1). (Yates 2007).

322. Position of the lesser trochanter in anterior view: near the center of the anterior face of the femoral shaft (0); close to the lateral margin of the femoral shaft (1). (Yates 2007).

323. Visibility of the lesser trochanter in posterior view: not visible (0); visible (1). (Yates 2007).

324. Height of the fourth trochanter: a low rugose ridge (0); a tall crest (1). (Yates 2007).

325. Position of the fourth trochanter along the length of the femur: in the proximal half (0); straddling the midpoint (1). (Yates 2007).

326. Symmetry of the profile of the fourth trochanter of the femur: sub-symmetrical without a sharp distal corner (0); asymmetrical with a steeper distal slope than the proximal slope and a distinct distal corner (1). (Yates 2007).

327. Shape of the profile of the fourth trochanter of the femur: rounded (0); subrectangular (1). (Yates 2007).

328. Position of fourth trochanter along the mediolateral axis of the femur: centrally located (0); on the medial margin (1). (Yates 2007).

329. Extensor depression on anterior surface of the distal end of the femur: absent (0); present (1). (Yates 2007).

330. Size of the medial condyle of the distal femur: subequal to the fibular + lateral condyles (0); larger than the fibular + lateral condyles (1). (Yates 2007).

331. Femoral distal transverse width: equal or lesser (0); greater (1) than 1·4 times its largest anteroposterior depth across the fibular condyle. (Novas et al. 2011).

332. Well-developed tibiofibular crest on distal femur: absent (0); present (1). (Smith & Pol 2007).

333. Distal surface of tibiofibular crest: as deep anteroposteriorly as wide mediolaterally or deeper (0); wider mediolaterally than deep anteroposteriorly (1). (Smith & Pol 2007).

334. Tibia: femur length ratio: greater than 1.0 (0); between 0.6 and 1.0 (1); less than 0.6 (2). Ordered. (Yates 2007).

335. Orientation of cnemial crest: projects anteriorly to anterolaterally (0); projecting laterally (1). (Yates 2007).

336. Paramarginal ridge on lateral surface of cnemial crest: absent (0); present (1). (Yates 2007).

337. Position of the tallest point of the cnemial crest: close to the proximal end of the crest (0); about half-way along the length of the crest, creating an anterodorsally sloping proximal margin of the crest (1). (Yates 2007).

338. Proximal end of tibia with a flange of bone that contacts the fibula: absent (0): present (1). (Yates 2007).

339. Position of the posterior end of the fibular condyle on the proximal articular surface tibia: anterior to the posterior margin of the proximal articular surface (0); level with the posterior margin of the proximal articular surface (1). (Yates 2007).

340. Shape of the proximal articular surface of the tibia: transverse width subequal to anteroposterior length (0); transverse width between 0.6- and 0.9-times anteroposterior length (1); anteroposterior length twice the transverse width or higher (2). Ordered. (Yates 2007).

341. Transverse width of the distal tibia: subequal to its craniocaudal length (0); greater than its craniocaudal length (1). (Yates 2007).

342. Anteroposterior width of the lateral side of the distal articular surface of the tibia: as wide as the anteroposterior width of the medial side (0); narrower than

the anteroposterior width of the medial side (1). (Yates 2007).

343. Relationship of the posterolateral process of the distal end of the tibia with the fibula: not flaring laterally and not making significant contact with the fibula (0); flaring laterally and backing the fibula (1). (Yates 2007).

344. Shape of the distal articular end of the tibia in distal view: ovoid (0); subrectangular (1). (Yates 2007).

345. Shape of the anteromedial corner of the distal articular surface of the tibia: forming a right angle (0); forming an acute angle (1). (Yates 2007).

346. Position of the lateral margin of descending caudoventral process of the distal end of the tibia: protrudes laterally at least as far as the anterolateral corner of the distal tibia (0); set well back from the anterolateral corner of the distal tibia (1). (Yates 2007).

347. A triangular rugose area on the medial side of the fibula: absent (0); present (1). (Yates 2007).

348. Transverse width of the midshaft of the fibula: greater than 0.75 of the transverse width of the midshaft of the tibia (0); between 0.5 and 0.75 of the transverse width of the midshaft of the tibia (1); less than 0.5 of the transverse width of the midshaft of the tibia (2). Ordered. (Yates 2007).

349. Proximal end of the tibia with a transverse/anteroposterior length ratio: narrow (ratio less than 0.7) (0) or broad (more than 0.7) (1) (Apaldetti et al. 2013).

350. Position of fibula trochanter: on anterior surface of fibula (0); laterally facing (1); anteriorly facing but with strong lateral bulge (2). (Yates 2007).

351. Depth of the medial end of the astragalar body in cranial view: roughly equal to the lateral end (0); much shallower creating a wedge-shaped astragalar body (1). (Yates 2007).

352. Shape of the posteromedial margin of the astragalus in dorsal view: forming a moderately sharp corner of a subrectangular astragalus (0); evenly rounded without formation of a caudomedial corner (1). (Yates 2007).

353. Dorsally facing horizontal shelf forming part of the fibular facet of the astragalus: present (0); absent with a largely vertical fibular facet (1). (Yates 2007).

354. Pyramidal dorsal process on the posteromedial corner of the astragalus: absent (0); present (1). (Yates 2007).

355. Shape of the ascending process of the astragalus: anteroposteriorly deeper than transversely wide (0); transversely wider than anteroposteriorly deep (1). (Yates 2007).

356. Astragalus with medial condyle anteroposterior depth: less (0); equal or more (1) than 1·6 times the depth of the lateral condyle. (Novas et al. 2011).

357. Posterior margin of astragalus: straight (0) or convex (1). (Otero & Pol 2013).

358. Mediolateral surface of distal astragalus straight (0), concave (1), or convex (0). (Otero & Pol 2013).

359. Posterior extent of ascending process of the astragalus: positioned anteriorly upon the astragalus (0); close to the posterior margin of the astragalus (1). (Yates 2007).

360. Sharp medial margin around the depression posterior to the ascending process of the astragalus: absent (0); present (1). (Yates 2007).

361. Buttress dividing posterior fossa of astragalus and supporting ascending process: absent (0); present (1). (Yates 2007).

362. Vascular foramina set in a fossa at the base of the ascending process of the astragalus: present (0); absent (1). (Yates 2007).

363. Distal articular surface of astragalus: relatively flat or weakly convex (0); extremely convex and roller-shaped (1). (Smith & Pol 2007).

364. Transverse width of the calcaneum: greater than 30 per cent of the transverse width of the astragalus (0); less than 30 per cent of the transverse width of the astragalus (1). (Yates 2007).

365. Lateral surface of calcaneum: simple (0); with a fossa (1). (Yates 2007).

366. Medial peg of calcaneum fitting into astragalus: present, even if rudimentary (0); absent (1). (Yates 2007).

367. Calcaneal tuber: large and well developed (0); highly reduced to absent (1). (Yates 2007).

368. Shape of posteromedial heel of distal tarsal four (lateral distal tarsal): proximodistally deepest part of the bone (0); no deeper than the rest of the bone (1). (Yates 2007).

369. Shape of posteromedial process of distal tarsal four in proximal view: rounded (0); pointed (1). (Yates 2007).

370. Ossified distal tarsals: present (0); absent (1). (Yates 2007).

371. Proximal width of the first metatarsal: less than the proximal width of the second metatarsal (0); at least as great as the proximal width of the second metatarsal (1). (Yates 2007).

372. Size of first metatarsal: maximum proximal breadth less than 0.4 times its proximodistal length (0); maximum proximal breadth between 0.4 and 0.7 times its proximodistal length (1); maximum proximal breadth greater than 0.7times its proximodistal length (2). Ordered. (Yates 2007).

373. Orientation of proximal articular surface of metatarsal one: horizontal (0); sloping proximolaterally relative to the long axis of the bone (1). (Yates 2007).

374. Shaft of metatarsal I: closely appressed to metatarsal II throughout its length (0); only closely appressed proximally, with a space between metatarsals I and II distally (1). (Smith & Pol 2007).

375. Orientation of the transverse axis of the distal end of metatarsal one: horizontal (0); angled proximomedially (1). (Yates 2007).

376. Shape of the medial margin of the proximal surface of the second metatarsal: straight (0); concave (1). (Yates 2007).

377. Shape of the lateral margin of the proximal surface of the second metatarsal: straight (0); concave (1). (Yates 2007).

378. Projection of ventral flange on proximal surface of second metatarsal: neither corner appreciably more developed than the other (0); laterally flaring (1); medially flaring (2). (Smith & Pol 2007).

379. Well-developed facet on proximolateral corner of plantar ventrolateral flange of mt II for articulation with medial distal tarsal: absent (0); present (1). (Smith & Pol 2007).

380. Length of the third metatarsal: greater than 40 per cent of the length of the tibia (0); less than 40 per cent of the length of the tibia (1). (Yates 2007).

381. Proximal outline of metatarsal III: subtriangular with acute or rounded posterior border (0); subtrapezoidal, with posterior border broadly exposed in plantar view (1). (Smith & Pol 2007).

382. Minimum transverse shaft diameters of third and fourth metatarsals: greater than 60 per cent of the minimum transverse shaft diameter of the second metatarsal (0); less than 60 per cent of the minimum transverse shaft diameter of the second metatarsal (1). (Yates 2007).

383. Transverse width of the proximal end of the fourth metatarsal: less than twice the anteroposterior depth of the proximal end (0); at least twice the anteroposterior depth of the proximal end (1). (Yates 2007).

384. Angle formed by the anterior and anteromedial borders of metatarsal IV: obtuse (0); right angle, or acute (1). (Smith & Pol 2007).

385. Transverse width of the proximal end of the fifth metatarsal: less than 25 percent of the length of the fifth metatarsal (0); between 30 and 49 percent of the length of the fifth metatarsal (1); greater than 50 percent of the length of the fifth metatarsal (2). Ordered. (Yates 2007).

386. Transverse width of distal articular surface of metatarsal four in distal view: greater than the anteroposterior depth (0); less than the anteroposterior depth (1) (Yates 2007).

387. Pedal digit five: reduced, non-weight bearing (0); large (fifth metatarsal at least 70 per cent of fourth metatarsal), robust and weight bearing (1). (Yates 2007).

388. Length of non-terminal pedal phalanges: all longer than wide (0); proximal most phalanges longer than wide while more distal phalanges are as wide as long (1); all nonterminal phalanges are as wide, if not wider, than long (2). Ordered. (Yates 2007).

389. Division of the length of the first phalanx of the digit I of the foot (at the midpoint) by the maximum height of the proximal end: 2.4 or more (0); 2.3 or less (1). (Müller et al. 2017).

390. Length of the first phalanx of pedal digit one: greater than the length of the ungual of pedal digit one (0); less than the length of the ungual of pedal digit one (1). (Yates 2007).

391. Length of the ungual of pedal digit one: less than at least some non-terminal phalanges (0); longer than all non-terminal phalanges but shorter than first metatarsal (1); longer than the first metatarsal (2). Ordered. (Yates 2007).

392. Shape of the ungual of pedal digit one: shallow, pointed, with convex sides and a broad ventral surface (0); deep, abruptly tapering, with flattened sides and a narrow ventral surface (1). (Yates 2007).

393. Shape of proximal articular surface of pedal unguals: proximally facing, visible on medial and lateral sides (0); proximomedially facing and visible only in medial view, causing medial deflection of pedal unguals in articulation (1). (Yates 2007).

394. Penultimate phalanges of pedal digits two and three: well-developed (0); reduced disc-shaped elements if they are ossified at all (1). (Yates 2007).

395. Shape of the unguals of pedal digits two and three: dorsoventrally deep with a proximal articulating surface that is at least as deep as it is wide (0); dorsoventrally flattened with a proximal articulating surface that is wider than deep (1). (Yates 2007).

396. Length of the ungual of pedal digit two: greater than the length of the ungual of pedal digit one (0); between 90 and 100 per cent of the length of the ungual of pedal digit one (1); less than 90 per cent of the length of the ungual of pedal digit one (2). Ordered. (Yates 2007).

397. Size of the ungual of pedal digit three: greater than 85 per cent of the ungual of pedal digit two in all linear dimensions (0); less than 85 per cent of the ungual of pedal digit two in all linear dimensions (1). (Yates 2007).

398. Number of phalanges in pedal digit four: four (0); fewer than four (1). (Yates 2007).

399. Phalanges of pedal digit five: present (0); absent (1). (Yates 2007).

400. Presence of growth marks (LAGs and/or annuli) in the cortical bone: growth marks in the whole cortex (0); growth marks absent or only formed in the outer cortex (1). (Cerda et al. 2017).

401. Relative abundance of woven fibered (WFB) or parallel fibered bone (PFB) in the primary compact bone: (0) PFB>WFB; (1) WFB>PFB. (Cerda et al. 2017).

402. Femoral length: less than 200mm (0); between 200 and 399mm (1); between 400 and 599mm (2); between 600 and 799mm (3); between 800 and 1000mm (4); greater than 1000mm (5). Ordered. (McPhee et al. 2018)

Appendix 2: Details of Phylogenetic Analysis

We used the Müller (2018) data matrix as a starting point, it is a modified version of the data set originally published by Yates (2007) and subsequently modified by other authors. Changes to the character scores of *Antetonitrus* and *Plateosauravus* based on the material in the above studies were made based on new material and first hand observations.

Scores for *Ledumahadi* were added to the Müller (2018) matrix from McPhee et al. (2018).

The following characters were added to the Müller (2018) matrix from McPhee et al. (2018): character 244, 272 and 402. Characters 199 and 278 from Müller (2018) were deleted as per McPhee et al. (2018)

The synthesised matrix represents 76 taxa and 402 characters. The data matrix was analysed in TNT 1.1 (Goloboff et al., 2008) using a heuristic search of 1000 replicates of Wagner trees followed by TBR branch swapping with 10 trees saved per replication. A final round of TBR branch swapping was performed as replications overflowed. All characters were equally weighted. Forty-four multi-state characters were treated as ordered based on Müller (2018). *Euparkeria* was used as the outgroup.

Seven unstable taxa were identified using the IterPCR procedure (Pol & Escapa, 2009) on the entire set of most parsimonious trees (MPTs), the following taxa were pruned from the MPTs a posteriorori of the heuristic tree searches in order to create a reduced strict consensus showing clades that are collapsed in the strict consensus. Instability in these taxa is due to character conflict and missing data.

The following taxa are unstable and collapse nodes in the strict consensus:

Meroktenos
The following characters support alternative positions in different trees:
312 321 322 323 324 401

Scoring the following characters may help to resolve its position:
1 3 5 7 9 11 14 21 25 26 27 28 33 34 35 36 39 41 42 45 47 49 50 62 66 71 73 81 83 86 89 101 103 105 107 111 114 115 117 121 122 126 127 128 136 140 143 144 151 152 153 167 168 175 179 184 188 189 195 199 200 201 205 207 208 214 225 226 227 228 229 236 237 239 240 241 242 248 254 255 256 259 263 266 271 273 274 277 292 304 320 332 339 341 344 346 349 351 352 356 357 358 360 362 363 365 371 377 379 381 383 385 386 387 390 395 396

Glacialisaurus
The following characters support alternative positions in different trees:
357 377
Scoring the following characters may help to resolve its position:
1 11 20 22 23 25 30 32 33 34 38 42 43 48 50 53 57 58 60 70 72 73 76 78 79 81 85 86 92 94 96 97 98 100 103 104 108 114 115 116 119 120 123 125 126 137 141 143 144 150 155 158 167 171 197 201 206 212 224 225 228 232 233 234 255 259 265 270 283 286 295 298 303 311 313 335 348 353 371 395 400 401

Chromogisaurus
Scoring the following characters may help to resolve its position:
46 76 115 131 143 158 181 222 224 226 305 307

NMQR3314
The following characters support alternative positions in different trees:
14 50 236 243 288 363 371 401
Scoring the following characters may help to resolve its position:
151 186 188 212 214 225 226 227 256 292 303 324 349 352 356 357 359 383

PVL_3808
Scoring the following characters may help to resolve its position:
11 20 29 57 60 73 81 115 116 125 126 133 137 362

Blikanasaurus
The following characters support alternative positions in different trees:
352 356 357 360 363 371 383 401
Scoring the following characters may help to resolve its position:

3 9 11 14 21 23 25 26 27 34 38 39 41 42 45 47 49 50 62 71 72 78 81 83 89 101 107 108 109 115 116 117 127 131 136 143 151 152 153 167 168 175 180 184 186 189 190 193 201 205 208 226 229 236 239 240 241 242 243 247 254 255 256 259 260 263 266 271 273 274 277 278 288 289 292 293 303 306 307 311 314 316 318 321 322 323 324 346

Ingentia

The following characters support alternative positions in different trees:

151 167

Scoring the following characters may help to resolve its position:

136 153 180 184 186 189 190 193 205 208 223 226 229 243 263 266 271 278 288 292 303 306 307 323 339 344 346 348 352 356 357 358 359 371 376 383 385 386 390 395

The following taxa form polytomies in which all descendants are unstable:

Plateosauravus

There are no characters to revise (with relevant information) for resolving the relationships of this taxon with others of the polytomy

---

The following taxa form an unstable clade that appears in the reduced consensus [absent from the strict consensus]):

This node includes the following taxa: 13 36 37 54

.

The following characters support alternative positions in different trees:

60 236

Leyesaurus

There are no characters to revise (with relevant information) for resolving the relationships of this taxon with others of the polytomy

---

Adeopapposaurus

There are no characters to revise (with relevant information) for resolving the relationships of this taxon with others of the polytomy

Strict consensus tree

Strict consensus of 3744 trees (0 taxa excluded)

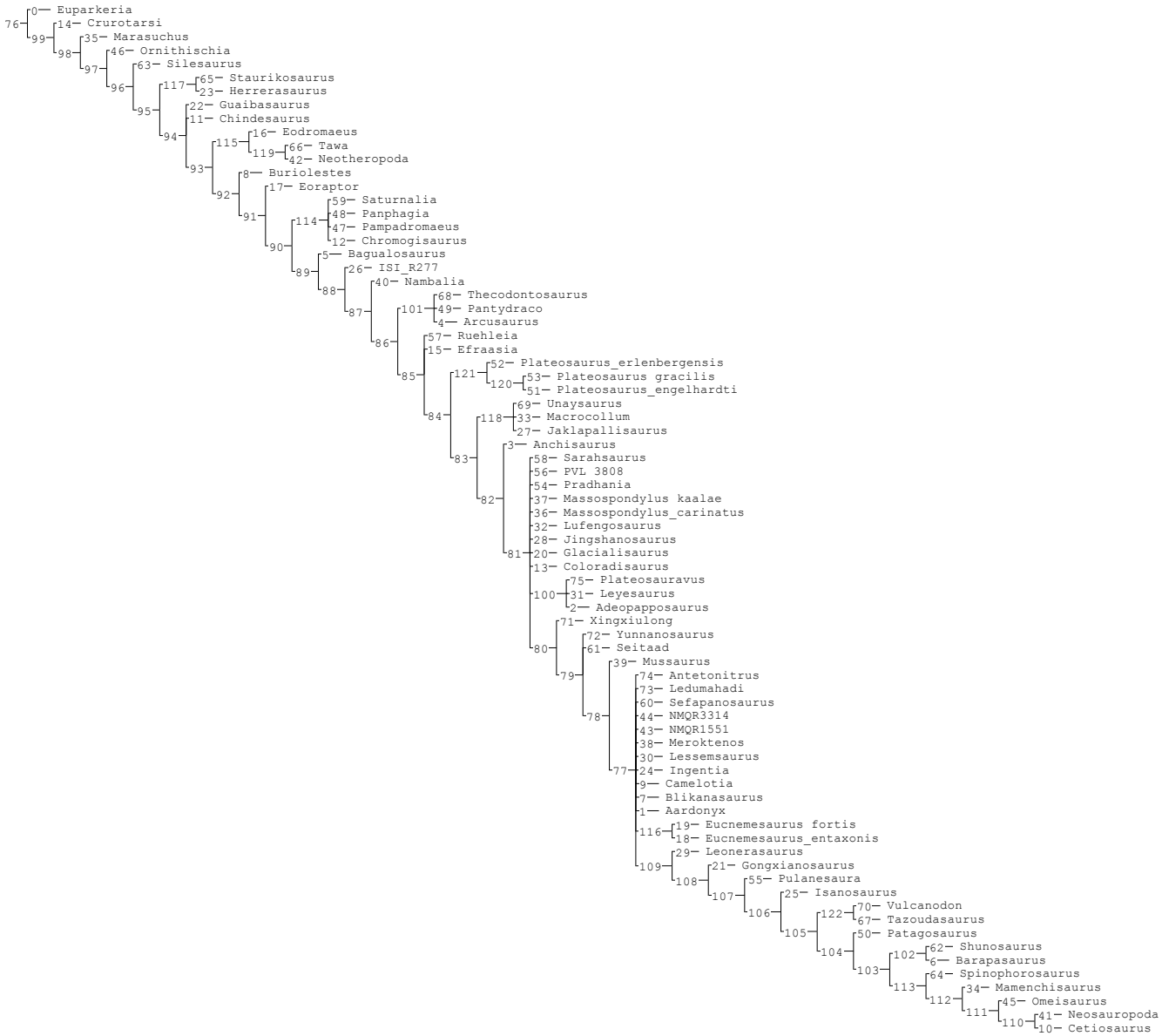

Reduced strict consensus tree

Strict consensus of 3744 trees (7 taxa excluded)

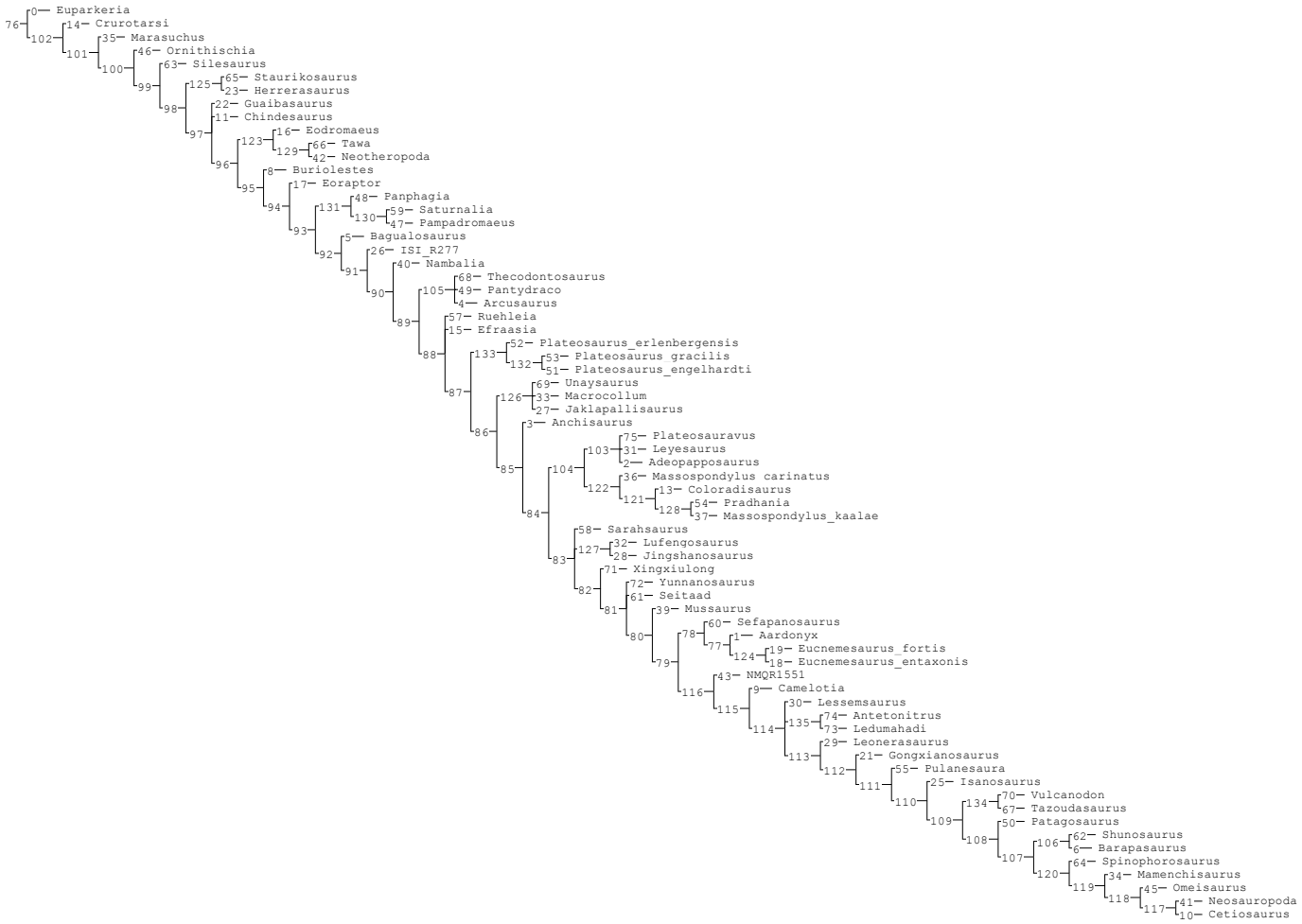

Sources for phylogenetic analysis:

Apaldetti, C., Martínez, R.N., Cerda, I.A., Pol, D. & Alcober, O. 2018. An early trend towards gigantism in Triassic sauropodomorph dinosaurs. *Nature Ecology & Evolution.* 2(8):1227.

Barrett, P.M. 2009. A new basal sauropodomorph dinosaur from the upper Elliot Formation (Lower Jurassic) of South Africa. *Journal of Vertebrate Paleontology.* 29(4):1032-1045.

Cabreira, S.F., Kellner, A.W.A., Dias-da-Silva, S., da Silva, L.R., Bronzati, M., de Almeida Marsola, Júlio Cesar, Müller, R.T., de Souza Bittencourt, J. et al. 2016. A unique Late Triassic dinosauromorph assemblage reveals dinosaur ancestral anatomy and diet. *Current Biology.* 26(22):3090-3095.

de Fabrègues, C.P. & Allain, R. 2016. New material and revision of Melanorosaurus thabanensis, a basal sauropodomorph from the Upper Triassic of Lesotho. *PeerJ.* 4:e1639.

Galton, P.M. 2001. The prosauropod dinosaur Plateosaurus Meyer, 1837 (Saurischia: Sauropodomorpha; Upper Triassic). II. notes on the referred species. *Revue De Paléobiologie.* 20(2):435-502.

Kutty, T.S., Chatterjee, S., Galton, P.M. & Upchurch, P. 2007. Basal sauropodomorphs (Dinosauria: Saurischia) from the Lower Jurassic of India: their anatomy and relationships. *Journal of Paleontology.* 81(6):1218-1240.

Langer, M.C., McPhee, B.W., de Almeida Marsola, Julio Cesar, Roberto-da-Silva, L. & Cabreira, S.F. 2019. Anatomy of the dinosaur Pampadromaeus barberenai (Saurischia—Sauropodomorpha) from the Late Triassic Santa Maria Formation of southern Brazil. *PloS One.* 14(2):e0212543.

Martinez, R.N., Sereno, P.C., Alcober, O.A., Colombi, C.E., Renne, P.R., Montañez, I.P. & Currie, B.S. 2011. A basal dinosaur from the dawn of the dinosaur era in southwestern Pangaea. *Science.* 331(6014):206-210.

McPhee, B.W., Benson, R.B., Botha-Brink, J., Bordy, E.M. & Choiniere, J.N. 2018. A giant dinosaur from the earliest Jurassic of South Africa and the transition to quadrupedality in early sauropodomorphs. *Current Biology.* 28(19):314-3151. e7.

Müller, R.T., Langer, M.C., Bronzati, M., Pacheco, C.P., Cabreira, S.F. & Dias-Da-Silva, S. 2018. Early evolution of sauropodomorphs: anatomy and phylogenetic relationships of a remarkably well-preserved dinosaur from the Upper Triassic

of southern Brazil. *Zoological Journal of the Linnean Society.* 184(4):1187-1248.

Müller, R.T., Langer, M.C. & Dias-da-Silva, S. 2018. An exceptionally preserved association of complete dinosaur skeletons reveals the oldest long-necked sauropodomorphs. *Biology Letters.* 14(11):20180633.

Nesbitt, S.J., Smith, N.D., Irmis, R.B., Turner, A.H., Downs, A. & Norell, M.A. 2009. A complete skeleton of a Late Triassic saurischian and the early evolution of dinosaurs. *Science.* 326(5959):1530-1533.

Novas, F.E., Ezcurra, M.D., Chatterjee, S. & Kutty, T.S. 2010. New dinosaur species from the Upper Triassic Upper Maleri and Lower Dharmaram formations of central India. *Earth and Environmental Science Transactions of the Royal Society of Edinburgh.* 101(3-4):333-349.

Otero, A., Krupandan, E., Pol, D., Chinsamy, A. & Choiniere, J. 2015. A new basal sauropodiform from South Africa and the phylogenetic relationships of basal sauropodomorphs. *Zoological Journal of the Linnean Society.* 174(3):589-634.

Pretto, F.A., Langer, M.C. & Schultz, C.L. 2019. A new dinosaur (Saurischia: Sauropodomorpha) from the Late Triassic of Brazil provides insights on the evolution of sauropodomorph body plan. *Zoological Journal of the Linnean Society.* 185(2):388-416.

Prieto-Márquez, A. & Norell, M.A. 2011. Redescription of a nearly complete skull of Plateosaurus (Dinosauria: Sauropodomorpha) from the Late Triassic of Trossingen (Germany). *American Museum Novitates.* 2011(3727):1-59.

Yates, A.M., Bonnan, M.F. & Neveling, J. 2011. A new basal sauropodomorph dinosaur from the Early Jurassic of South Africa. *Journal of Vertebrate Paleontology.* 31(3):610-625.

Appendix 3: Chapter 2 and 3 Phylogenetic Analysis OTU Scores

Euparkeria

00000000?00000?000000000?000?10010000000000000
0000?000000000000100000000000000100?000000??00?0100
00?00?000?000000000?10000000000000000000000?000000000
0000???000000??000000000?00?0?00??000000000000000000
0000?00?0?????0????0000?00200000000000000???????00000
0000001?0??0?00000???00?000?0000?01100000000000100000
0000000?02?000??01000000??1?000?100000?00000000?0???
0?0?0010??0000?0????0?00?1?10?0000000?00[0 1]00

Aardonyx

1101?00210?002?1?01?11????1110?1011000???????1?
010??0??110110???0?1?????????1?0??????????0???????????
????????1??0?0?1?0?????1??1?00101011001??1???????001
0?01101 00??101101?0000011?00110001000020000010?100??
0110000?01110?0?00??????11??????????11100??00???????1
31101???1??10??1?0?????????????????111010?001011?0?10
110?101?1111000011110 00?1????????1101110??0???01????
??????????01201111[0 2]0?0010?0?2???00?0???0??3

Adeopapposaurus

100110021 0?00211?01?11?11011011111010000101101 0
000110[0 1]11110111100010001 02001[0
1]00110101100011100 1?10000101101000001011[0
1]1010100111111110[0
1]10011110011?1100200010010100101101100[0
1]00111001100000000000000100101000100000001000000000
0101010[1
2]21100010100000110111101111010110020010000001000[0
1]1003100000[0
2]01101100 01?1100010110010001101000010[1

2]1010?100000001110110011001111?0001000011101000011110000010200011100001100001

Anchisaurus

10???00??00102?1?0??11?????111011?010?001010?1?0001100?111?101100?10??????01?001101?1??0011?10????00010??????10?10?000?10001?0000101?11?01?11?001?1???100?100111??1011?10000?010?001100?000??0000000??1000?0???000?00?10?0????11[0 1]?0???2?1100101100?00??0??1101011010010020110000?02000[0 1]1013100000?1111100001011?000101001010110100010[0 1]11101?0100000111011 0?1??01?0100?0???010111?0?0011????0?01?1?00?1000001001??1

Arcusaurus ?0?1??0[1 2]1??0????????0?010?1??????????????????????0???????0?00??0????0?01010?????0??11?0101010000??00???????????????????0?0???0??[1 2]????0?0???????

Bagualosaurus 10?1?00[1 2]??11?1[0 1]?100?1??????101?010?1000?10?10????0?100?10???0?0000010?????0111000101000?00???????????????????????????????0??001??0?1???10?0?0000000?0?01??001???????0?0???0??000011000202?00?00??0?????????????000??0111000101110????100000?0?01??01?0????????????????????0???1????0?0??0110?????????????2

Barapasaurus

???

??
????????????????????????????????1?111211????????????1
?1?????00????002??100101??00201102111120121100?[1
2]10001?1?1?1??1????0????1010?00?21???????20010?????
???????0?????????????????????1111031011000111110001 1??
11?110010?????????????????????1????1?1?????????1??1???
??000??1???????????20?????????????????2?1????????5
Blikanasaurus
??
??
??
??
??
??
??
??????????????????????????0000?1110111?10?010010100
1111101110012011110 01?1112102?120000100???2
Buriolestes
0001?001??0100?110001110?1100100100100001001000
000?10?1100110100001?00001?01?00110101????1?100????0
?0?0?????000000010100100001000000000000111?00111000
01010011?00101101000000100011101100000000000000?01??0
010???0???0?0????????1?1?11211000??0??0???????????
????????????????????000001100210 1?0???????1?11?00?0
?1?10000101110001011000010000000 1??0????1000????0???
????0???????000?????0??1?0??00???0????0???0
Camelotia
??
??
??
1????????????????0??0??001??00210000000??00?0????????
??1???0??011??
????????????????????????????????1??????????1???00

111?1110111101111?1??1101???00000????????????????????
????????????????????????????[1 2]????000??????4

Cetiosaurus

1??
??
??2??001?11101
110110100??100020?2001?1??1020??1[1 2]11102010100??[1
2]??????20111?00100?0??0111110103211001000 20?10?????
??1????????????????????????111103?0210?0110?1?0011?1
10?1?00???211112??0???010?111???2101002100101110????
??5

Chindesaurus

???
??
???0??
???????????????01?0??0?1??0?1??????000??00?????00???
?1?0?????1000?0?????????????????????????????????????
???????????????????????????0???001??????00??????????
????000010111000101110000??????11111100??0?01?110??0
100???????????????????????????????????????1

Chromogisaurus

???
??
??
??1000
0??10?0??11?????????????????????????0???????????????
?????????????????????0????11002102??????????????????
?????0??????1???10110?????[0 1]00000[1
2]01010001?0??????????????????????????????????0??0??
??000??????0

Coloradisaurus

?00?1002??010??1?011111?1??1110??011000?10??0?0
?10?100?1101111000010010 0?10100111110101001111 00?100

001?????1?1001011010011???10001010100011?11?00?11002
0001001010 0?01100?00?001?1001100000000000000101????0
0?11000?011???0????0100010121110011?????????????????
????1???????????0?????0?0?31100???011?11100201100010
11000000110100001021110?1110000011101100?1?011110010
?001??????0000111111010102000?1[0 1]00002100002

Crurotarsi 0000000000?000?0??[0
1]000000000?0001000000[0
1]000000?0000000?000?0000?0000000000000000000?00000?
??[0 1]?01[0
1]00??0000000000000000000000??0000000000000?00000000
00000000???00??00??000002000?00?0?00??00002000000000
0000000000000000000[0 1]00?0[0
1]0??002?0000000000?0?0000000000000000000000100000?0[
0 1]00000000?0000?0[0
1]000000000000000000000000?00?000000000000000?1?0000[
0
1]00000?00?00000?0???0?0000000000?00000000?00?0010?0
000000000??[0 1]

Efraasia
100?1001?0010??1?0?111?112?1110?100???00100100?
000??0??10???01?0??1??????10?00???????100?1111001?00
??00??????10010010??11?01111001010 10000?1???1??11001
1001001010010110100000001??001?00000000000000000?0000
0100000?01100000?0?010?0112012000111001001101012010?
1010000011010100001000010031000101000010000001100010
1101000011110000101100001000000011101?0010?011010010
?0??01?111000001??0?0?01?1?0011[0 1]00001000??2

Eodromaeus
00???????0?????1?10??1?????0000?00?0?1?????????
????????1???
?????????????0?000???0?0?0000000000000001???????????
?0?1?????11??????000??01??011?????????0?????1??10???

??????????1?1??1???01010??01110??0?10??20?????020?00
0??100?00001000?0?????00001000210[0
1]000?10?001?1??????????0?0010111000101????0??000?11
100?110??0??100100?010???????????????????????????0??
??????????0
Eoraptor 00?1?00[0
1]?001010??000111001110100100100001101000000?1001100
11010??011000010011???1?1??????????????????????????0
0000010???0?001?00?10000000001??????110000101001???0
1011??000??01?00??100?000??00000011?10????10???001??
0??0000?010?0??10?10??00100100?????020?000011?000100
1000000[0
1]010000010002101??0??0?0?0??10??1011?10??0?01110001
01100001?00?1?0111010??10?0?00????????001????0?000??
???0?0??00100000000??00??0
Eucnemesaurus_entaxonis
???
??
??
??????????????????0?0?01??0????0???000??0000?001011?
0?10?00?01????0?????????????????????????????????????
?????????????????????0?1??3?000100??1??0??0??11??010
110?1?1?011101001010110?10?0?????110111?1??0??0?????
????0??????11011112??001?[1 2]?00?11000???????2
Eucnemesaurus_fortis
???
??
??
??????????????????0???01??001100[0
1]10000??00?0??????????10000?01100???????????11?????
??
????110????0??????????????0110111010?1010110????0000

01110110??0??
??????????[2 3]

Glacialisaurus

??
??
??
??
??
??
??
?????0??????????????????00?11??????????????????0???10100
10[0 1]0????1100?0111111?1010????????????????????

Gongxianosaurus

1?????0????????????????12????????????????????????
??
??
????????????????????????0??0???1??2121?????????????0
??????????????1??0??001??0??????0?0??00000?????????
??????0?0?1?0??000?011????2?110????1?????????????????
????????????????????0?100???0??????????????????????
????[1
2]111?2??????0???110???1??????1?0??1????0?1?1???????
?1?11??01?0??????1?0???2?11?120002000??5

Guaibasaurus

??
??
??
????????????????????0???01??0110010000??00000??00000
0?00000?01?0??0[0
1]00??1?1?????110????1?0?0?????????0????0110??0?11?00
???0?0?000?0[1
2]1002101100100?00000100?10110000001001000010110??
?[0
1]00?0?111111001000?011?0?01?0001011100000000000001?
0110000000000??1

Herrerasaurus

00000000?0010100?000000000000?0000000000000001000
0000100001001010000010000110100000010 1?00?1???0??0?0
0000?1000?00000000?100000000000000000000110100001 0000
0001000000000?00001000001 1??0010[0
1]1000000200000010000010110010011101001 00?111?0??001
1000000001200000012000000001000001010110010010000020 0
0000010000001 0??01??0101001000010111000101100000010 0
0011000100010001001000010000100110000001000000000100010
000000000?0112

Ingentia

???
??
??
11?1????0??1011?0??0????????????????????????????????
????????????????????????????110001011110??1?10?00111
3110110?????????????0???????????????????????????????
??
??01?

Isanosaurus

???
??
???0??
0??????????????2??10??0???????????????2?011000??????
??????????????????101??0????????????????????????????
??
????211112??0???001?1?0111??????????????????????????
???1???????????????0????????????????????113

ISI_R277

???
??
???001
0????????00???1???????????0??????????????000??001???

01??
????????????????????????????2?1??201????????????????
?????0?0101100001011O??????0????????????????????????
??
Jaklapallisaurus
??
??
??
????????????????????0???0????????????????????????????
????????1??
??
????????????????????001???0000111101O??0?011011O?0
??00???????0?0???1????0???1??0????????????
Jingshanosaurus
1001?002???10211??111100?0?11101110110O?102001?
??1?100?11011110?001000????011000101012?1?????????
??1000??1?10110010??1110??1100101211001?????11?1??01
0????????1?????10100??0011100?1???000000000000?10???
011000000010000000?001?0??121201011O??0???00??0011?
3?100100?0110001?020000100310000020110011002?110?010
110?[1 2]0[0
1]011010000101111O???10100011101O?1?201101???0?00??
?????0120?1112?1?01?20001120000010???4
Leonerasaurus
?0??
??
????????????????0?0?????????1?1101011001?1???00?1??01
0?[0
1]1?????????1100?00?0?10000110000000??00000100111?00
1????????????????0100????1100000????????????????????
????????????????????1101310?????????0?????11???1?1
????0??
??????????1001110200????????????0??????00?

Lessemsaurus

??
??
??0?0
11???0100?????101?0000011?00[1
2]10000000111000000?????????????????????????000?1???
?11000101 1??00???????0???3110?????00?0??1????001003
100000?01111000 01??1???10110?111011?10???01111?01???
00000111 01?1??1?01101002100 11?????????????112????1?21
01???00??0???014

Leyesaurus

?001?00?10?00211?0??11????1010?110100001011010
?00?100111111111?00100010[0
2]0011??????????00?11?00??1?0?0?110??1?00?10110??1010
?1?1111010[0
1]0001??1???1?1100200010011100101 1????0????????????
????????????????????0000?001????000????????????
??
??????1?00????????????????????????????????????
????????????????????????010??????????0?1020001???
?0????0?00?

Lufengosaurus

110???02????0211?0?1?11?1111111101010010101101?
000010111100111 1?0010?1????0110??1010??00011??0?????
??100?00101001 0????0111???1100101010001 11?00?1?11002
00?110111???0110100020011100110000000000000010010 1?0
011000000[0 1]1000000000 11?0111212[0
1]101110?000110111101113010010120010001002000010031 1
000020110110002011010101100101010110100001021110?11101
000111011001000111 1???0?00001?11100[0
1]0111101010102000111 0000[1 2][0 1]00??4

Macrocollum

100110021001021111111111121111001001000010010 00

00011000100110100001000001101???????????0??????????0
?0?0?10???1001011010?1?0??11001010100001111?011111002
0001001110010110100000011101110100000000000010010??0
010000000010000100?010001111120000110000?11011120101
0010100021010000?010000100210001020 0?0?0?0010110?010
1110100000110000101100011010000[0
1]11101100100011011010100001011100001101000001011000
0000001000??1
Mamenchisaurus
11000113?1?11201??10120000000101112??001112010?
1010111?11111012?100000111221010010111?2?1?11?1?0??1
010??????2?11[0
1]00001001000??1111111112111?3?0001?110121001000 01??
10002?1110101010020110?01102012100001100111211111011
001?0111111?000322100100120000110011011000?100011?0?
?10?1??31?1111031011?001111100011001100100100211112?
?0???010?011???21010?0??0???????10101???11111??????1
120?1????2?1??2?12?1211102??0??5
Marasuchus
00???????0??0??????????????0?00???????0????????
????0?????????????????????????????00???0?0?0?100100?
?????????????????????????0?00?00000000??1?1000000000
0100???00?0?0??00?000000?00???00??000?00000000?00000
000??0010100000000?000??012?1000?00000??????????????
?0???????????????????00000000000?0100010000000000000
0001000000011000100000000??00000010001000100010000000
0?0?0000000000?000??0?00?0?00??0??00???1??0
Massospondylus_carinatus
1001100210100211?011111112111101001100001011010
0001100111111111000100010200100011010110001[0
1]10011100001111000110011110100010[0
1]1110010101100111100?101100200010011100101101000200
11100110000000000000001011010001[0

1]00000000000000?01[0
1]00111212010111000001101111011120100101211100000020
00010031000[0 1]000110110001011000101110[0
1]0101101000010[1 2]1010?10[0
1]000001110110010001111?010100?011111000011111100?010
200011100002100002

Massospondylus_kaalae

?0???002???00211???101????110?100110000100102?
??0?10?1?10??01???????????1??0????????????????????
???0???????0??0101?????0??0100101000000????????????
??
??
??
??
????????????????????????????????????

Meroktenos

??
??
??
??
??
????????????????????0??0?31?0000101?000001???????
????11111110?00011111?????????????????????????????
??????????????01?0?????????????????????2

Mussaurus

??????????????????0????????????????????????????
???????1????????0????????????????????????????????
??001
000????????10110??0000?1??00100000000?0000010?1?1??
0111?0000111?0?????01110??10110001111110?1?11?00101
201011012011000000200???0?3100010?011??1?001011???10
110?10101101000010111?0?1?100000[1

2]1101110100011O1?1101010?????0110111100000112001?1
100001100[0 1][0 1]3
Nambalia
??
??
??
??
????????????000????????????????????????????????
????????0?010??00?10???????2?0??20??0???????????1?????
111?0100110101001011O?0000???????1101?0????011010O?0
??000101???0?00101?0?00101110O??00?????00??0
Neosauropoda 1100011311[0 1]11201?0101200000101O111[0
2]11101112010?101011[0 1]?111?10121100[0
1]10112221110010111112[0 1][0 1]0[0 1][0 1][0 1 2]1000[0
1]10100001020111000012010O0[0 1]1[0 1]111111[0 2]12[0
1]1112[0 1]0000?1110011?110100??110020121010101[0
1]020111[1 2]0110201211000210001120111111[0 1]1000[0
1]0100111?0003?21001[0
1]00200101100010100000000011002O1??1??30011110310210
00111110001101110O[0 1]10[0
1]00211012??0???010?111111210l0?0100001l1?1101010021
11111011??11211100??2?10?2012112111021101l5
Neotheropoda 00[0 1]1[0 1]002[0 1]00102010100110000l[0
1]0000000000001100000000010[0 1][0 1]100?[0 1]01000001[0
1]0001[0 1 2]0100000101100001?[0
1]?0100000011100010000000l?000000000000000000011011
0011100000010000[0
1]11100001020000101011001000000100000000[1
2]10000110010000001001000010000l0?1100000100100010000
120000000l0?00010011O?0[1
2]0101010300021110101000011110100011010000l?0110001
00000001000[0

1]011111111002000101100?00000111110000??0?0000000?01
0000000000001[0 1][0 1]2

NMQR1551

???
??
??
?????????????11???00?001??002100000000100000000?2?110
0120000?0[0
1]11000????01010??2?????00011110????????????2?1?????
??1??????????001003100000[0
1]0110100001????????????11101111001110[0
1]1110?11100000111011001000?101?0?010000??????110111
12?000?????1?120000??????3

NMQR3314

1001?10310?00211?0111101?1110101111???101010110
0101100?11011011?000000102201101110 10??20011????????
??10011011101?00111?1000??110?100211001?10?010?11001
?00110100??1011[0
1]10000001??0??100??0?0?10000000?1111001?0100?0?1??0
0?????1?????[2 3]01100?0?11??01??????0010?2?100101[1
2]0??000100200001003100 0[0 1]0[1
2]????????????1???10110?????????????1???110?11100000
11?011?01??0??0????0???100111001201111201001?2?01?1[
1 2]00001100??3

Omeisaurus

11000113110112 01??101200000101011?201001112010?
1010111?110?10121100000112221110010111???0??????????
??0???1???11100001?0?0001?1110111112111?3??001?11012
000110101??11002?1210101011020110?011020121100?21???
1?20111100100??0111101000032210010002 0?10??????01000
0010001100?01001??3101111031011000111110001100110110
0100211012??0???010?010???210100?1?0??111??01101???0
?11???1????121?110??2?10?2012?1211102?10??5

Ornithischia 0010000000[0 1]000?000000000?000?10110001001 00?10000000100[0 1]100?001000000[0 1]000100100000000010000 10?[0 1]?01?000000010010[0 1]01[0 1]0000001001[0 1]11100111010000110000000000100100[0 1]000?00??010000000?00?0?00?000000000000000[1 2]10000000000010000010000 10?0111[0 2]1100000100?000000000000000000000000000000?000001101 3100010001??0000?00110000000010000 1?01011110200000?0 00000[0 1]1011100020?01?[0 1]10??000000111100000?000?00?00?0[0 1]00?0000000001[0 1][0 1]0

Pampadromaeus

00?1?00?10110??1100011????1000?100100001????01 0????0?1100?1??????1?????1?????????????????????????? ??????????00??000???0?000100010100000000???????????? ?? ??????????1????????111?????????????????????????????? ??????????????????????000001100??0?????????????????? ????000010111000101110001 00?????????????????????????? ??????????????????????????????????????0

Panphagia

??????????????????????????0?1?????????????????1 0??1??????????1?0?????????10?1?0?1????0???????????00 ??????????0?0?0?1010000???10?0101000000???????????001 0101001110 0?01101?000?01???01?10?00?000000000????0?0 0??0000?01100?0?0??011?1?????????????????????????????? ??????????????????????0??0?1[0 1]0021010?00?0?00??11???0?110?????????????????????? ?00100101010 0??0?0100????010?0?????????????????0????? ???????????????????

Pantydraco ?0???0????0?????1????[0 1]00?0???1??1????000100100000010?01000001?00???????

?00?000?1?10??00?101100??00??011?000?00?01010??00001
1?1001010100001100 1???1100110010100100101101?00???1?
???1???????????????????????0??1?0000100000100??????1
1?01?00???0010
021100001??????????011?0?10110?00??????????1?1?00000
??0000010?01?0010?????????????????????00001110000010
1?00000000001001???
Patagosaurus
11???
??
???????????1?00001????????0??0111012111????????11001
012100000??110020?2001010?00201?021111201 21?00?21000
11[1
2]0?01?0?100????0?111??00??2100100?2??10????????????
????????????????????11110310100001111100011011101100
10?211112??0???0011111???10100[0
1]??0????????????0?????????????????????????????????
?????????115
Plateosaurus_engelhardti 1001100110110201101[0
1]111112111100101100001001010010110001101011000 11001
0011011011101011100110200010000000101111001011010111
11?1100101010000111001101100110 0100[0
1]0100101101000200111001100000000000000001010100001[0
1]00000001000000000100011111[1
2]00001100000110111101011010010010010000?01000010031
1001020010100000111101010111110001111000001011000 11010
000[0
1]11101100100011010110100001011100001110000001011001
1100001000013
Plateosaurus_erlenbergensis
??01100110?10111??1110??121111?01011000001110??
010010???00?0010?0????100100?1??????????????????????
????1101??10010?10101111??1100101010001?????????????

??
??
??
??
??3
Plateosaurus_gracilis
?00??001?0?102?1?010111?1??1110?101??00?10?101?
0?0??0??100?0110???10??????????????????1????????????
???????????0??0110?????1?11100101010?00?1??????1100?
?001???01??101101?00?001?1001100000000000000010?01000
0100000000010000?00????0????11200?01100?00?1011?10101
0010000???010??????0?00100311001020010100001111010 10
11??[0
1]0001111000010110?01??10000?1??0110??0???????01????
??????????0??????????????01?0??????????[2 3]
Pradhania
?????????????????????????????1???????00????????
?????????????????????????????????10?????????????????
???????????0???1?1????????????1?1010???????????????2
0?????????????10????????????????????????????????????
??
0?1?????20??0???????????????????????????????????????
??
???
Pulanesaura
???
??
??????????????????????????????10?012011??????????001
?111?0100????11?????0??1??00[1 2][0
1]?0010?0120001000????????2?111?011???0?0???????????
????10??[1
2]???0??
??????????11?0?1?11???????????????????????0?00000210

0101???1??
????????
PVL_3808
????????????????0????????????????????????????
??
??1?0?11?11001
100111101 00?011[0
1]1?00100111001100000000000000101101?00110000?011000
0?????????10321210011 10??00????????????????????????
???????00100311001020?10100001????1???????1?01010101
0010111?0?10100000111011001 10??????01????????????????
????????????????1???????????00?
Ruehleia
??
??
??
??01?11001
?00????01?????101?00200 11?00110010000011000010?10000
01?0?00?0110???????0100011101200011100100?0100??0101
10101000????0??000???00100311000020??1100001011 01?10
110?10100101000010210000??10?00?111011001 0?0?001???0
100???3
Sarahsaurus
10?1?00?10???201?0??11????1110111???0?010?0110
010010??1101001000010?0???00100011 1?01?0001????????
??1011??1?10?10010?????0?111001010100 01?1?00110110?1
000111111001011?1100200111001?00?000000000010?10??0
011000000?0000000001010101[0
2]12100011000001101111011?1010?10121110000?020000100
310[0
1]00020010 11?0010110?0101110??1011010000100 10?0?1010
0000?1?011001?001101?0001?0001111101[0
1]01?11200?0102000??[0 1]000?1100??[1 2]

Saturnalia

?0?????????????????????????????1??1????00?100?0??
????????????????0??10?????1??00???0?0??0101?1?00?000
0?0??????????00000?????????000100000000???????????001
01010010?00?01101?000001000011001000000000000001000
010???0??1100???0??111001111110001010002???????????
?????????????????????0000011[0
1]021010000000001011000100100000010111000101100001000
000001010100010001001000010000100010000000000001001
10?00?000?00?010

Sefapanosaurus

??
??
??
??00?
?0?1100?????0?10??00?001????1?00000001??0000???1????
??11?00??011?????0?0?01010??1?00????11100?1011??0101
311010??10110???1????????????????????????????????
?????0?1111100000??11[0
1]??????000000??????0?0001101?010111?0001??0?????11?
0??0??2?0????????????????

Seitaad

??
??
??
??
???????????????????00?[0
1]?1??00??00?001????0000?????????????????????????00
10?011??11000111?00?11?11100111301O?00?2111O??0????
0????????????0?10000001?????????????????????????
???????0?00?11101?0????01101?0?010?00??11?00??11????
0?010???1?1[0 1]0000010????

Shunosaurus

11000113?1?10201??101200000001011?201001112010?
1010100?11011012000010011121010001111?1200?????0??11

?1???1102001100001201000??1111111212111?2??000?11?10
012?1?100??10012?1100001011021?0??01??2012100001 1??0
0?101?1101100 11?111?1??0002221001100?001?1000?101100
10?0001100200??1??3101111031011000111 11?00110?110110
0100211112??0???000?011???21010?[0
1]1?0????1?10?101??????1?1011??1121?110???2?00?2?12?1
21?102110??5

Silesaurus

00?0??00?00000?0000100000??0?00?0?01010????????
??0010?0?0?1???0?????????????00?0?0?1000??0001111000000
??0?????1?00?0?010???0?0?1000010001000011 0?000?00000
0000???0000100000000000101000011000000000000000?10000
0100000?0?0????????111??1110000010000000?????????????
??????????????????????0000000000200100000000?0100100
?0?10000110110001001000000100011110000000?000000100
0??011?1??002???00000000?0?10????000?0010[0 1]1

Spinophorosaurus

1????1??????????????????????????????????????2????
??????????0??????1?????????0??100111111201???21?0?1?
01?????????1?????????????????100111012?11?2??????11?11
0101?0?01???0002?110??01????[1
2]?11???1?12?1010?0????????[1
2]???11011?001?1??111?0?03?2[1
2]0?10???
?[1 2]????1?1???01[1
2]?0110??001??21111111 0?1101??0?0???20?1002??0??11??
10??0????0?01?????????????????????????????????????
?

Staurikosaurus

00???
??
??????????000000000100???00?000000000?????????000
10?????00???01001?000011?000?000000000200000 1?010?1

01100?00110010000??1?1?????????????????????????????
????????????????????00000200110000110?0010?00100?00
000100001??000?0101?0000??000001100000001????01????
??1

Tawa

0?1?000??00100?10010110011111?0?00?????1010100
0?0?101??1??1010???0[0
1]00101??10????0????0?0?????????????????????000000000?
??1??00100000000000??1??????110?100???????11???????0?
???0?????[1
2]??????????00????00?00???????????0?0?10?100?000?0??1
?010????1??????????020??0???1???0?0??0000?1000?00??2
0010110?1????????2????????????0?0?0?0110?1?1?0????0??1
0??01???????????0?1??????0?101?11??0??01?????0?0??0?
10?????0????????0

Tazoudasaurus

11??
??????????0?10????????????[0
2]011???1???1?????????????????????????00?00000???0???
?10?1111012101????000???0010120????????0002??100001?
?00200101011020121000?????????21?11?111?????11??????0
1?22100100?[1 2]10??????????010?[0
1]0100001001?00010?310?1???3101??0?111000?002?11?0?1
??1??2110111100111101?01???00100201010102??110101010
1111??011????1?????20????????1???10?1???????5

Thecodontosaurus

?0?????????????????????????????1??1??1000??????0?
?0?0?0????0?00????????????10?0?0?1010?10001??000?10?
??0????????00?11010????????1100101010000??1???????000
1001010?1???01101?000001??00110000000000000000?0000?
0101000?01000?0?00?010?011201100010102??0011000120100
0011000010010000?0101000002100000?1???0?0?00?011???01
010?[0 1]000111100001011000000?[0

1]0000010101100?1?011010??0100?????1100?0?111??0??1?
?0000??00?0???????1

Unaysaurus

100110021001O??111?1111?1??1110?10?1000????????
?????0?0?00??????01???000??0?10??1?10??10?110?0??100
??0????????10?1011O?????0??1100101010000????0?1??????
0??1?0?????????????0??0?11?00?10100?0??00000?????????
?????0???010000?00?010001 1?1120000110000???????????
1010????2101???0???0?????????????????????????????????
??????????????????????????????????1101 10????011011010
?00????????0???1100??????????00???0????????1

Vulcanodon

??
??
??
??
??????????????????????????[1
2]??????????????????1??????01?11?0?00??0?0???1????2
?[1 2]10?10?0[1
2]0010?????????????????????????????????????310[1
2]?00?011110000101110110010?1110111100100 11?1?????[1
2]0?10021?0???110?10101010101111011??111?10102?10010
20111111 0?121?0??5

Xingxiulong

??????????????????0????????1???1?1111???0?10?0??0
??01100?110?0110000?000101?01?00110101?0??1?????????
??1???????0??????????001????000?????????? 1100 11?11001
000110?01???0110100020011100110000000000?0000110110??
?1110000001?????00?000?0????120?01111??00????1??????
1?101?????????????????001003110000[1
2]0?1011?002?11?0??0?100101011110000101101 0?10?00000
[0
1]10?11001?001101???0?0?0?011?00110111000000 1?2100?1
10000210 0??2

Yunnanosaurus

100?1002???00??1??0011001??101?111???00101110?
?00??0??110?1111?001000001?01?0?01010???????????????
??????????000?0010???0?????00010?21000??1???11?1100[
0
1]100110100???0110100000011000110000000001000000?101
?10110000?00?0???0??001?00??121200?111[0
1]??00??01??0011?20101100201100[0
1]0020?00100310000000011010?001?110?010111?[0
1]01011010000101101 0?1?101000110011001 1?01101???0100
001111001?0?1110?0?011???111?0000110????2

Ledumahadi

???
??
??
??0?????????????1?0??0011???[1
2]?0000010121001000???1????1?000?01?????????????????
?????????1??01???????????[2
3]?1????????????11??????????????????????????????????
??????0??????????????????10?????????????????????????
?????????????????????????????????0?????????[4 5]

Antetonitrus

???
??
??????????????????????????????1??01101???????????0?[
0 1]0???????????0??00?0000011?00[1
2]00002010121001000?[1
2]1???0?10?00?01100?0??0?010010032110001011101?????
?00101[2
3]1100???10?10????????000003?00000201101000010 11?1?1
1010?111[0 1]1111001[0
1]11111011110000001101110101001012000 11???????1[1
2]011102010011201[1 2]111000[0 1]110?01?

Plateosauravus

??
??
??00?
0??1000????0110??001??1??0?1?0?00000011 00??1???????
????000??010?????????01????111001[0
1]1?00??
???????????1????1?1????????????????????????000000
110111??0????????????????????????????1100?00??????????
??????????